LAMINAR FLOW HEAT TRANSFER IN A PIPE PRECEDED BY A 180° BEND

By

NITIN D. MEHTA

Bachelor of Science in Chemical Engineering

Oklahoma State University

Stillwater, Oklahoma

1978

Submitted to the Faculty of the Graduate College
of the Oklahoma State University
in partial fulfillment of the requirements
for the Degree of
MASTER OF SCIENCE
December, 1979

LAMINAR FLOW HEAT TRANSFER IN A PIPE PRECEDED

BY A 180° BEND

Thesis Approved:

Kenneth J. Bell
Thesis Adviser

John H. Erbar

Jerald D. Parker

Norman N. Durham
Dean of the Graduate College

PREFACE

Experiments were conducted to study heat transfer mechanisms in laminar flow in a pipe preceded by a U-bend. The U-bend had a curvature ratio (R_c/r_i) of 7.66. Ethylene glycol was used as a test fluid. Straight sections of the tube were heated by passing DC current through the tube wall. The local heat flux was approximately constant for each run. Local outer surface temperatures were measured peripherally along the test section. Reynolds numbers ranged from 62 to 528 while Prandtl numbers ranged from 75 to 132.

I am gratefully indebted to my adviser, Dr. Kenneth J. Bell, for his expert guidance during the course of my study. I am also thankful to members of my advisory committee, Dr. J. H. Erbar and Dr. L. S. Fishler, for their constructive criticism and suggestions. The assistance of Dr. Mohammad A. Abul-Hamayel, Dr. C. B. Panchal, and Dr. Mahmood Moshfeghian is appreciated. I would also like to thank Dr. B. L. Crynes and the faculty of the School of Chemical Engineering for providing the opportunity to work on this thesis.

My appreciation is extended to the School of Chemical Engineering for providing me with an assistantship during the course of my study.

I am grateful to Mr. E. E. McCroskey for his assistance in the fabrication of the equipment.

I shall always be indebted to my parents, brothers, and sisters for their abundant love and encouragement. I am especially grateful to my uncle, Mr. M. V. Mehta, my aunt, Mrs. R. M. Mehta, and my cousin, Dr. M. J. Mehta, for their moral and financial support throughout my studies.

TABLE OF CONTENTS

LIST OF TABLES

LIST OF FIGURES

Figure | Page

NOMENCLATURE

AAPD	average absolute percent deviation
C_p	specific heat of fluid
D_c	U-bend diameter
De	Dean number, Re $\sqrt{d_i/D_c}$
d_i	inside diameter of tube
D_c/d_i	curvature ratio
d_o	straight tube outside diameter
emf	electromotive force
g	gravitational acceleration
Gr	Grashof number, $d_i^3 \rho^2 g \Delta t/\mu^2$
Gz	Graetz number, WC_p/kL
h_{ij}	local heat transfer coefficient based on tube inside diameter
$\bar{h}_i$	peripheral average local heat transfer coefficient based on tube inside diameter, defined by Equation (6.2)
$\bar{h}_i^*$	peripheral average local heat transfer coefficient based on tube inside diameter, defined by Equation (6.3)
h_o	circumferential mean heat transfer coefficient based on tube inside diameter
I	current in test section
J_H, j_x	heat transfer parameter, $Nu/\rho r^{0.4} (\mu_b/\mu_w)^{0.4}$
k	thermal conductivity of the fluid
k'	thermal conductivity of the stainless steel 304
ℓ	length of heated portion of test section--both straight portions
Nu	Nusselt number, hd_i/k

Pr	Prandtl number, $C_p\mu/k$
P_w	tube wall parameter, $hd_i^2/k_w t$
$(\dot{q}_r)_{ij}$	local heat flux
$(\bar{\dot{q}}_r)_i$	peripheral average local heat flux
r_i	inside radius of tube
Ra	Rayleigh number, Gr•Pr
Re	Reynolds number
R_c	bend radius, measured to tube axis
R_c/r_i	curvature ratio
t	tube wall thickness
T_b	bulk fluid temperature
$(T_w)_{ij}$	local inside wall temperature
$(\bar{T}_w)_i$	peripheral average inside wall temperature
W	mass flow rate of the fluid
x	distance along test section
x_i	distance between thermocouple stations
(x/d_i)	nondimensional distance

Greek Letters

β	coefficient of volume expansion of fluid
μ	fluid viscosity
ρ	fluid density
ρ	electrical resistivity in Appendix D
θ	angular position

Subscripts

avg	average

b	bulk fluid
b	bottom, in conjunction with heat transfer coefficient
cr	critical
exp	experimental
f	evaluated at fluid film temperature, $(T_{wi} + T_b/2.0)$
i	inside of tube, or index
in	test section inlet
j	index
M	Moshfeghian
MB	Morcos-Bergles
o	outside of tube
out	test section outlet
W	wall
x	local value

CHAPTER I

INTRODUCTION

In the petrochemical, food, and biomedical process industries, the use of U-tubes in double pipe heat exchangers, shell-and-tube heat exchangers, and kettle reboilers is common. In spite of that fact, the present understanding of laminar flow heat transfer downstream of the U-bend is not sufficient and warrants study. Figure 1 shows a sketch of a double pipe exchanger.

In isothermal laminar fluid flow, the velocity profile is parabolic about the center line in a circular tube. The fluid velocity is maximum at the tube center and zero at the wall. When the tube has a 180° bend, the fluid is subjected to a centrifugal force. The centrifugal force is directly proportional to the square of the fluid velocity and inversely proportional to the radius of curvature of the bend. The effect of the centrifugal force is to move the more rapidly flowing fluid towards the wall and the slower moving fluid at the wall towards the bend-axis. This, in effect, superimposes a secondary flow pattern on the primary flow pattern in the downstream section of the tube.

The objective of the present investigation was to study the laminar flow heat transfer mechanisms in a single phase fluid downstream from the bend.

Experiments were made with ethylene glycol as the test fluid. Ethylene glycol was chosen as the test fluid because its properties are well-

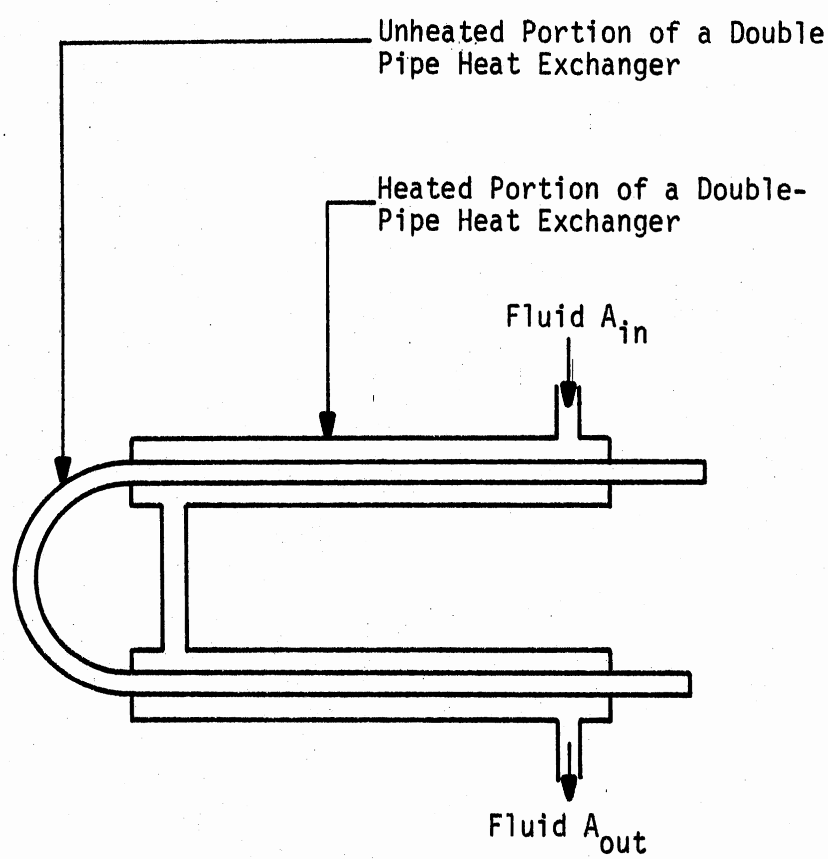

Figure 1. Sketch of A Double-Pipe Heat Exchanger

known. The straight portions of the U-bend were heated electrically in parallel. The apparatus allowed the measurement of the outside local wall temperature, thus permitting the calculation of the local inner wall temperature and radial heat flux. This allowed evaluation of the local heat transfer coefficients, which should be useful in shedding some light on the laminar flow heat transfer process.

The U-bend was made of seamless stainless steel (type 304) with an outside tube diameter of 10.05 mm (0.75 in.) x 1.65 mm (0.065 in.) wall thickness. The bend radius was 60 mm (2.375 in.) to the center line of the tube. The heated straight length of the tube was 2.743 m (9.0 ft) on either side of the U-bend.

CHAPTER II

LITERATURE SURVEY

In spite of the use of U-bends in various process industries, there has not been much work reported in the open literature on heat transfer in U-bends. The summary of some of these investigations is presented in this chapter.

Turbulent flow heat transfer in the U-bend was studied by Lis and Thelwell (1). The experimental configuration was a vertical pipe, with upward flow, followed by a 180° bend. In this case the vertical pipe on the downstream side of the 180° bend was electrically heated, giving a uniform heat flux boundary condition and with large temperature difference between the tube wall and the bulk of water. Lis and Thelwell used three test sections with bend to pipe radius ratios of 2, 3, and 4. Table I includes other relevant information. They made the following observations:

1. The local heat transfer parameter

$$J_x = Nu(Pr)^{-0.4} \; (\mu_b/\mu_w)^{-0.14}$$

in the entrance region on the downstream side of the tube depends on tube length, ratio of bend radius to tube radius, and the Reynolds number. The dependence of J_x on the ratio of bend radius to tube radius and the heated tube length downstream of the bend decreases with increasing Reynolds number.

2. The variation of circumferential heat transfer coefficient (h_θ) just after the U-bend exit was very irregular and a distance of almost 12 diameters was required before the coefficient became uniform. The distribution of heat transfer coefficient was symmetrical about the plane of the bend. The minimum value of the heat transfer coefficient was observed to be on the inside of the tube with respect to the bend.

Lis and Thelwell proposed a correlation for the heat transfer parameter J_x for the range of variables covered in the investigation.

$$J_x = \frac{Nu}{Pr^{0.4}\ (\mu_b/\mu_w)^{0.14}} = 0.0239\ Re^{0.826}\ (x^*/d_i)^{-0.064}$$

$$\times\ (R_c/r_i)^{-0.062} \tag{2.1}$$

where x* is the distance measured from the exit of the 180° bend. The range of variables for which the above correlation is valid is listed in Table I.

TABLE I

RANGES OF VARIABLES COVERED BY THE LIS AND THELWELL STUDY

Variable	Units	Range
Heat Flux	W/cm^2	5-50
Water Mass Flow	kg/h	440-5070
Water Inlet Temperature	°C	10-20
Water Temperature Rise	°C	5-12
Wall-to-Water Temperature Drop	°C	7-65
Prandtl Number	---	5.5-9.7
Reynolds Number	---	8,000-94,000
Water Viscosity Ratio, μ_w/μ_b	---	1.42-2.87
Ratio of Bend Radius to Tube Radius		2/1-3/1-4/1

The 5 percent thermal entrance length (x/d) is defined by Lis and Thelwell as that length for which the value of $J_x/J_{x\delta}$ ($J_{x\delta}$ is the value of the heat transfer parameter at which fully developed conditions exist) equals 1.05. Lis and Thelwell observed that the 5 percent thermal entrance lengths decreased with increase in Reynolds number.

Ede investigated heat transfer effects in and near a 180° bend in the tube (2). Ede studied heat transfer in turbulent, laminar, and transitional regimes using three bends of different bend radius to tube radius ratio. The test section was placed in the horizontal plane. Water was used as a test fluid. The test section consisted of straight sections upstream and downstream of the U-bend and the U-bend. The U-bend was heated by passing current through the tube wall. The Prandtl number ranged from 4.2 to 10.9.

Ede explored the nature of the variation of the local heat transfer coefficient in and near the bend. He found the flow mechanism to be complex in the laminar flow regime.

Ede observed that the disturbance due to a 180° bend produced higher heat transfer coefficients than in a straight tube not preceded by a 180° bend. He concluded that velocity (of the fluid) near the outside of the bend becomes much higher than that near the inside of the bend, and as a consequence secondary circulation develops. Ede observed that secondary circulation had considerable impact downstream of the bend in the laminar flow regime. Ede attributed the cause of higher heat transfer coefficient on the outside of the bend (compared to the inside) to the secondary circulation. These effects were observed to be accentuated in the laminar flow regime. In the case of laminar flow, the heat transfer coefficients were observed to be as much as 30 times the terminal value (the value of the heat transfer coefficient for Nusselt number 4.36) immediately after the bend.

Ede suggested the possibility that incipient laminar flow was the cause for the low heat transfer coefficient in the transitional regime. Ede's finding agrees well with Ito's correlation to determine critical Reynolds number for fluid flowing through the curved pipes (3). Ito's correlation to determine critical Reynolds number is

$$Re_{critical} = 20{,}000\ (r_i/R_c)^{0.32} \qquad (2.2)$$

The upper and lower limits for R_c/r_i ratio in Equation (2.2) are 860 and 15, respectively.

Heat transfer from a single phase fluid flowing through 90° and 180° bends was studied by Staddon and Tailby (4). They compared their results with those of Ede (2) and Lis and Thelwell (1). In the Staddon and Tailby investigation, hot air was blown inside a test section immersed in a constant temperature bath. Reynolds numbers were studied in the range of 10,000 to 50,000. They also made flow visualization studies and confirmed the presence of secondary flow. Staddon and Tailby made the following observations and suggestions:

1. The ratio of the heat transfer coefficient at the outside wall to that at the inside wall was observed to be 1.5:1 compared to Ede's (2) ratio of 4:1.

2. The ratio of the bend radius to the tube radius (R_c/r_i) has considerable impact on the local heat transfer coefficient. The value of the local heat transfer coefficient was observed to increase with the decrease in the curvature ratio. For a given value of x/D (x is the distance from the beginning of the bend) the local heat transfer coefficient

ratio between the maximum and the minimum was observed to decrease with decreasing curvature ratio (R_c/r_i) along the bend.

3. The variations in the peripheral mean heat transfer coefficient (as a function of x/d) increased with decrease in the (R_c/r_i) ratio. However, the peripheral mean heat transfer coefficient returned to the straight pipe value within 30 diameters of the beginning of the bend.

4. The ratio of the peak heat transfer coefficient in the bend to that in the straight pipe was in the range of 1.25 to 1.51.

Staddon and Tailby suggested the following correlation for the ranges of variables covered:

$$\frac{Nu}{Pr^{0.4}} = 0.0341\ Re^{0.82}\ (R_c/r_i)^{-0.11}\ (x/d_i)^{-0.14} \qquad (2.3)$$

where x is the distance measured from the beginning of the 180° bend. The above equation was obtained by a multiple regression computer program. The ranges of variables for which the equation is applicable are

$$10{,}000 \le Re \le 50{,}000$$

$$4 \le R_c/r_i \le 14$$

$$7 \le x/d_i \le 30$$

The exponent of R_c/r_i was observed to agree well with the one obtained by Lis and Thelwell (1), unlike the exponent of x/d_i (see page 4).

Moshfeghian (5) investigated fluid flow and heat transfer in a 180° bend using four bends of different curvature ratios (R_c/r_i). In his investigation three fluids--distilled water, Dowtherm G, and ethylene glycol--were used. The test section consisted of the straight section upstream of the bend, the U-bend, and the straight section downstream of the bend. It was electrically heated by passing DC current through the tube wall. Reynolds numbers ranged from 55 to 31,000. Moshfeghian's (5) findings and conclusions are summarized below.

1. In the case of low Reynolds numbers, natural convection was observed upstream of the bend, resulting in higher heat transfer coefficients at the bottom of the tube than at the top.

2. The peripheral distribution of heat transfer coefficient was nonuniform in the bend. The local heat transfer coefficient on the outside of the bend was higher than on the inside. This phenomenon was more pronounced in the laminar flow regime than in the turbulent flow regime.

3. The secondary flow has considerable impact on the local heat transfer coefficients downstream of the bend. The net effect is to increase the peripheral mean heat transfer coefficient.

4. In the case of laminar flow, the secondary flow tends to be counteracted by natural convection effect, the net result being a decrease in the peripheral mean heat transfer coefficient downstream of the bend as compared to a straight pipe not preceded by a 180° bend.

The following correlation was proposed by Moshfeghian for the straight section downstream of the bend:

$$J_x = 0.031\ Re^{0.825}\ (x/d_i)^{-0.116}\ (R_c/r_i)^{-0.048} \tag{2.4}$$

where x is the distance beginning from the start of the bend. The ranges of variables for which the above correlation is valid are:

$$10^4 \le Re \le 3 \times 10^4$$

$$\pi/2\ (R_c/r_i) \le (x/d_i) \le 160$$

$$4.83 \le (R_c/r_i) \le 25.62$$

For the bend-portion of the test section the following correlation was developed:

$$J_x = 0.0285\ Re^{0.81}\ (x/d_i)^{0.046}\ (R_c/r_i)^{-0.133} \tag{2.5}$$

where x is the distance from the beginning of the bend. The ranges of variables for which the above equation is valid are:

$$10^4 \leq Re \leq 3 \times 10^4$$

$$0 \leq (x/d_i) \leq \ /2\ (R_c/r_i)$$

$$4.82 \leq (R_c/r_i) \leq 25.62$$

For laminar flow downstream of the bend the following equation was proposed:

$$J_x = 0.00275\ [Re^{\{0.733\ +\ 14.33\}(R_c/r_i)^{0.592}\ (x/d_i)^{-1.169}}]$$

$$[1.0 + 8.5(Gr/Re^2)^{0.429}][1.0 + 4.79e^{\{-2.11(x/d_i)^{-0.237}\}}] \tag{2.6}$$

where x is the distance from the inlet of the bend. The ranges of variables for which the above equation was developed are:

$$Re \leq 2100$$

$$\pi/2 \leq (x/d_i) \leq 160$$

All equations were developed by regression analysis using a computer.

CHAPTER III

DESCRIPTION OF THE EXPERIMENTAL SYSTEM

Single phase heat transfer was studied using ethylene glycol as the test fluid in a 180° bend tube. A sketch of the experimental setup is shown in Figure 2. Since the experimental setup and equipment used are more or less similar to those used by Singh (6), Farukhi (7), and Moshfeghian (5) in their dissertations, some parts of this chapter are taken from these manuscripts.

Description of Components

Test Section

The test section was made of stainless steel type 304. The test section was fabricated from initially-straight tubing. The test section had an outer diameter of 19.05 mm (0.750 in.) and a wall thickness of 1.65 mm (0.065 in.). The other relevant details about the test section are summarized in Table II.

Bonded fiberglass tape was wrapped around the test section in order to insulate it thermally. On top of this several layers of fiberglass wool were wrapped. The outer surface of the test section was then covered with silver-colored vapor seal wrap in order to minimize radiation losses. The test section was electrically isolated from the rest of the system by connecting it with neoprene tubing at each end of the test section.

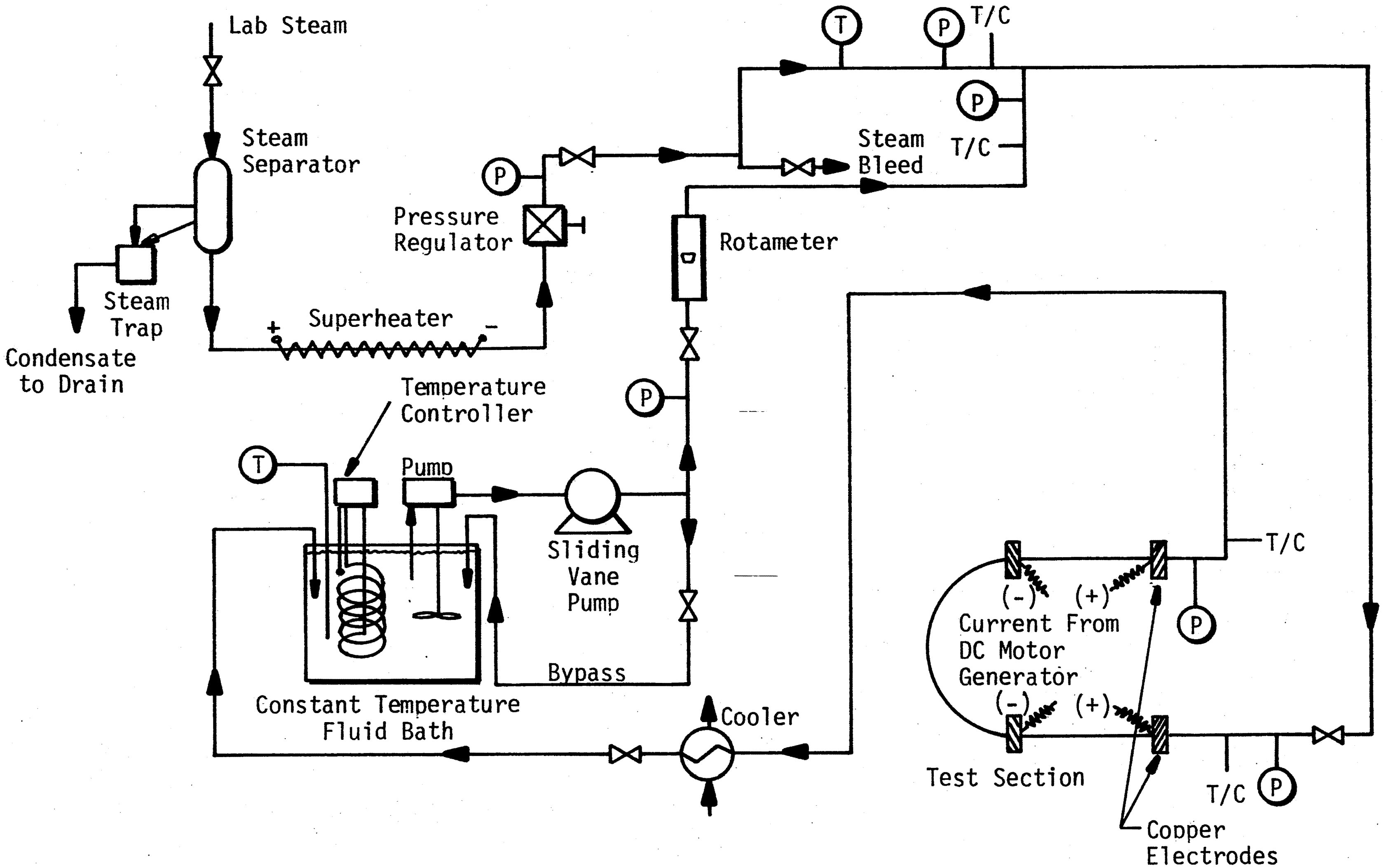

Figure 2. Heat Transfer Loop

TABLE II

SPECIFICATION OF THE TEST SECTION

Material	Bend Radius mm (in.)	Tube Diameters Outside mm (in.)	Inside m (in.)	Straight Section m (in.)	Curvature Ratio R_c/r_i
Seamless Stainless Steel 304	60 (2.375)	19.05 (0.750)	15.75 (0.620)	3.480 (137)	7.66

Two copper bars were silver soldered on the straight sections on either side of the U-bend. The distance between each pair of copper bars was nine feet. DC current was passed through the tube wall such that straight sections on either side of the bend were heated in paralel. In this manner the U-bend portion was not heated.

Experiments were conducted with the U-bend in the vertical plane. Ethylene glycol was pumped into the test section at the bottom and exited at the top.

Fluid Bath

A "Lo-Temprol" 154 constant temperature circulating system type bath was used during the investigation. The bath has a rated capacity of 2.75 gallons. It is controlled by an ultrasensitive micro-set thermo-regulator, a 250-500-1000 watt immersion-type (tape heater) electric heater. The bath allows the set-point to be varied from -10°C to 100°C. A Brooklyn P-M mercury-in-glass thermometer having a range from 0°F to 230°F, graduated in 2°F intervals, was used to measure bath temperature.

The circulating system has a guaranteed accuracy to maintain the bath temperature within 0.06°C of the set-point temperature (8).

Pump

A sliding vane pump manufactured by Eastern Industries, Inc. was used to pump ethylene glycol through the experimental loop. The pump is a positive displacement type and has a rated capacity of 0.273 m^3/hr (1.2 gpm) of water. It has a rated head of 42 m (138 ft).

DC Power Source

A Lincolnweld SA-750 DC generator generated the DC current which was passed to the test section via two silver-soldered copper bars at either side of the test section. The fluid was heated by resistance heating generated on account of the DC current flowing through the tube wall. All the experiments were carried out under approximately constant heat flux conditions. The DC generator has a maximum rated output power of 30 kilowatts.

The reason for choosing DC resistance heating over AC resistance heating are summarized below:

1. The cyclic nature of the AC electrical current may cause cyclic temperature variations in the test section, a condition which is to be avoided at all times. DC heating provides a constant heat source compared to AC heating.

2. Inherent complex AC induction and skin effects are avoided when DC is used.

3. The possible vibrations caused by the cyclic nature of the electrical forces of AC are avoided.

4. The possibility of inducing thermal stresses in the test section on account of the cyclic nature is eliminated.

5. Induced spurious emf effects in the thermocouple wires are avoided.

A motor-generator was used instead of a rectifier because:

1. It was available.

2. A motor-generator provides relatively smooth power output and eliminates large magnitude superimposed sine waves unlike the rectifier.

3. The resistance to overload is better than with rectifiers.

4. The transient voltage peaks that occur in switching the unit on and off are reduced remarkably when a motor-generator is used.

Heat Exchanger

A 1-shell-pass-4-tube-pass heat exchanger manufactured by the Kewanee-Ross Corporation was provided on the downstream side of the test section to cool the test fluid. The shell side fluid was ethylene glycol and tube side fluid was water. Water from the laboratory cooling tap was used. The heat exchanger is a size 502, "BCF" type (9).

Measuring Devices

Insulated wire thermocouples made from 30 B&S gauge copper-constantan were used to measure the inlet and outlet bulk temperatures, and outside wall temperatures of the test section tube. Copper-constantan thermocouples were chosen instead of iron-constantan because:

1. Copper-constantan thermocouple has more resistance to corrosion than iron-constantan.

2. Copper-constantan thermocouple has equal sensitivity as iron-constantan for practical purposes.

3. Copper-constantan thermocouple wire was available. The thermocouples were fabricated in the laboratory using a thermocouple welder.

The thermocouples were placed at eleven stations on the surface along the test section. The position of each station along the test section is shown in Figure 3 and tabulated in Table III. At each station eight thermocouples were placed 45 degrees apart around the tube periphery.

Each of the thermocouples was numbered such that the first number (which ran from 1 to 11) specified station number and the second number (which ran from 1 to 8) specified location of the thermocouple around the tube periphery. Thermocouples at each station were numbered in such a fashion that the number one thermocouple was always on the outside. Thermocouple layouts upstream, in the U-bend, and downstream are shown in Figure 4.

The thermocouples were placed along the test section in the following manner. First, the surface of the test section was cleaned using sand paper. Then a thin layer of Sauereisen cement was placed at the desired location and made smooth using mild to medium sandpaper. The purpose of putting the thin layer of Sauereisen cement on the tube was to electrically insulate the thermocouples. Then the thermocouple wires were placed at the desired location along the tube periphery. The thermocouples were held in place by means of a hose clamp placed about 7 mm to 12 mm from the intended location. In order to prevent any accidental short-circuiting of the thermocouple wire, the duct tape was placed between the hose clamp and the wires. In similar fashion, a second hose

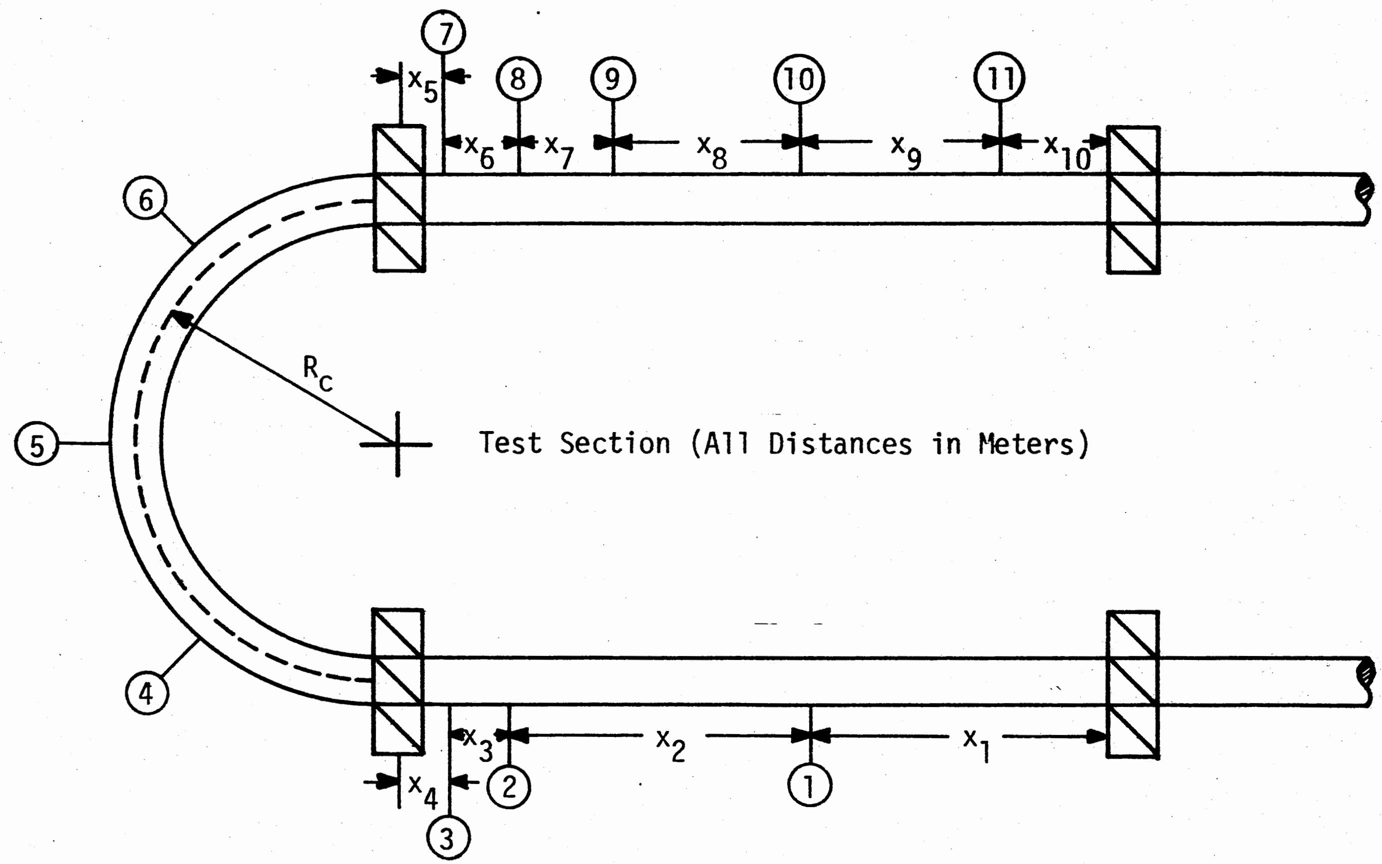

Figure 3. Location of Thermocouple Stations Along Test Section

TABLE III

THE VALUE OF x_i AS SHOWN IN FIGURE 2

Location of Thermocouple Station, meter (ft)									
x_1	x_2	x_3	x_4	x_5	x_6	x_7	x_8	x_9	x_{10}
1.219	1.143	0.325	0.056	0.046	0.335	0.381	0.762	0.762	0.457
(3.999)	(3.750)	(1.066)	(0.184)	(0.1509)	(1.099)	(1.250)	(2.500)	(2.500)	(1.500)

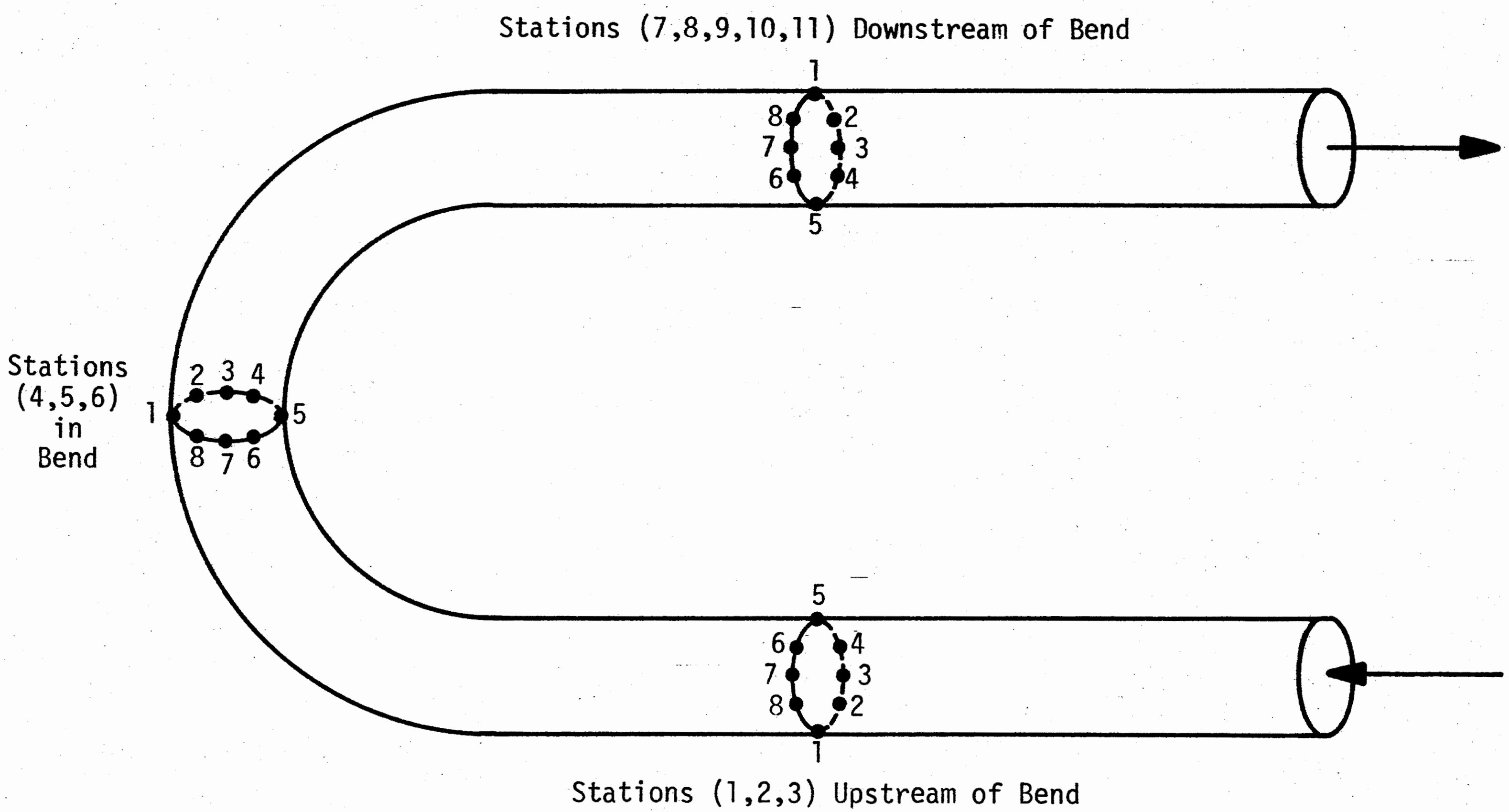

Figure 4. Identification of Test Points in U-Bend Tests

clamp was placed about 5 mm from the first one to hold the thermocouple wires in place. A wire made of iron-constantan was wrapped around the tube periphery in order to hold the thermocouple bead at its intended location. This wire was later removed when the thermocouples were cemented properly in their locations. After the Sauereisen cement was placed on the top of each thermocouple bead, it was assured that the cement patches did not overlap each other. The Sauereisen cement was allowed to dry for about 24 hours. After this the thermocouple wires were led off to the thermocouple selector switchboard.

All outside wall thermocouples were connected to an array of barrier strips which in turn were connected to 13 two-pole non-shorting switches. The rotary switches were mounted on a panel and enclosed in a constant temperature box. The outputs from the rotary switches were brought to a master rotary switch. This was connected to a Type T, model DS 350 Thermocouple Indicator which gave a digital output in °F.

Rotameter

A Brooks "Full-View" rotameter was used to indicate and measure fluid flow rate. The rotameter specifications are given in Table IV.

TABLE IV

ROTAMETER SPECIFICATIONS

Rotameter Model Number	1110-08H2B1A
Rotameter Tube Number	R-8M-25-4
Float Number	8-RV-14
Maximum Water Flowrate, gpm	1.45

DC Ammeter and Voltmeter

The power input to the test section was measured by a Weston model 931 DC ammeter in conjunction with 50 millivolt shunt. The ammeter has a range of 0 to 750 amperes and the voltmeter has a range of 0 to 50 volts.

The voltmeter was connected across the two electrodes connected by a copper strip on either side of the U-bend. The ammeter was connected across the shunt.

The ammeter and voltmeter were calibrated by the manufacturer. They were guaranteed to be accurate with 1 percent of their full range; that is, $\pm$7.5 amperes and $\pm$0.5 volts, respectively. A digital multimeter, model 283-105-130 VAC, manufactured by Dynascan Corporation was used to read voltage drop across the test section.

Mercury-in-Glass Thermometer

Mercury-in-glass thermometers were used to measure the bath fluid temperature and to measure room temperature. The thermometer used to measure fluid bath temperatures had a 0°F to 230°F range, graduated at 2°F intervals. A 23-inch long, 65°F to 90°F ASTM calorimeter thermometer was used to measure the room temperature.

Digital Thermocouple Indicator

A digital thermocouple indicator, Type T, model DS 350 was used to measure thermocouple outputs. The indicator is provided with the capability to convert a thermocouple emf fed to the instrument into its corresponding temperature reading. The reading is displayed directly in °F on the digital readout panel.

The thermocouple indicator has the following stated accuracies: $\pm$0.4°F below 0°F and $\pm$0.3°F above 0°F. The maximum linearization error is less than $\pm$0.1°F (10).

Auxiliary Equipment

All measuring devices except the DC ammeter and voltmeter were calibrated using auxiliary equipment. The DC ammeter and voltmeter had been previously calibrated by the School of Electrical Engineering laboratories at Oklahoma State University.

Rotameter Calibration and Fluid Flow Rate Measurement Equipment

The following accessories were used for rotameter calibration and fluid flow measurement equipment:

1. Stop watch: a 10-minute stop watch with main dial range of 10 seconds was used to time the fluid flow rate. The watch has a precision of 0.1 seconds.

2. Weighing equipment: a 5 kilogram capacity Ohaus Pan Balance was used to weigh the amount of the fluid collected for fluid flow rates less than 1.0 gpm. The balance has a sensitivity of 0.5 grams. A set of calibrated weights was used in conjunction with the balance.

A single-beam platform weighing scale was used to weigh the collected fluid for flow rates greater than 1.0 gpm. The weighing scale has a rated capacity of 300 lbs and an accuracy of 0.125 lb. The beam is graduated in pounds and ounces.

CHAPTER IV

EXPERIMENTAL PROCEDURE

In this chapter calibration, startup, data gathering, and shutdown are described.

Calibration Procedure

Thermocouple Calibration

The insulated copper-constantan wire thermocouples were calibrated in-situ by bleeding saturated steam at about atmospheric pressure from the laboratory steam line. The steam was passed through a separator to remove condensate. Then steam was allowed to pass through the test section at atmospheric pressure. The outlet of the test section was kept open to the atmosphere and the condensate was collected at the outlet. To prevent condensate accumulating inside the bend, the steam was bled through the upper arm of the U-bend (placed in the vertical plane). The calibration run lasted about 12 hours. In addition to this, water at room temperature was also passed through the test section to observe thermocouple response.

After determining atmospheric pressure, the temperature of the saturated steam at that pressure was found from steam tables. Knowing the temperature of the saturated steam, the deviations between saturated steam temperature and the surface thermocouples, and the inlet and outlet thermocouples were determined. Deviations for the surface thermocouples are presented in Table VII (Appendix B). The deviations for inlet and outlet thermocouples were also determined and are given in Table VIII (Appendix B).

The heat loss from the test section was calculated using:

1. Atmospheric pressure and saturated steam temperature at that pressure.

2. The heat of vaporization for steam, found from the steam tables.

3. The condensate mass flow rate. Heat loss calibration data are given in Table IX (Appendix B).

The thermocouple calibration and heat loss calibration data were incorporated into a computer program for calculating heat balances, local heat transfer coefficients, and other pertinent variables for each experimental run.

Rotameter Calibration

A rotameter was used as a guide to set the mass flow rate. At the time of execution of each run the mass flow rate of ethylene glycol was measured by the procedure outlined below:

1. Fluid flow was adjusted to the desired float setting on the rotameter.

2. After steady state was reached, ethylene glycol was collected in a previously weighed empty jar for a set time interval. The time interval varied from fifteen seconds to two minutes, depending on the flow rate.

3. The bath fluid temperature was recorded and was assumed to be the temperature of the fluid in the rotameter.

4. The jar with ethylene glycol was weighed and the weight of ethylene glycol collected was determined, giving the mass flow rate.

Digital Thermocouple Indicator

The Digital Thermocouple Indicator was calibrated periodically as described in section IV of the Owner's Manual (10).

Start-Up Procedure

After the test section was installed, ethylene glycol was passed through the test section to check for possible leaks. The fluid was passed through the test section at the highest possible flow rate. No leaks were found.

The following step-by-step procedure was followed to take the data:

1. The impeller and heater in the fluid bath were activated and the fluid was brought to the desired temperature (80 to 92°F). The test fluid was allowed to pass in the bypass line.

2. Cooling water was started through the heat exchanger.

3. The DC generator was started with the polarity switch in the "off" position. This was allowed to warm up for 30 minutes.

4. The Digital Thermocouple Indicator was turned on.

5. After about 25 minutes, the flow control valve located upstream of the rotameter was opened and the fluid was allowed to flow through the test section. Care was taken to remove all the air bubbles.

6. After about 5 minutes the polarity switch located on the generator motor was switched to "Electro Positive" allowing DC current to pass through the test section. The shunt was adjusted to the desired current.

Data Gathering Procedure

The data gathering procedure consisted of the following steps:

1. The fluid flow rate was adjusted to the desired value.

2. The current to the test section was adjusted to the desired value.

3. Cooling water flow rate was adjusted so that bath temperature stayed at the desired value (between 80° and 92°F).

4. The experimental setup was operated for about one and one-half to two hours to allow the system to achieve steady state. Only minor adjustments were made as deemed necessary in the above variables to keep the system at steady state.

5. Usually after about two to two and one-half hours of operation, steady state was achieved. The following experimental data were taken:

   a. The surface temperatures of the test section.

   b. Inlet and outlet bulk fluid temperatures.

   c. Room and bath temperatures.

   d. The DC current passing through the test section and voltage drop across it.

   e. Mass flow rate of the ethylene glycol.

6. Steady state was assumed to have been achieved if the two sets (after about 30 minutes) of temperature measurements agreed within $\pm$0.3°F. If steady state was not achieved, steps 4 through 5d were repeated until the agreement between two sets of data as defined by the above criterion was satisfied. After steady state was reached, three sets of data were taken for each flow rate. For each run the above procedure was repeated.

Shutdown Procedure

After at least three sets of data were obtained, the following shutdown procedure was followed:

1. The immersion heater located on the constant temperature bath was turned off.

2. The polarity switch was turned to "off" position and the generator was turned off.

3. After about five minutes the fluid flow was shut off (by closing a valve) to the test section. The pump was turned off.

4. The Digital Thermocouple Indicator was turned off.

5. The main power switch was turned off.

6. Cooling water to the heat exchanger was shut off.

CHAPTER V

DATA REDUCTION

Experimental data were obtained using ethylene glycol. Nine runs were made keeping approximately constant heat flux (314 to 332 Btu/hr ft^2). The power input was kept almost constant (1086 to 1153 Btu/hr) to the test section for all runs. The raw experimental data are presented in Appendix A. A computer program was written to reduce experimental data using the IBM 370/158 computer. The computer program listings are presented in Appendix G.

The physical properties measured for each run are listed in item 5 in the data gathering procedure, Chapter IV. The peripheral outside wall temperatures were measured at 11 stations, each station having 8 peripheral positions around the tube. The thermocouple locations are shown in Figure 4.

In order to calculate the inside wall temperature, the thermal conductivity, k, and the resistivity, ρ_e, for stainless steel 304 were evaluated at the outside wall temperature (6). All fluid properties were evaluated at the arithmetic average of the mean inside wall temperature and the bulk fluid temperature unless specified. The bulk fluid temperature was assumed to increase linearly with the distance through the heated portion of the tube. Average bulk fluid temperature for the entire test section was assumed to be the arithmetic average of the inlet and exit bulk fluid temperatures.

The regression correlations developed by Curme were used to evaluate the physical properties of ethylene glycol (11). The regression correlations of these properties are presented in Appendix C. These properties were incorporated into the computer program for data reduction.

Data as outlined in the following steps were reduced:

1. Calculation of percent error in the overall heat balance.
2. Calculation of inside wall temperatures and inside heat fluxes.
3. Calculation of the local heat transfer coefficients.
4. Calculation of the pertinent dimensionless numbers. The dimensionless numbers calculated are presented in Table V.

TABLE V

LIST OF DIMENSIONLESS NUMBERS EVALUATED

Dimensionless Number	Symbol	Definition
Reynolds	Re	$4W/d_i$
Prandtl	Pr	$C_p\mu/k$
Nusselt	Nu	hd_i/k
Graetz	Gz	WC_p/kL
Grashof	Gr	$(d_i)^3(\rho)^2 g\beta(\Delta t)/\mu^2$
Rayleigh	Ra	(Gr)(Pr)
Dean	De	$Re\sqrt{d_i/DC_c}$

Calculation of the Error Percent in Heat Balance

The error percent in the heat balance for each run was calculated as follows:

1. The heat input to the test section was calculated knowing power input to the test section and heat loss from the test section. The heat loss from the test section was determined from calibration data as explained in Table IX (Appendix B).

$$\dot{Q}_{input} = (3.41213)\ (I)\ (V) - \dot{Q}_{loss} \tag{5.1}$$

where

I = current to the test section, amperes;

V = voltage drop across the test section; volts;

$\dot{Q}_{loss}$ = heat loss from the test section, Btu/hr; and

$\dot{Q}_{input}$ = heat input to the test section, Btu/hr.

2. The heat output rate was determined from mass flow rate, inlet and outlet temperatures, and the specific heat evaluated at the average of the inlet and outlet bulk temperatures.

$$\dot{Q}_{output} = WC_p\ [(T_b)_{out} - (T_b)_{in}] \tag{5.2}$$

where

W = mass flow rate of fluid through the test section, lbm/hr;

C_p = specific heat of the fluid, Btu/lbm-°F;

T_{in} = corrected inlet bulk temperature, °F; and

T_{out} = corrected outlet bulk temperature, °F.

3. From the above information the percent error was determined.

$$\text{Percent error} = \left(\frac{\dot{Q}_{input} - \dot{Q}_{output}}{\dot{Q}_{input}}\right) \times 100$$

Calculation of Inside Wall Temperature and Radial Heat Flux

A computer program was written to calculate inside wall temperature and heat flux. Some portions of the computer program were taken from the one written by Owhadi (12), Crain (13), and later modified by Singh (6), Farukhi (7), and Moshfeghian (5). The computer program calculates inside wall temperature and radial heat flux using equations derived by making a shell balance. Appendix D shows the derivation of the equations used in determining inside wall temperatures and inside radial heat fluxes. The computer program listings are presented in Appendix G.

Calculation of the Local Heat Transfer Coefficient

After calculating the inside radial heat flux, the fluid bulk temperature, and the inside wall temperature at each station, the local heat transfer coefficient was determined using the following equation:

$$h_{ij} = \frac{\dot{q}_{r_{ij}}}{[(T_w)_{ij} - (T_b)_i]} \tag{5.3}$$

where

h_{ij} = local heat transfer coefficient, Btu/hr-ft^2-°F;

$\dot{q}_{r_{ij}}$ = local inside radial heat flux, Btu/hr-ft^2;

$(T_w)_{ij}$ = local inside wall temperature, °F; and

$(T_b)_i$ = bulk temperature at station i, °F.

The subscript i denotes the station number and j denotes the peripheral position of the thermocouple.

Calculation of the Pertinent Dimensionless Numbers

The dimensionless numbers calculated at the film temperature (i.e., at arithmetic mean of the average inside wall temperature and the bulk fluid temperature) at each station were Reynolds, Prandtl, Nusselt, Graetz, Grashof, Rayleigh, and Dean numbers. Some of these dimensionless numbers were also calculated at the bulk temperature as required for comparison.

The graph of the peripherally averaged local Nusselt numbers versus the inverse Graetz numbers were plotted. The comparison was made with the classical Graetz solution for a constant heat flux case.

All the experimental data gathered were reduced in the above mentioned fashion. Sample calculations for data run 151 are given in Appendix E.

CHAPTER VI

RESULTS AND DISCUSSION OF RESULTS

Experimental data were gathered for the straight sections of the U-bend. The curvature ratio (R_c/r_i) was 7.66. Ethylene glycol was a test fluid. Reynolds numbers ranged from 62 to 528, while Prandtl numbers ranged from 75 to 132. The results of this study along with a discussion of the results are presented in this chapter.

General Discussion

For each run the following parameters were computed at each thermocouple location.

1. Local heat fluxes.
2. Local heat transfer coefficients.
3. Average local heat transfer coefficients.

These values are summarized in Appendix F for all experiments.

The average local heat transfer coefficient at each station was defined as follows:

$\bar{h}_i$ = average local heat transfer coefficient

$$= \frac{1}{8} \sum_{j=1}^{8} [\dot{q}_{ij}/(T_w)_{ij} - (T_b)_i] \qquad (6.1)$$

$$= \frac{1}{8} \sum_{j=1}^{8} [h_{ij}] \qquad (6.2)$$

where i indicates a station number and j denotes the peripheral position on the tube cross section at the station. The average local heat transfer coefficient obtained using Equation (6.2) was then used to compute the average local Nusselt number for the station. All physical properties of the test fluid in calculating the above dimensionless numbers were evaluated at film temperature unless otherwise specified.

The average local heat transfer coefficient at a station may also be defined as follows:

$$\bar{h}_i^* = [(\bar{\dot{q}}_r)_i / \left((\bar{T}_w)_i - (T_b)\right)_i] \qquad (6.3)$$

where $(\bar{\dot{q}}_r)_i$ and $(\bar{T}_w)_i$ are calculated as follows:

$$(\bar{\dot{q}}_r)_i = \frac{1}{8} \sum_{j=1}^{8} (\dot{q}_{r_{ij}}) \qquad (6.4)$$

and

$$(\bar{T}_w)_i = \frac{1}{8} \sum_{j=1}^{8} (T_{w_{ij}}) \qquad (6.5)$$

The ratio of heat transfer coefficients defined by Equations (6.1) and (6.3) tends to unity as the inside wall temperature becomes uniform. The heat transfer coefficient calculated by Equation (6.1) was always greater than the one calculated by Equation (6.3). However, the ratio never exceeded 1.05.

Peripheral Distribution of the Heat Transfer Coefficient

In order to understand the flow mechanism, the peripheral heat transfer coefficients were plotted against the peripheral positions for stations upstream and downstream of the U-bend.

Straight Section Upstream of the Bend

Figure 5 shows peripheral distribution of the heat transfer coefficient for runs at average local Reynolds numbers of 85 and 528. The average heat fluxes for these runs were 329.3 Btu/(hr-ft^2) and 315.4 Btu/(hr-ft^2).

For a Reynolds number of 85, one observes that there is considerable variation in the heat transfer coefficient around the tube periphery. The heat transfer coefficient at the bottom is much higher than the heat transfer coefficient at the top. Relatively, the observed dip in the peripheral distribution of the heat transfer coefficients is almost the same at all stations and the peripheral distribution of the heat transfer coefficient is almost symmetrical. The observed behavior is typical if natural convection is present.

The above phenomenon can be explained by the fact that the fluid near the wall is warmer, and hence lighter and less viscous than the fluid in the core. As a result, the heavier and colder fluid in the core flows down and the fluid at the bottom flows along the tube periphery upwards. As a consequence, the apparent heat transfer coefficient at the bottom is higher than the one at the top. Natural convection flow mechanisms were also observed by Morcos and Bergles (14) in a circular horizontal tube. The idealized natural free convection flow mechanism observed for the ideal case in a horizontal circular tube is shown in Figure 6.

For a Reynolds number of 528, the peripheral distribution of the heat transfer coefficient is quite uniform compared to that for a Reynolds number of 85. The dip in the peripheral distribution of the heat transfer coefficient has almost vanished. The temperature around the tube

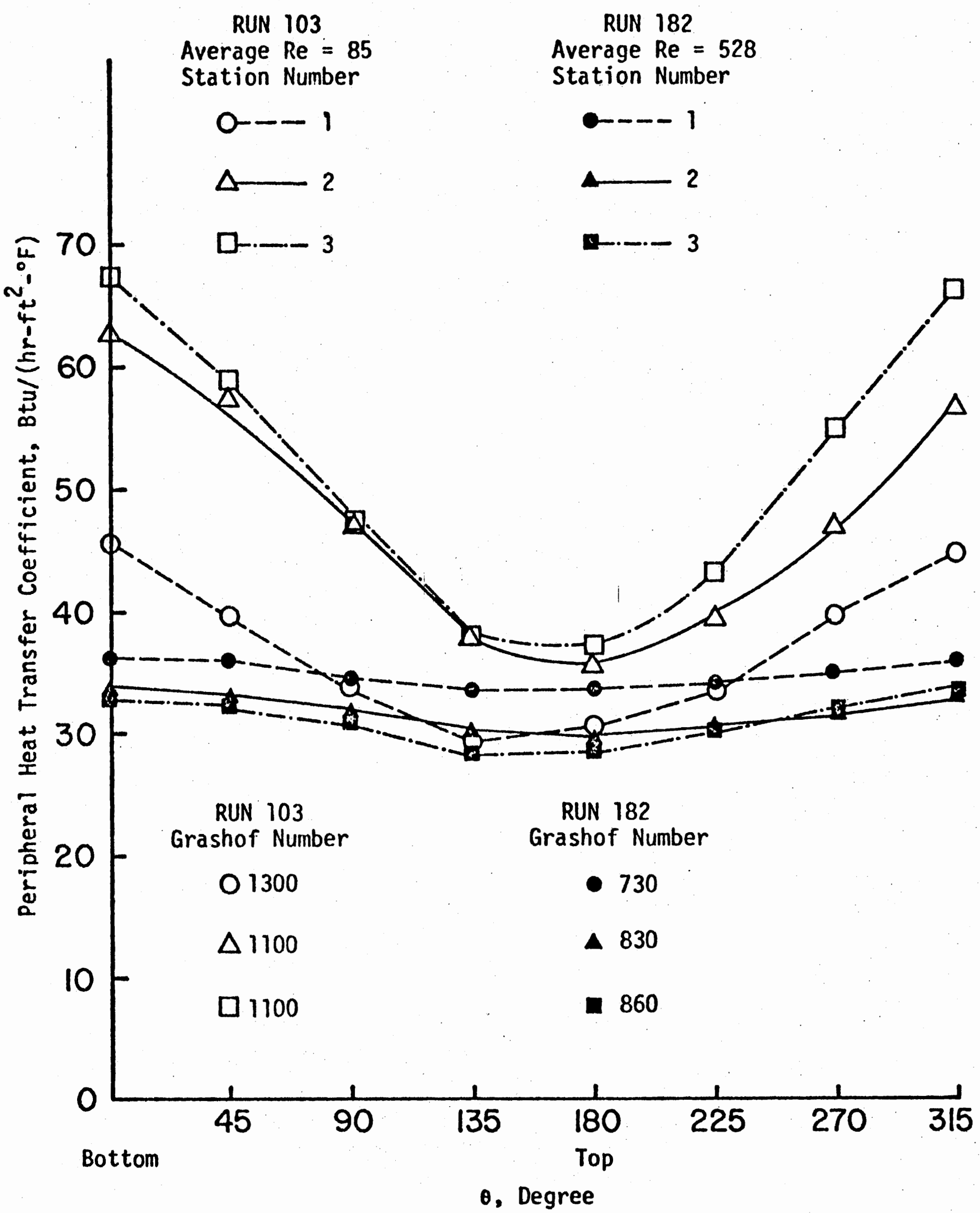

Figure 5. Peripheral Distribution of Heat Transfer Coefficient for Stations Upstream of the U-Bend

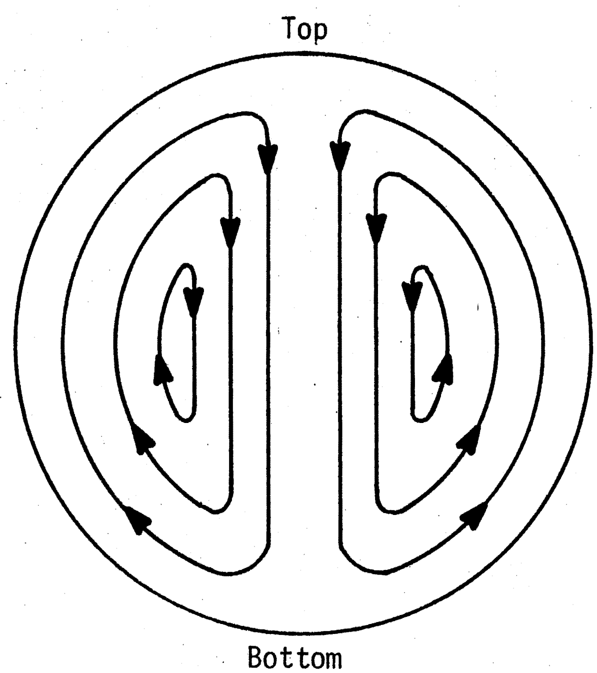

Figure 6. Idealized Natural Convection Flow Patterns Downstream From the U-Bend

periphery is nearly constant (and there is no appreciable [large] difference between fluid near the wall and in the core).

Straight Section Downstream of the Bend

Figures 7 and 8 show the distribution of peripheral heat transfer coefficients downstream of the U-bend.

From Figure 7 (Re 85) one observes that the variation in the peripheral heat transfer is not as significant as for the fluid upstream of the U-bend. The variation in the peripheral heat transfer coefficient grows as the test fluid moves down the tube. The heat transfer coefficient at the bottom increases almost by 50 percent while that at the top only increases by 2 percent. Also, one observes that the heat transfer coefficients at station 7 (where local Dean number is 30.7), immediately following the U-bend, are the lowest (compared to those at any other position down the tube).

From Figure 8 one observes that there is considerable variation in the peripheral heat transfer coefficients immediately following the U-bend. At station 7, the heat transfer coefficient at the top is higher than the peripheral heat transfer coefficient at the bottom. The peripheral heat transfer coefficients are quite uniform at stations 8 through 11 compared to run 103 (for which the Reynolds number is 85). Also, one observes that the heat transfer coefficients immediately following the U-bend (at station 7) are highest compared to those at any other station down the tube. The values of the heat transfer coefficient decrease as the fluid moves down the tube.

The observed trends in the heat transfer mechanism (Figures 7 and 8) can be explained on the following basis.

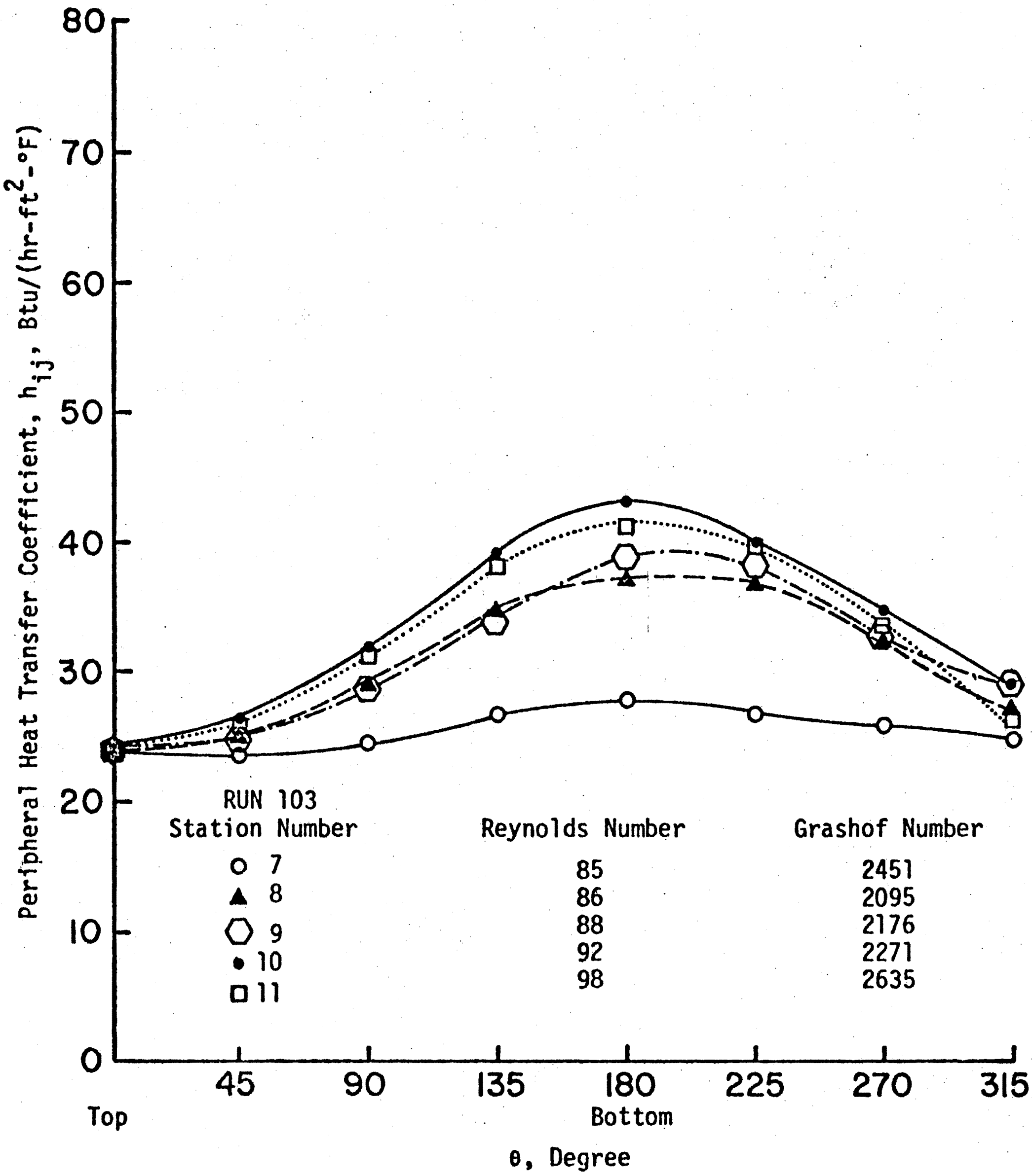

Figure 7. Peripheral Distribution of Heat Transfer Coefficient for Stations Downstream of the U-Bend

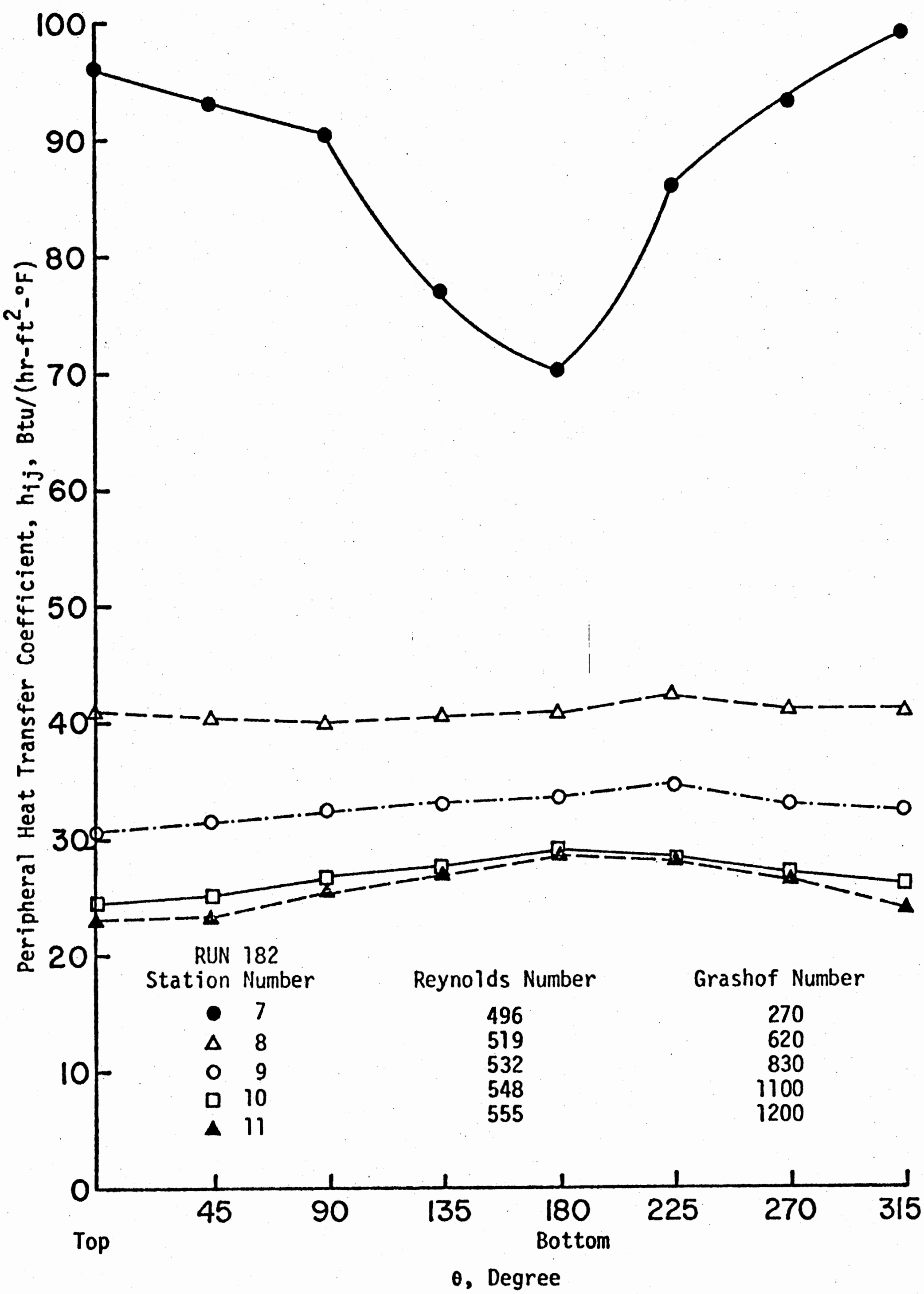

Figure 8. Peripheral Distribution of Heat Transfer Coefficient for Stations Downstream of the U-Bend

The effect of the U-bend is to impose a secondary flow on the primary flow. The secondary flow mechanism for the ideal case is shown in Figure 9. The effect of secondary flow is to move the cold, faster-moving fluid in the core nearer to the wall, while the hot, slower-moving fluid near the wall is moved into the core. The effect of the secondary flow immediately following the U-bend is quite significant even at low Dean numbers. The secondary flow effects are enhanced with increase in Dean number. The secondary flow effects decay as the fluid moves down the tube. Natural convection effects are gradually reconstituted as the fluid moves down the tube. The flow arrangement causes the secondary flow and natural convection to act in opposite directions downstream from the bend.

The above discussed heat transfer mechanisms could be used to explain some facts about Figures 7 and 8.

1. The variation in the peripheral heat transfer coefficients for a Reynolds number of 528 immediately following the U-bend (where the Dean number is 179) is a consequence of the strong secondary flow. The heat transfer coefficient at the top is about 95 Btu/(hr-ft^2-°F) while that at the bottom is 70. The Dean number is 179 and the Grashof number is 270 at station 7.

2. The distribution of the peripheral heat transfer coefficients at stations 8 and 9 is quite uniform, which implies that the contribution of natural convection and secondary flow to the heat transfer processes is equal. However, as the fluid moves down the tube, the effect of secondary flow decays and natural convection increases. This is supported by a change in the Grashof number from 270 (at station 7) to 1200 (at station 11), while the Dean number only changes from 179.3 to 200.5.

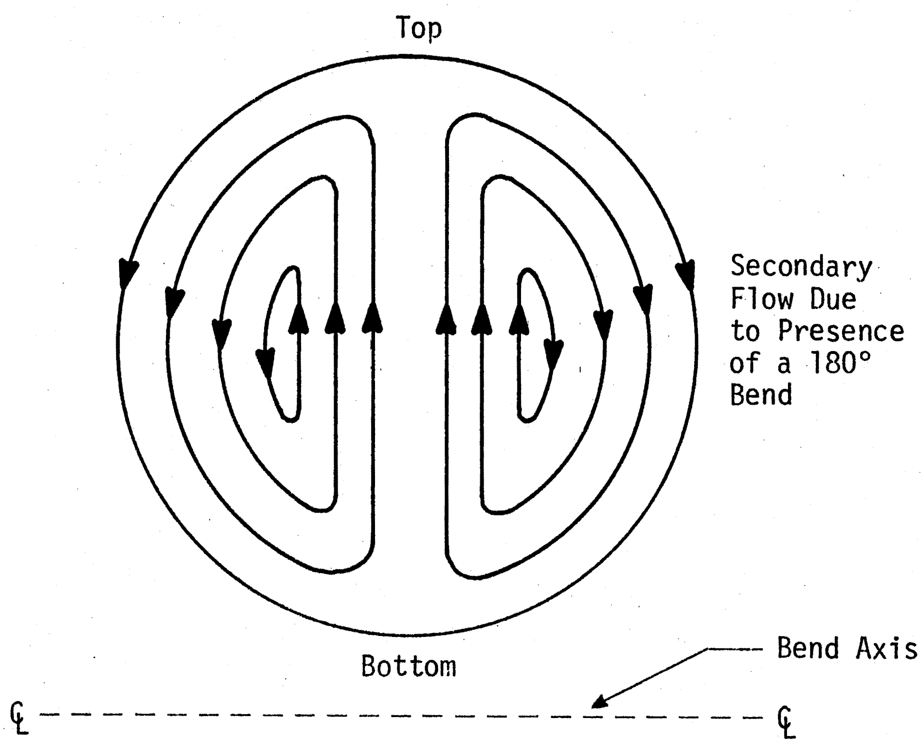

Figure 9. Idealized Secondary Flow Patterns
Downstream From the U-Bend

Effect of Reynolds Number on the Interaction Between Natural Convection and Forced Convection Upstream of the U-bend.

In order to study the effect of the Reynolds number on natural convection and forced convection, the ratio of the heat transfer coefficient at the top of the tube to that at the bottom was plotted against the station number with Reynolds number as a parameter (Figure 10). As the Reynolds number is increased, the ratio of the heat transfer coefficients approaches unity.

The error in the measurement of the heat transfer coefficient depends on the error associated with the measurements of the primary variables like test section current, test section voltage, test section dimensions, inside wall temperature, room temperature, bulk fluid temperature, and accuracy of the Thermocouple Indicator. Based on the error analysis performed by Abul-Hamayel (15), the maximum error in the heat transfer coefficient is estimated to be about 15 percent. After making allowance for the experimental scatter, the following criterion is suggested to determine the comparative significance of natural convection.

$(h_{bottom}/h_{top}) > 1.45$;	natural convection is governing primary flow mechanisms
$(h_{bottom}/h_{top}) < 1.20$	natural convection is significant but not necessarily governing primary flow mechanisms

Effect of Reynolds Number on the Interaction Between Secondary and Natural Convection Downstream of the Bend

Interaction between secondary and natural convection flow downstream

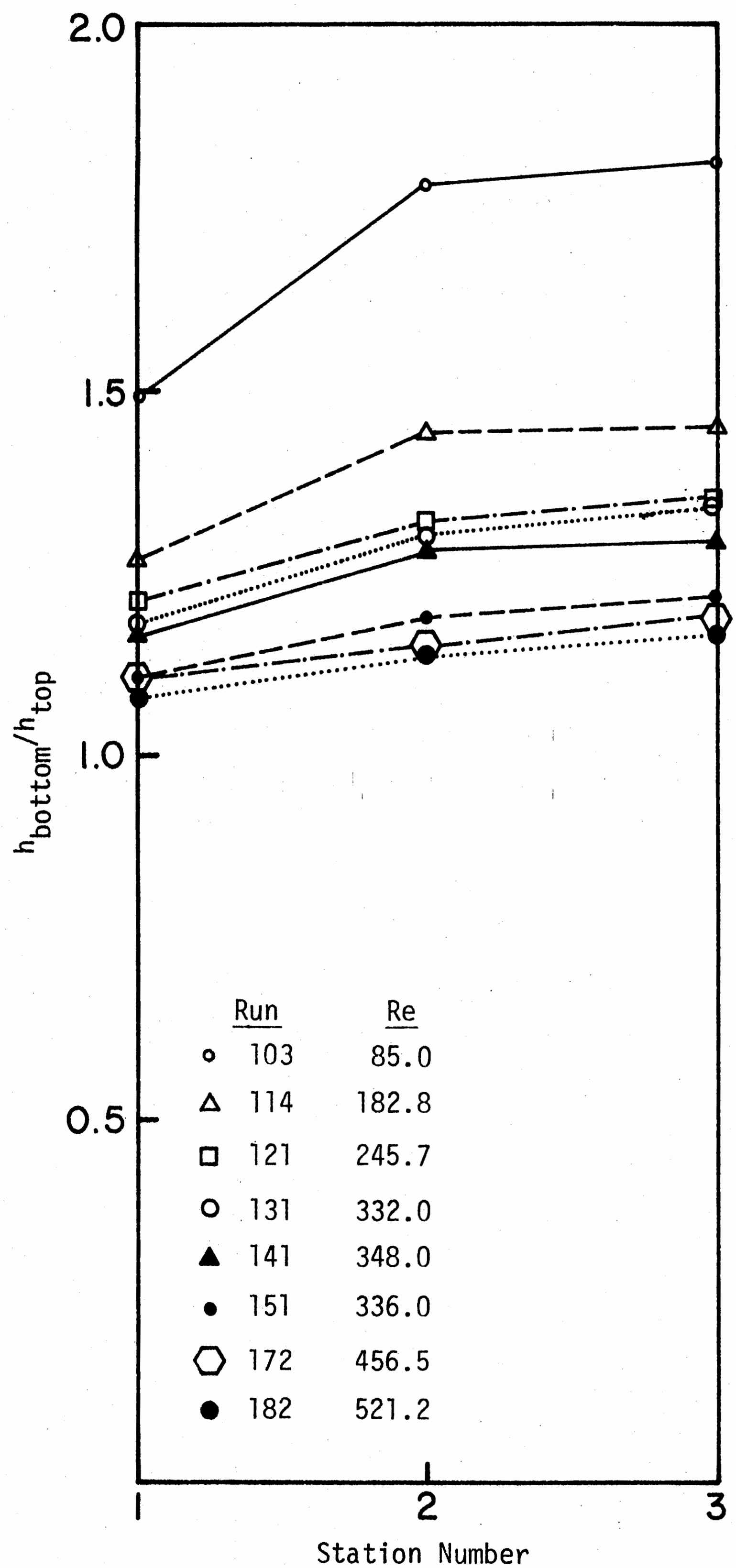

Figure 10. Effect of Reynolds Number on the Interaction Between Forced and Free Convection

of the U-bend depends on the Reynolds number, the ratio of bend radius to tube radius (presumed, but not tested), and the intensity of natural convection upstream of the U-bend. In Figure 11 the ratio of the heat transfer coefficient at the bottom is plotted as a function of station (i.e., axial position) with average Reynolds number as a parameter. One observes that as the Reynolds number is increased, the ratio goes down from 1.16 to 0.73 at station 7 (immediately after the U-bend) and 1.69 to 1.29 at station 11 (farthest from the U-bend). The slope (the ratio of the heat transfer coefficients to the axial position) also gradually decreases with the increase in Reynolds number. As mentioned earlier, this suggests that the secondary flow effects downstream are felt for greater axial distances with an increase in Reynolds number. Values of h_{bottom}/h_{top} greater than 1.3 suggest that natural convection is a major contribution to heat transfer. A ratio of less than 0.8 or 0.9 suggests that the secondary flow is more important. The ratio of unity suggests that the primary flow is a major contribution to heat transfer and the natural convection and the secondary flow are equal in magnitude, giving rise to nearly uniform heat transfer coefficients around the tube periphery. Based on the ratio of the heat transfer coefficient at the bottom to the heat transfer coefficient at the top, the following criterion is proposed:

$h_B/h_T > 1.60$;	natural convection is the governing heat transfer coefficient
$1.3 < h_B/h_T < 1.45$;	natural convection contribution to heat transfer mechanisms is significant
$1.0 \leq h_B/h_T < 1.15$;	natural convection and the secondary flow contribution are nearly equal

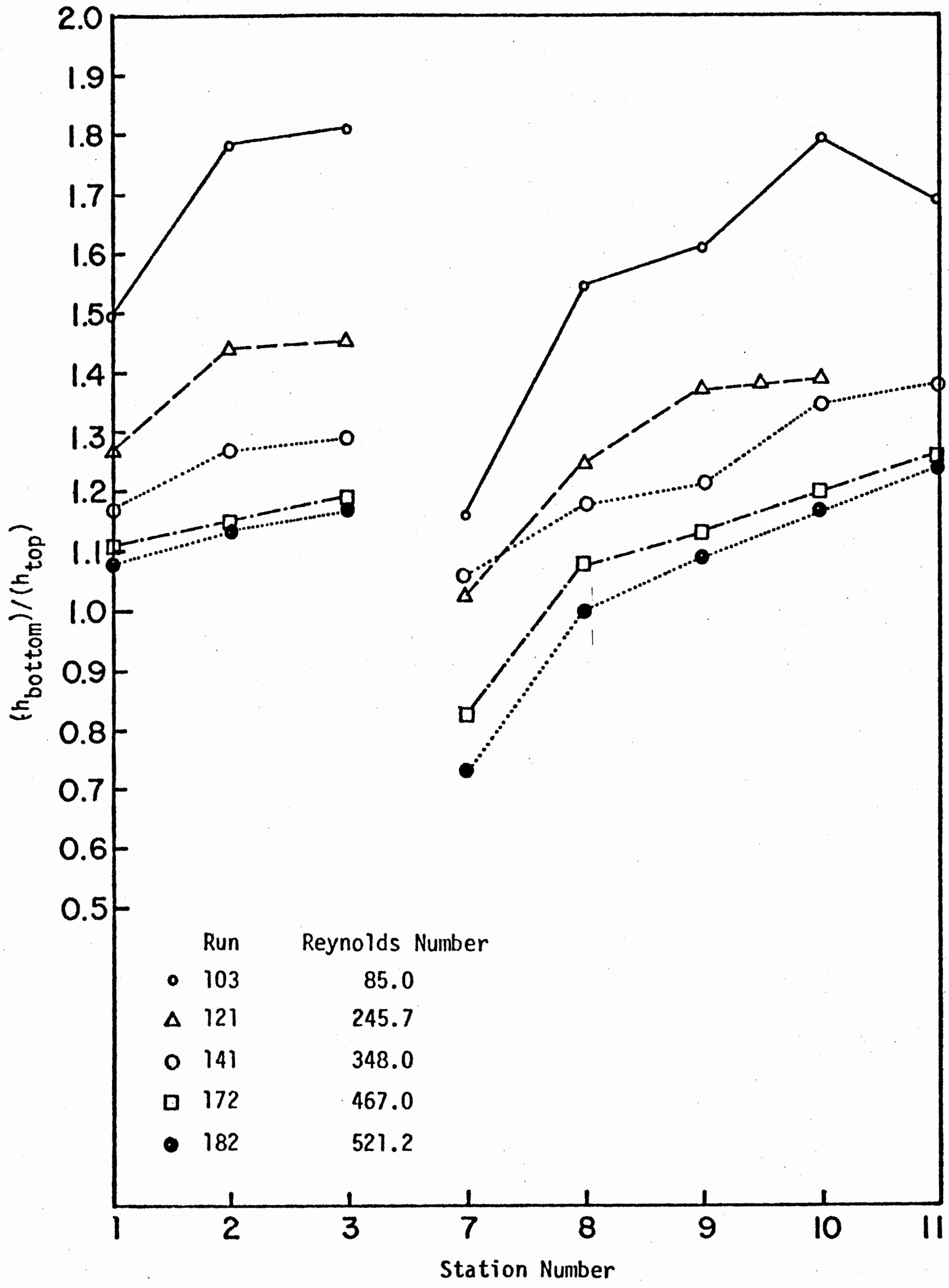

Figure 11. Effect of Reynolds Number on the Interaction Between Natural Convection and Secondary Flow

$0.6 \leq h_B/h_T < 0.85$; secondary flow contribution to heat transfer mechanisms is significant

$h_B/h_T < 0.60$; secondary flow is the governing heat transfer mechanisms

The above mentioned criteria could be useful in determining the heat transfer mechanisms prevailing downstream from the U-bend. This could serve as a guide in the correlation development.

Comparison With Graetz Solution (16)

The peripheral average local Nusselt number was plotted as a function of peripheral average inverse Graetz number. The peripheral average local Nusselt number was calculated using average local heat transfer coefficient defined by Equation (6.2). The comparison has been subdivided into one for points upstream of the U-bend and another for points downstream of the U-bend.

Comparison With the Graetz Solution Upstream of the U-Bend

Figure 12 shows the peripheral average local Nusselt number as a function of peripheral average inverse local Graetz number with the Reynolds number as a parameter. From the graph it is evident that at low Reynolds numbers, the Nusselt number is considerably higher than one obtained by the Graetz solution. At low Reynolds numbers, the Nusselt number is observed to increase (unlike the Graetz solution) as the fluid moves down the tube. The experimental curve approaches the Graetz solution as the Reynolds number is increased. However, the data points fall near the nonconstant Nusselt number region rather than in the constant Nusselt number of the "4.36" region.

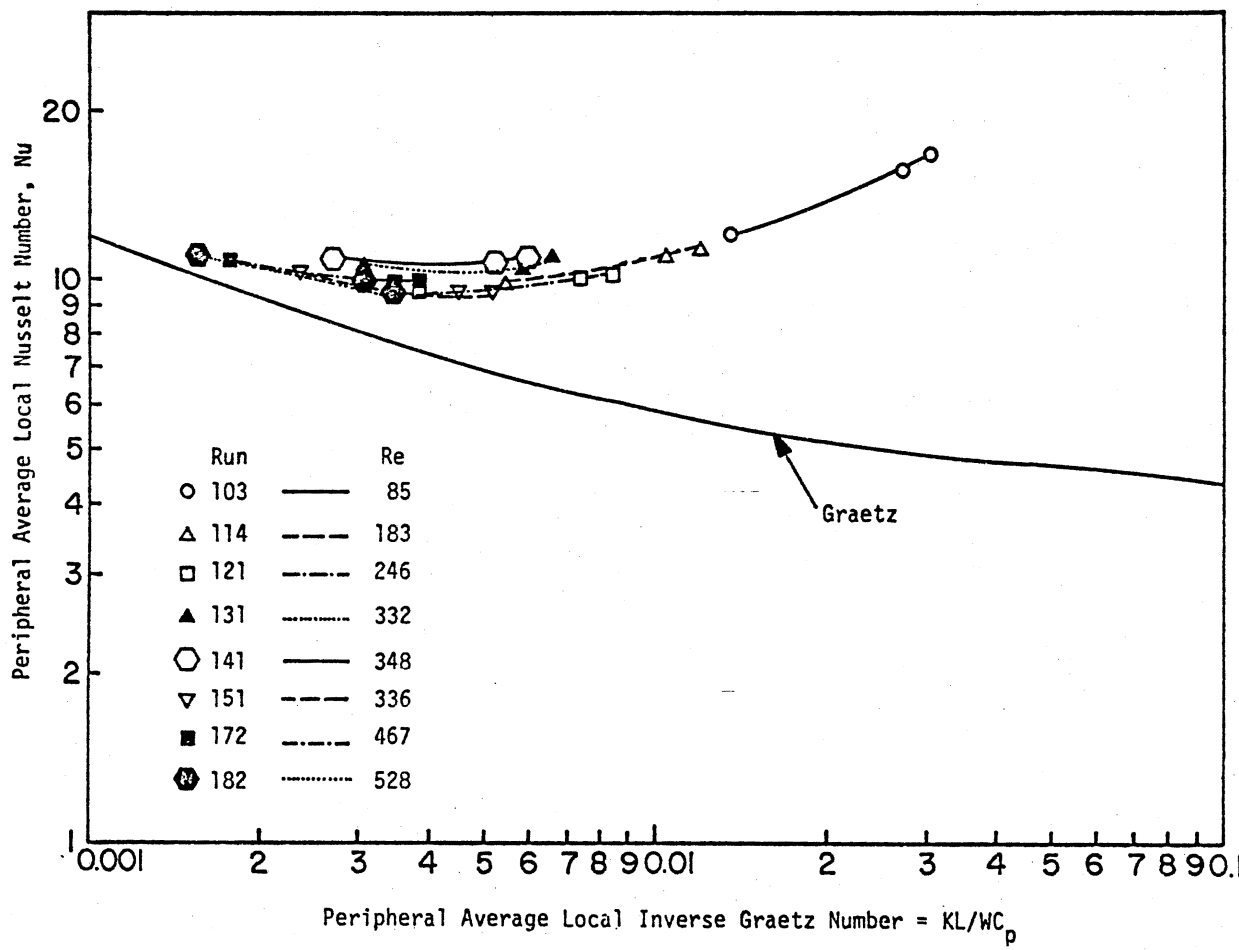

Figure 12. Peripheral Average Local Nusselt Number Versus Peripheral Average Local Inverse Graetz Number for Points Upstream From the U-Bend

This behavior could be explained by the following considerations. The Graetz solution is for fluids with constant density and fully developed velocity profile. However, the assumption of constant density is not valid. The test fluid (ethylene glycol) has a temperature dependent density. The effect of the variation in density with temperature is to cause natural convection (due to density gradients). This alters velocity and temperature profiles, yielding a Nusselt number (heat transfer coefficient) different from one predicted by a constant property assumption. This also accounts for the variation in the heat transfer coefficient. The boundary layer at the surface is also strongly influenced by temperature dependence of the viscosity.

In order to check the relative importance of natural convection and forced convection, the value of Gr/Re^2 was studied. Parker et al. (17) suggest the following criterion to determine the type of heat transfer mechanisms:

1. $Gr/Re^2 \ll 1$, forced convection
2. $Gr/Re^2 \simeq 1$, mixed convection
3. $Gr/Re^2 \gg 1$, free convection.

The criterion Gr/Re^2 revealed the mixed convection at low Reynolds number, and as the Reynolds number was increased the flow was primarily forced convection. This is the reason why the experimental curve tends to agree well (at higher Reynolds number) with the Graetz solution which is valid only in the absence of natural convection. The Grashof number remained nearly constant for all the runs. Reynolds number was the variable.

In Figure 13, h_{bottom}/h_{top} is plotted as a function of Gr/Re^2 with x/d_i as a parameter (for stations upstream of the U-bend). Here x is

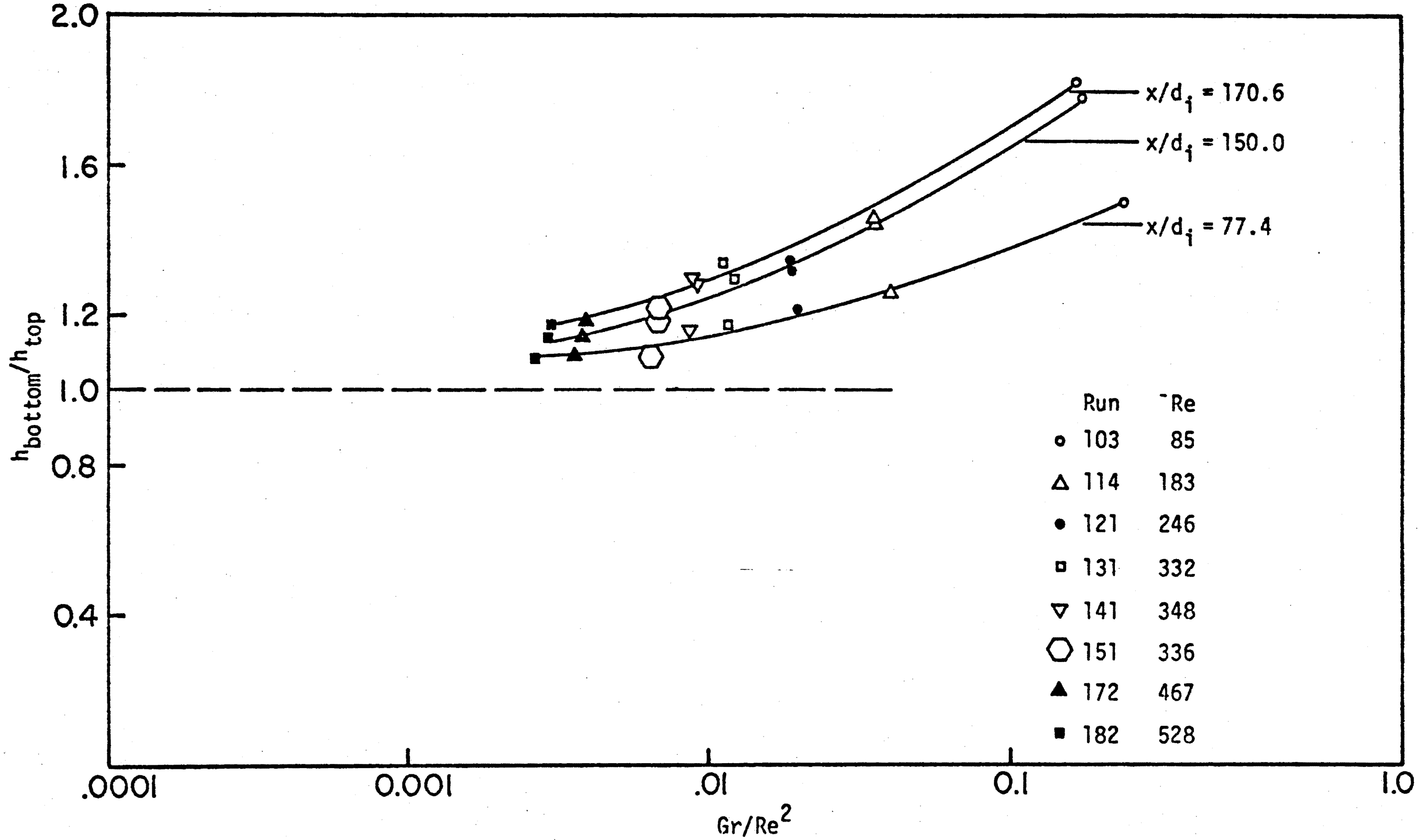

Figure 13. Ratio of the Heat Transfer Coefficients (Bottom to Top) Versus Gr/Re^2 for Stations Upstream of the U-Bend

the distance from the beginning of the heating section. The criterion of h_{bottom}/h_{top} described earlier for the stations upstream of the bend can be used.

Figure 14 shows local Reynolds number as a function of product of Grashof number and Prandtl number. Figure 14 also shows limits suggested by Metais and Eckert (18) (for the case of a horizontal pipe) to determine flow regime. From Figure 14 it is observed that limits suggested by Metais and Eckert do not agree very well with the experimental data. This may be because the limits to determine flow regime (Metais and Eckert) are for the case of a horizontal pipe with a uniform wall temperature. However, Metais and Eckert did suggest that the limits may be adjusted when more results become available.

Comparison With the Graetz Solution Downstream From the U-Bend

Figure 15 shows a comparison between the Graetz solution and reduced experimental data for stations downstream of the U-bend. The heat transfer mechanism downstream from the bend is more complicated because of the interaction between secondary flow and natural convection. It is observed from Figure 15 that (except for the lowest Reynolds number) for all Reynolds numbers, the Nusselt number has a value of about 8. The asymptotic region begins at about a peripheral average inverse Graetz number of 0.002.

The above phenomenon can be understood on the following basis: as mentioned earlier the effect of the U-bend is to throw the (cold) faster moving fluid outwards downstream of the bend, while the (hot) slower moving fluid is moved into the core. As the fluid moves down the tube, the

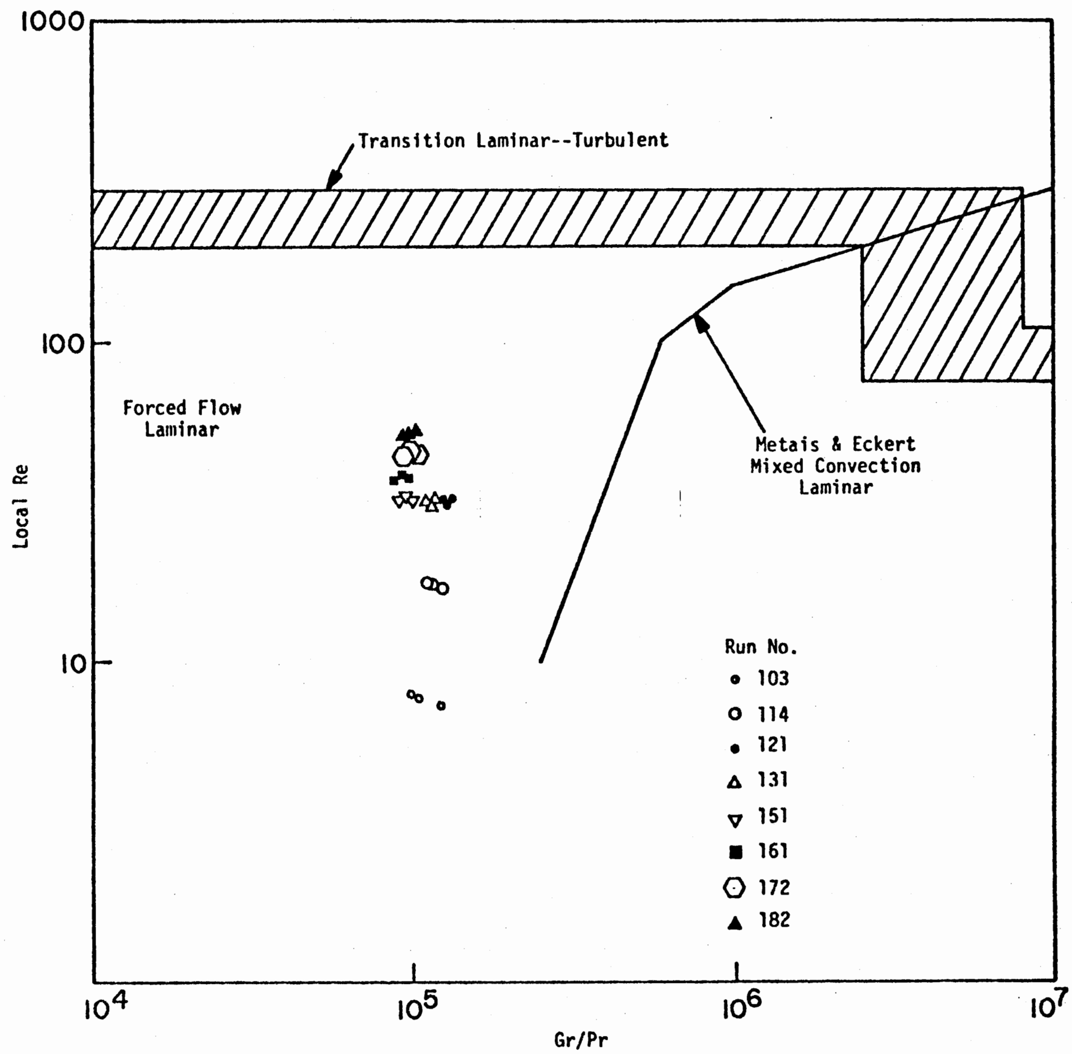

Figure 14. Local Reynolds Number Versus GrPr for the Straight Section Upstream of the U-Bend

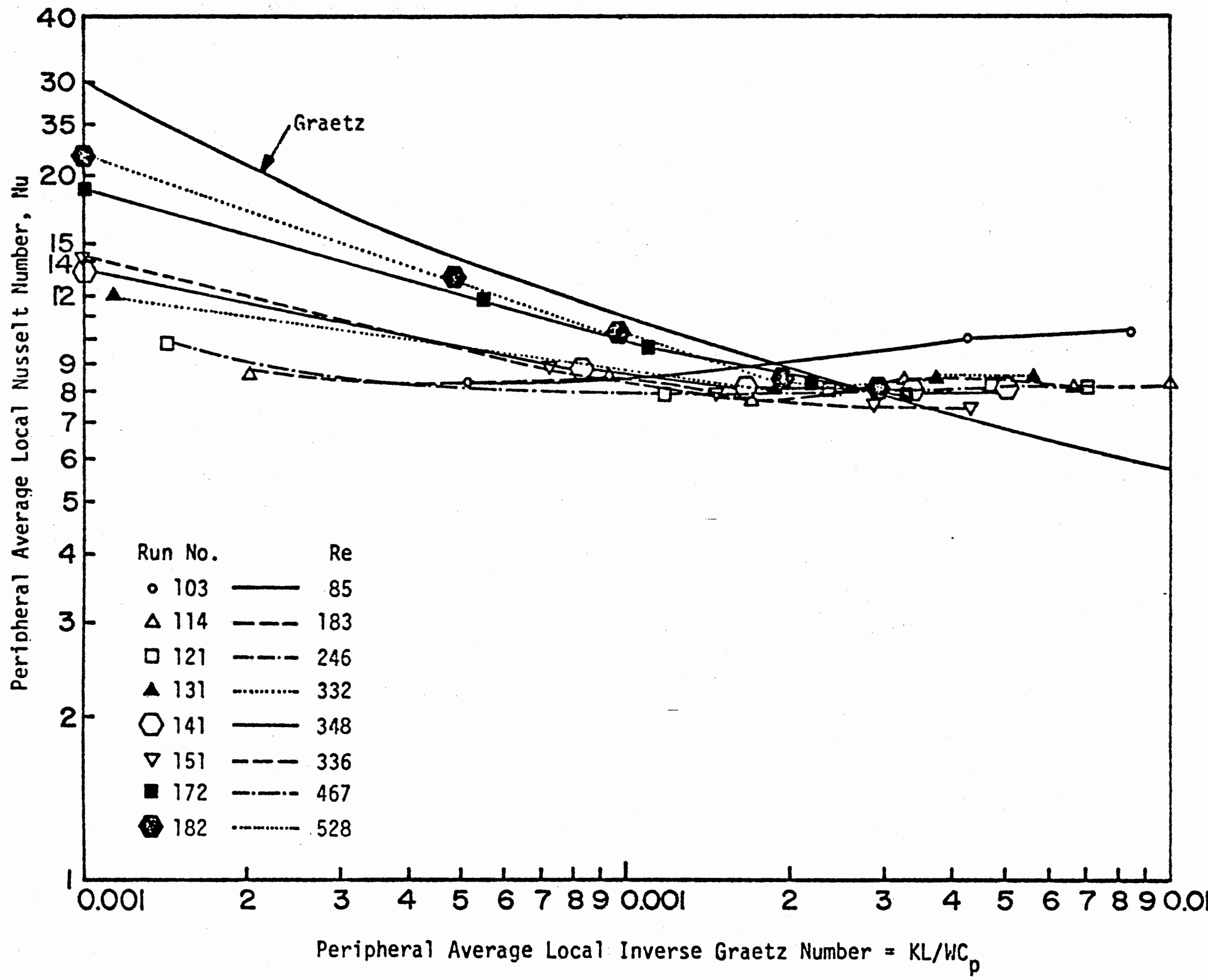

Figure 15. Peripheral Average Local Nusselt Number Versus Peripheral Average Local Inverse Graetz Number for Stations Downstream From the U-Bend

fluid near the wall gets warmer due to constant heat flux at the wall. However, as the fluid moves down the tube (after secondary flow effects have decayed substantially), the temperature difference between bulk and the fluid near the wall tends to remain nearly constant, giving constant Nusselt number. In other words, temperature profile is not altered much and behaves like a fully developed temperature profile case. In order to check this, Grashof numbers were checked for these stations (9 through 11). As expected, Grashof numbers for these stations did not change appreciably (they remained nearly constant). The above behavior may be due to low heat flux at the surface.

In Figure 16, h_{bottom}/h_{top} is plotted as a function of Gr/Re^2 with x/d_i as a parameter. Here x is the distance from the beginning of the heating section on the downstream of the U-bend. The criterion described earlier can be used to determine the relative importance of the flow regimes.

Figure 17 shows local Reynolds number as a function of product of Grashof and Prandtl numbers. Figure 17 also shows limits suggested by Metais and Eckert (18) to determine the flow regime. As discussed earlier, the limits suggested by Metais and Eckert do not agree well with the present study, and need some adjustment.

However, it is predicted that if the heat flux were increased so as to enhance the effect of natural convection, the Nusselt number would increase (as in the case of the lowest Reynolds number). If, on the other hand, the flux were decreased, the effect of secondary flow would be to give higher Nusselt numbers. The experimental data so obtained may agree with or give higher values than the Graetz solution in this case.

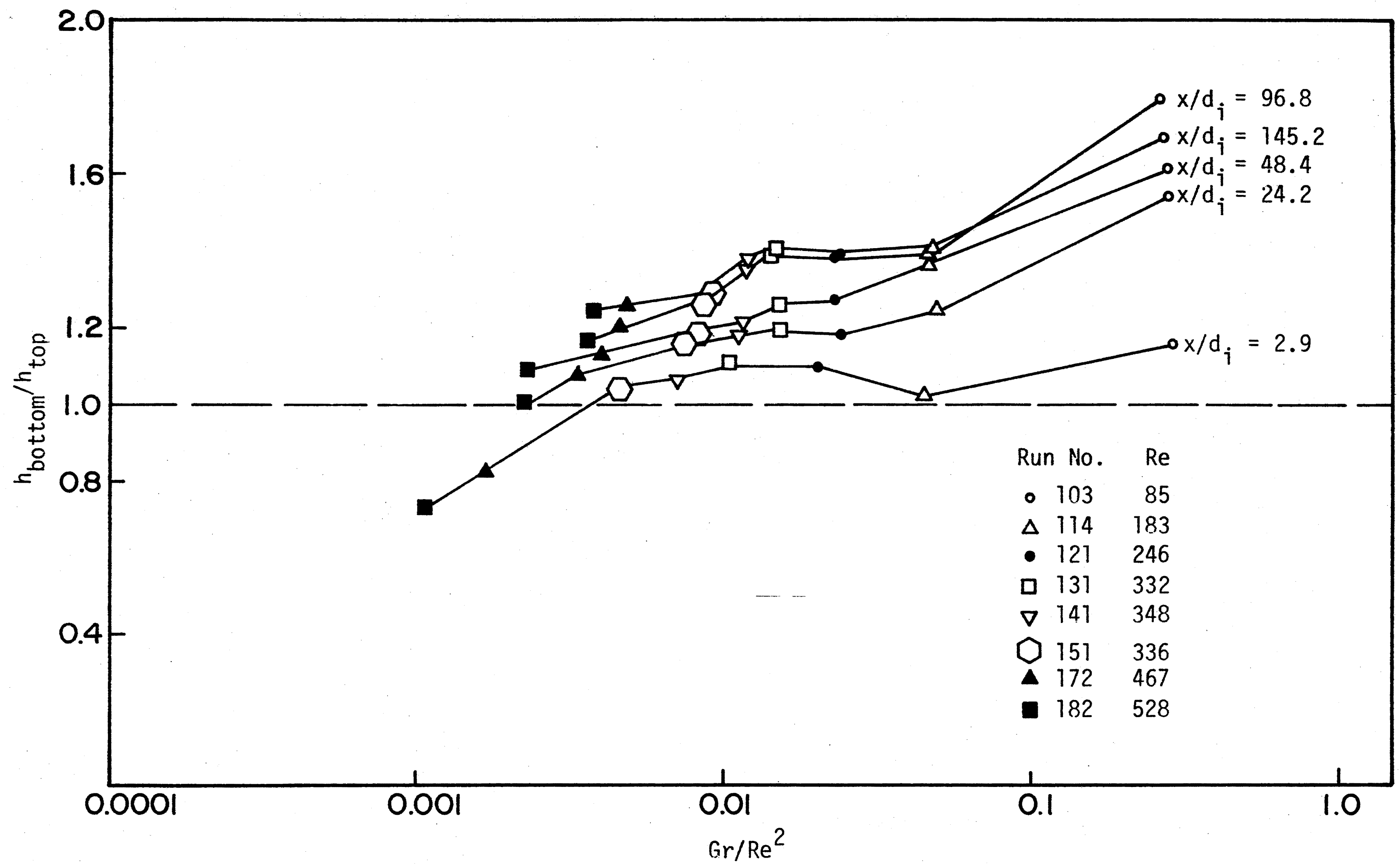

Figure 16. Ratio of the Heat Transfer Coefficients (Bottom to Top) Versus Gr/Re^2 for Stations Downstream of the U-Bend

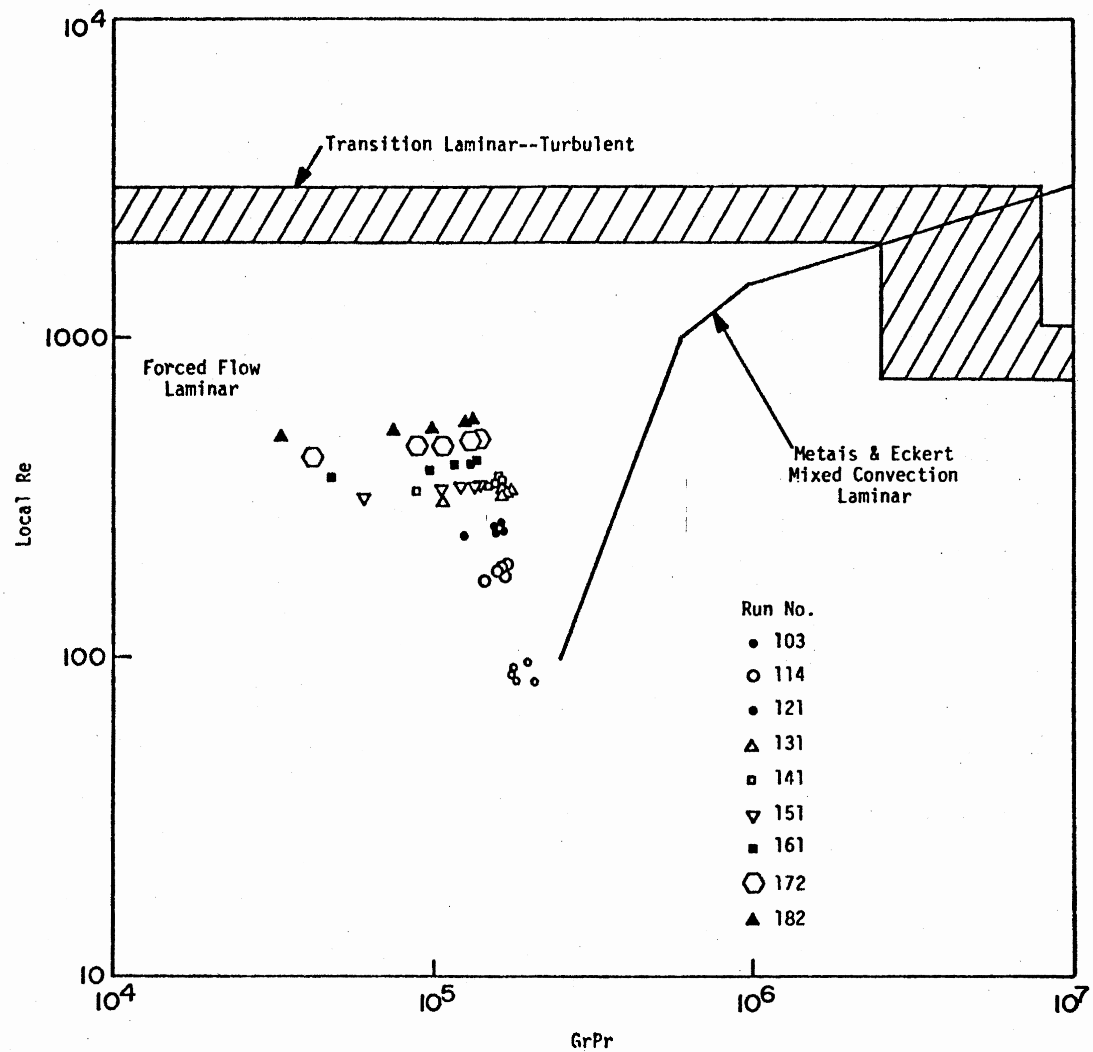

Figure 17. Local Reynolds Number Versus GrPr for the Straight Section Downstream of the U-Bend

Comparison With Morcos-Bergles Correlation

For stations situated upstream of the U-bend, comparison was made with the Morcos-Bergles correlation (14). Figure 18 shows comparison of the Nusselt number predicted by the Morcos-Bergles correlation to that obtained experimentally as a function of axial distance (stations 1 to 3) with average Reynolds number as a parameter. The correlation proposed by Morcos and Bergles (14) is

$$Nu_f = \left\{ (4.36)^2 + \left[0.055 \left(\frac{Gr_f \, Pr_f^{1.35}}{P_w^{0.25}} \right)^{0.4} \right]^2 \right\}^{1/2} \tag{6.6}$$

for

$$3 \times 10^4 < Ra < 10^6, \; 4 < Pr < 1.75, \text{ and } 2 < P_w < 66$$

where

$$P_w = hd_i^2/K_w t \tag{6.7}$$

In Equation (6.7), h is the average local heat transfer coefficient calculated by Equation (6.3), d_i is the inside tube diameter, k_w is the thermal conductivity of the wall, and t is the tube wall thickness. In Figure 15, data are compared only for the range suggested by Morcos and Bergles. The Morcos-Bergles correlation tends to be conservative, but the experimental data agreed quite well within the suggested range.

However, about two-thirds of the experimental data reduced did not meet the criterion of P_w greater than 2.0. Most of the values of P_w ranged from 1.80 to 1.99. For this range the Morcos-Bergles correlation overpredicts the Nusselt number (heat transfer coefficient) by as much as 12 to 20 percent. Thus for the values of P_w less than 2.0 and greater than 1.80, a correlation similar to Morcos-Bergles is proposed.

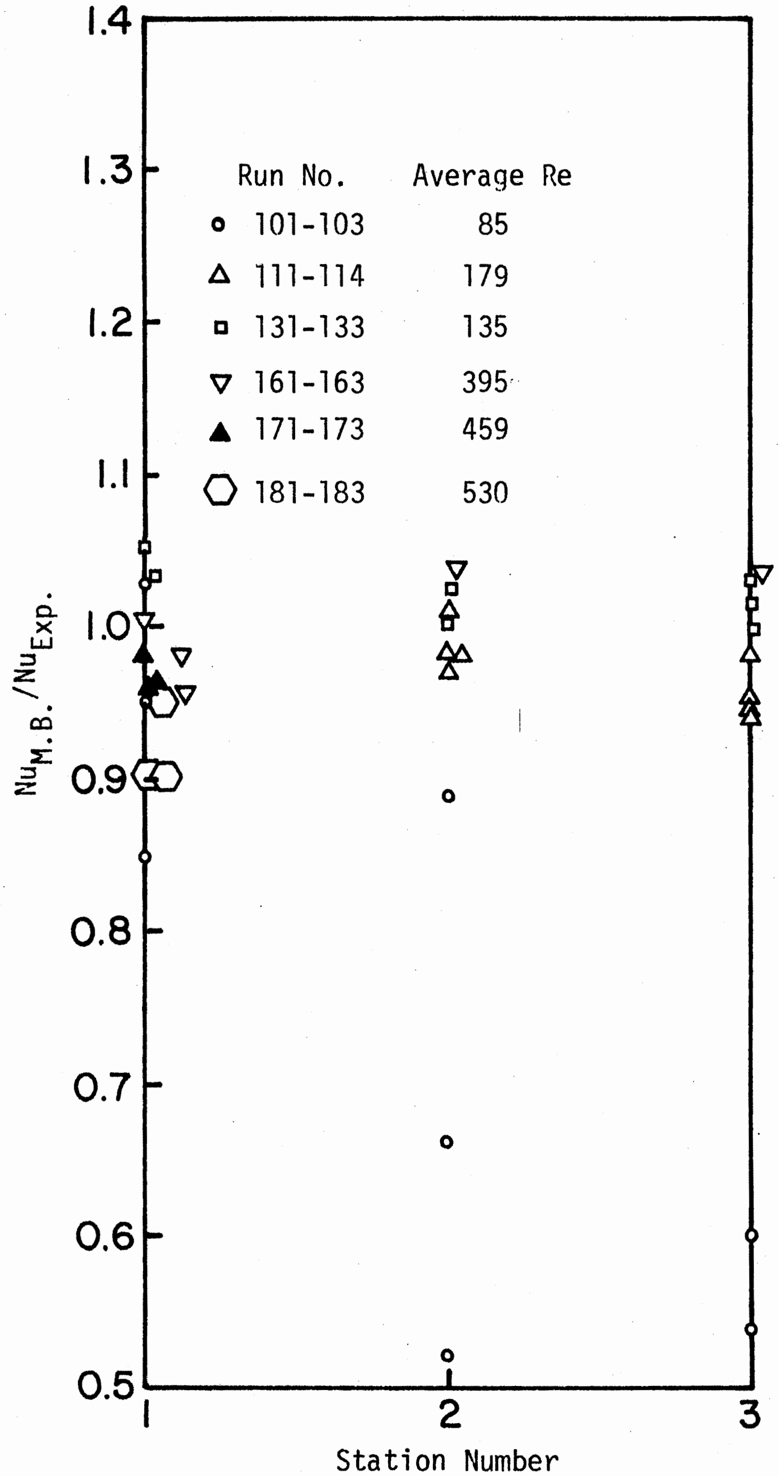

Figure 18. Comparison of Experimental Nusselt Number With That Predicted by Morcos-Bergles Equation

$$Nu_f = \left\{ (4.36)^2 + \left[0.05 \left(\frac{Gr_f \; Pr_f^{\;1.35}}{P_w^{\;0.25}} \right)^{0.4} \right]^2 \right\}^{1/2} \tag{6.8}$$

Figure 19 shows the comparison between values of the Nusselt number obtained by Equation (6.8) to that obtained experimentally. The agreement is fairly good for the data obtained. The above modification predicts a Nusselt number about 10 percent higher than that obtained experimentally for $P_w \leq 1.80$. Hence a precaution needs to be exercised for low values of P_w.

Comparison With Moshfeghian's (5) Correlation

A comparison was made between the Nusselt number predicted by Moshfeghian's (5) correlation and that obtained experimentally for stations located downstream of the U-bend. The correlation suggested by Moshfeghian (5) is

$$J_x = [Re^{\{0.733 + 14.33(R_c/r_i)^{-0.593} (x/d_i)^{-1.619}\}}]$$
$$[1.0 + 8.5\,(Gr/Re^2)^{0.424}][1.0 + 4.79e^{\{-2.11(x/d_i)^{-0.237}\}}] \tag{6.9}$$

where

$$Re \leq 2100, \; \pi/2\,(R_c/r_i) \leq x/d_i \leq 160,$$

and x is the distance from the inlet of the bend (just after the end of the upstream straight section), and

$$J_x = Nu/Pr^{0.4}\,(\mu_b/\mu_w)^{0.14} \tag{6.10}$$

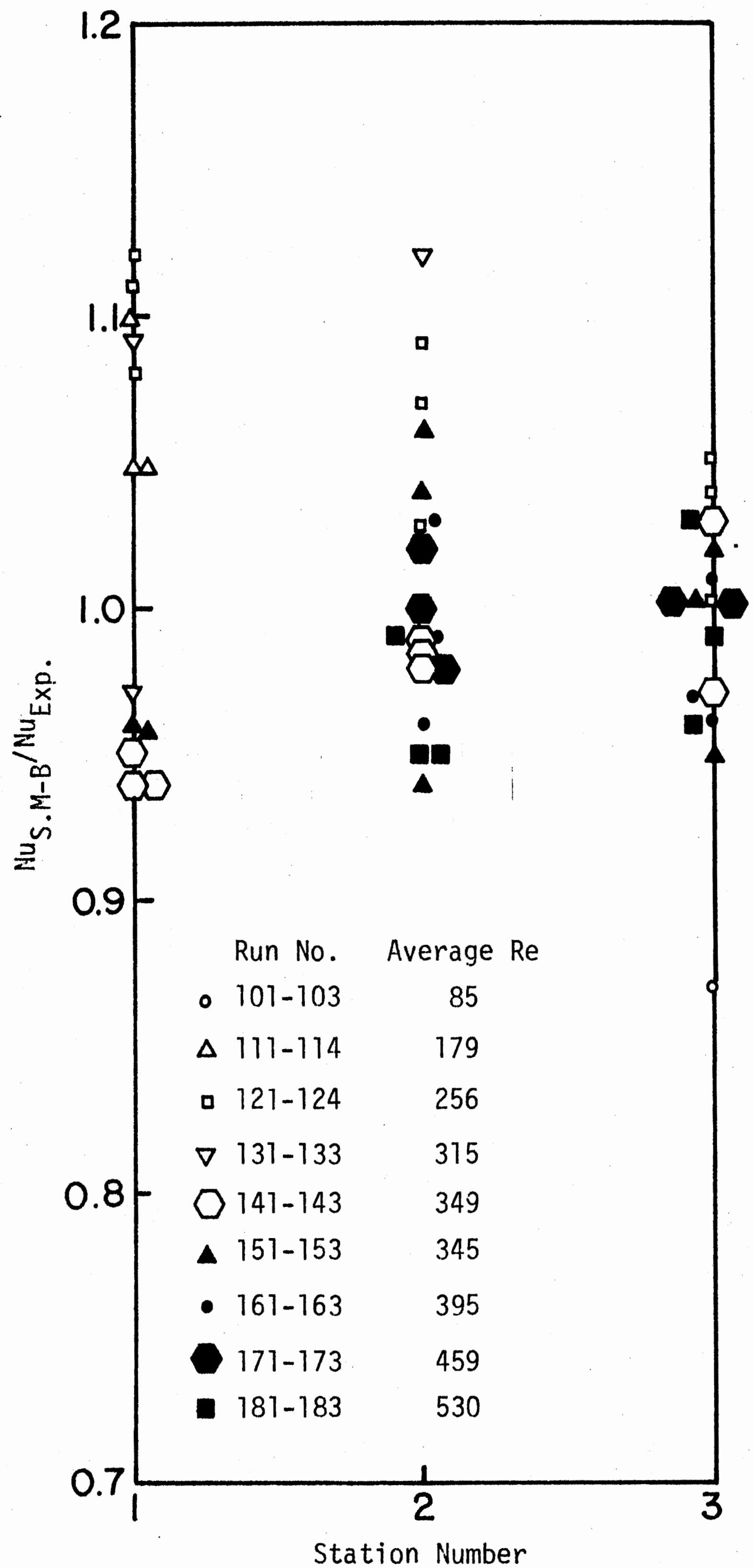

Figure 19. Comparison of Experimental Nusselt Number With the Nusselt Number Predicted by Equation (6.8)

The ratio of the Nusselt number calculated using Equations (6.9) and (6.10) to the experimentally obtained Nusselt number is plotted as a function of axial distance (stations 7 through 11) with the Dean number as a parameter in Figure 20. It is observed from Figure 20 that at the lowest Dean number (about 23), Moshfeghian's correlation gives conservative values of the Nusselt number. The correlation overpredicts the Nusselt number for Dean numbers between 57 to 142 after station 8. At higher Dean numbers (about 155 and above) the correlation gives quite conservative estimates of the Nusselt number up to station 9 (about 60 diameters down the tube), and then overpredicts the Nusselt number (as much as 10 to 40 percent). The overprediction (of the Nusselt number) is seen to increase as fluid moves down the tube after station 8.

In order to explain the above behavior, a detailed examination of parameters measured and calculated by Moshfeghian was made. In the case of Moshfeghian, heat flux was greater than in the present case as much as two to four times. In Moshfeghian's study, the U-bend was heated. Also, the ratio of Gr/Re^2 was observed to increase significantly up to station 9 or 10. Thus in the case of Moshfeghian's contribution of the natural convection to heat transfer process was significantly high, unlike the present study.

Testing of Literature Correlations

The Morcos-Bergles (14) correlation for stations situated upstream of the U-bend and Moshfeghian's (5) correlation for stations situated downstream of the U-bend were tested against the experimental results. The average absolute percent deviation (AADP) was used as a measure to determine the degree of fit of proposed correlations to the experimental

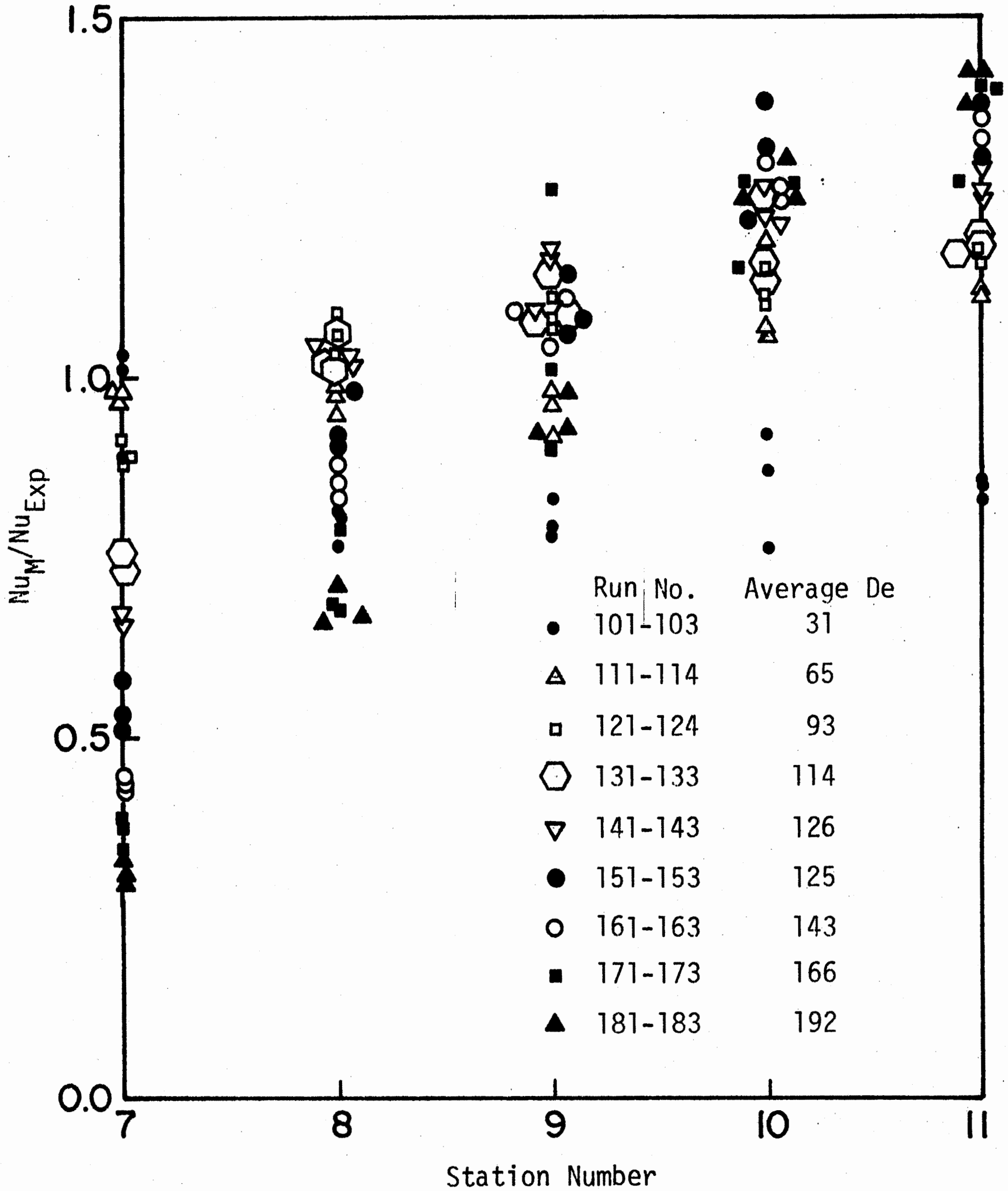

Figure 20. Comparison of Experimental Nusselt Number With Nusselt Number Predicted by Moshfeghian's Correlation

data. Results of the tests are given in Table VI. A total of 32 data points were tested with the Morcos-Bergles correlation, while 135 data points were tested with the Moshfeghian correlation.

The AADP is defined as follows:

$$\mathrm{AADP} = \frac{\sum_{i=1}^{h}\left[\left|\left\{\frac{(\text{Calculated Value})-(\text{Experimental Value})}{(\text{Experimental Value})}\right\}(100)\right|\right]_i}{n} \tag{6.11}$$

where n is the total number of data points evaluated and the summation is performed over all data runs evaluated.

Suggestion for Development of a Correlation

The heat transfer process downstream of the U-bend is a combination of forced flow, secondary flow, and natural convection. The specific effect due to each one of them would be difficult to analyze experimentally. But one may attempt to express the Nusselt number as a product form assuming that these three factors do not interact. The Nusselt number correlation then may be written as

$$\mathrm{Nu} = \begin{pmatrix}\text{forced flow}\\ \text{contribution}\end{pmatrix}\begin{pmatrix}\text{correction factor}\\ \text{for secondary flow}\end{pmatrix}\begin{pmatrix}\text{correction factor}\\ \text{for natural}\\ \text{convection}\end{pmatrix} \tag{6.12}$$

The correction factor for secondary flow may be expressed as

$$[1.0 + f(\mathrm{Re},\ R_c/r_i,\ (x/d_i)]\cdot g(\mathrm{Pr})$$

The correction factor $[1.0 + f(\mathrm{Re},\ R_c/r_i,\ (x/d_i)]$ should approach 1 at low Reynolds number and as the value of (R_c/r_i) tends to infinity. Also, as (x/d_i) increases, the contribution of the secondary flow should

TABLE VI

TEST RESULTS OF LITERATURE CORRELATIONS FITTED TO EXPERIMENTAL DATA

Investigator(s)	Reference	Stated Range of Applicability	AADP (%)	Stations
Morcos-Bergles	(14)	$3 \times 10^4 < Ra < 10^6$ $4 < Pr <$ $2 < P_w < 66$	8.8	1, 2, 3
Moshfeghian	(5)	$\pi/2\ (R_c/r_i) \leq x/d_i \leq 160$ $Re \leq 2100$	20.9	7, 8, 9, 10, 11

decrease. The correction factor should increase proportionately with the Dean number. The criterion of h_{bottom}/h_{top} may be used as a guideline.

The correction factor for the natural convection may be expressed as $[1.0 + f\ (Gr/Re^2)]$. This correction factor will increase with a decrease in the Reynolds number.

CHAPTER VII

CONCLUSIONS AND RECOMMENDATIONS

An experimental study of the single phase (liquid) laminar flow heat transfer processes was conducted in the straight sections upstream and downstream of the U-bend. The test fluid (ethylene glycol) was passed through the U-bend placed in the vertical plane. The radius ratio (R_c/r_i) of the U-bend was 7.66. The straight sections upstream and downstream of the U-bend were heated by DC current through the tube wall. Available literature correlations were tested.

The following conclusions were arrived at as a result of the total study:

1. The effect of natural convection was detected in the straight section upstream of the U-bend. This is due to temperature dependence of fluid density. This dependence caused density gradients around the tube periphery and established natural convection. The net effect is to cause higher heat transfer coefficients at the bottom than at the top. For a given heat flux, the natural convection contribution to the heat transfer process decreases with the increase in the Reynolds number. The average heat transfer coefficients are higher than those predicted by the Graetz solution.

2. The laminar flow heat transfer mechanism downstream of the U-bend is a function of forced convection, natural convection, and the secondary flow.

3. The contribution of secondary flow to the heat transfer process increases with the increase in the Dean number. The intensity of the secondary flow increases with the Dean number and is carried further downstream from the bend. The net effect of the secondary flow is to enhance average local heat transfer coefficients.

4. When the contribution of the natural convection and secondary flow to the heat transfer mechanism is equal in magnitude, nearly uniform heat transfer coefficients around the tube periphery are obtained.

5. The temperature and velocity profiles determined by primary flow are quite sensitive to secondary flow and natural convection.

6. A minor modification in the Morcos-Bergles correlation is proposed for values of the dimensionless number P_w less than 2.0 and greater than 1.80.

There still exist several gaps in the complete understanding of the heat transfer mechanisms downstream of the U-bend. The following recommendations are made based on the present study:

1. In spite of the low heat flux (about 325 Btu/(hr-ft^2), natural convection effects were detected. It is recommended to carry out experiments at still lower heat fluxes. This will help to study the secondary flow contribution to heat transfer processes downstream of the bend. The comparison to the Graetz solution of such experimental data for the section downstream of the U-bend would be helpful in design of double pipe heat exchangers.

2. The experimental data were obtained using only one test fluid and one bend. Further study should be made using several fluids and test sections of various curvature ratios under similar conditions. This would help to produce a more general correlation.

3. The experiments should be conducted by placing the bend in a horizontal plane. However, it is felt that results similar to the present study would be obtained.

BIBLIOGRAPHY

(1) Lis, J., and M. J. Thelwell. "Experimental Investigation of Turbulent Heat Transfer in a Pipe Preceded by a 180° Bend." Proc. Inst. of Mech. Engrs., V. 178, Pt. 3I (1963-64), p. 17.

(2) Ede, A. J., "The Effect of a 180° Bend on Heat Transfer to Water in a Tube." Third Intl. Heat Transfer Conf., Chicago, Ill., V. 1, 1966, p. 99.

(3) Ito, H. "Friction Factors for Turbulent Flow in Curved Pipes." Trans., Journal of Basic Engineering, ASME, D81 (1959), p. 123.

(4) Staddon, P. W., and S. R. Tailby. "The Influence of 90° and 180° Pipe Bends on Heat Transfer from an Internally Flowing Gas Stream." Fourth Intl. Heat Transfer Conf., Paris-Versailles, V. 2, FC4.5, 1970.

(5) Moshfeghian, M. "Fluid Flow and Heat Transfer in U-Bends." (Unpublished Ph.D. thesis, Oklahoma State University, Stillwater, Oklahoma, 1978.)

(6) Singh, S. P. "Liquid Phase Heat Transfer in Helically Coiled Tubes." (Unpublished Ph.D. thesis, Oklahoma State University, Stillwater, Oklahoma, 1973.)

(7) Farukhi, M. N. "An Experimental Investigation of Forced Convective Boiling at High Qualities Inside Tubes Preceded by 180 Degree Bends." (Unpublished Ph.D. thesis, Oklahoma State University, Stillwater, Oklahoma, 1974.)

(8) Precision Scientific Company Catalog 65, October, 1967.

(9) American Radiator and Standard Sanitary Corp. Ross Type BCF Exchanger Bulletin 1.1 KG, 1975.

(10) Digital Thermocouple Indicators Owner's Manual. Manual 350-4440-03. San Diego, Calif.: Doric Scientific.

(11) Curme, G. O., Jr., and F. Johnston, eds. Glycols. New York: Reinhold Publishing Corporation, 1952.

(12) Owhadi, A., K. J. Bell, and B. Crain, Jr. "Forced Convection Boiling Inside Helically Coiled Tubes." Intl. J. of Heat and Mass Transfer, V. 11 (1968), p. 1779.

(13) Crain, Berry, Jr. "Forced Convection Heat Transfer to a Two-Phase Mixture of Water and Steam in a Helical Coil." (Unpublished Ph.D. thesis, Oklahoma State University, Stillwater, Oklahoma, 1973.)

(14) Morcos, S. M., and A. E. Bergles. "Experimental Investigation of Combined Forced and Free Convection in Horizontal Tubes." Trans., J. of Heat Transfer, ASME (1975), p. 212.

(15) Abul-Hamayel, Mohammad A. "Heat Transfer in Helically Coiled Tubes With Laminar Flow." (Unpublished Ph.D. thesis, Oklahoma State University, Stillwater, Oklahoma, 1979.)

(16) Graetz, L. Ann Physik, 18, 77 (1883), and 25, 337 (1885).

(17) Parker, J. D. et al. Introduction to Fluid Mechanics and Heat Transfer. Reading: Addison-Wesley Publishing Company, Inc., 1974.

(18) Metais, B., and E. R. G. Eckert. "Forced, Mixed, and Free Convection Regimes." Trans., J. of Heat Transfer, ASME, V. 86, Series C, No. 2 (1964), p. 295.

APPENDIX A

EXPERIMENTAL DATA

Only those experimental data which were referred to are presented here. The rest of the experimental data are available from:

School of Chemical Engineering
Oklahoma State University
Stillwater, OK 74074

Attn: Dr. Kenneth J. Bell

RUN NUMBER 103

FLUID MASS FLOW RATE	=	78.58	LBM/HOUR
UNCORRECTED INLET BULK TEMPERATURE	=	88.60	DEGREES F
UNCORRECTED OUTLET BULK TEMPERATURE	=	110.70	DEGREES F
VOLTAGE DROP IN THE TEST SECTION	=	2.07	VOLTS
CURRENT TO THE TEST SECTION	=	162.50	AMPS
ROOM TEMPERATURE	=	83.00	DEGREES F
BULK BATH TEMPERATURE	=	91.00	DEGREES F

OUTSIDE SURFACE TEMPERATURES - DEGREES F

	1	2	3	4	5	6	7	8	9	10	11
1	100.8	103.5	104.5	99.5	98.0	102.8	113.9	115.2	116.8	119.8	122.8
2	101.9	104.0	105.2	100.1	98.0	102.7	114.0	114.5	116.3	118.6	122.2
3	103.3	105.2	106.6	101.3	98.7	102.5	113.6	112.7	114.3	116.5	119.9
4	104.8	107.0	108.3	105.7	100.2	102.7	112.4	110.9	112.6	114.5	117.8
5	104.4	107.6	108.5	106.0	101.2	102.7	111.9	110.3	111.5	113.7	117.2
6	103.5	106.6	107.3	104.3	100.1	102.3	112.4	110.4	111.6	114.4	117.4
7	101.9	105.3	105.6	101.2	98.8	102.4	112.8	111.6	113.0	115.6	119.2
8	101.0	104.1	104.6	100.0	98.0	102.3	113.5	113.6	114.3	117.5	121.8

RUN NUMBER 114

FLUID MASS FLOW RATE	=	205.00	LBM/HOUR
UNCORRECTED INLET BULK TEMPERATURE	=	84.90	DEGREES F
UNCORRECTED OUTLET BULK TEMPERATURE	=	93.60	DEGREES F
VOLTAGE DROP IN THE TEST SECTION	=	1.99	VOLTS
CURRENT TO THE TEST SECTION	=	160.00	AMPS
ROOM TEMPERATURE	=	89.80	DEGREES F
BULK BATH TEMPERATURE	=	90.00	DEGREES F

OUTSIDE SURFACE TEMPERATURES - DEGREES F

	1	2	3	4	5	6	7	8	9	10	11
1	96.1	96.6	97.0	89.2	88.1	91.5	101.5	104.2	105.2	106.8	108.0
2	96.8	97.0	97.5	89.7	88.2	91.4	101.6	104.2	104.4	105.8	107.5
3	97.8	97.9	98.7	90.7	88.6	91.5	101.6	103.5	103.2	104.3	105.5
4	98.9	99.5	100.4	94.5	89.9	91.7	101.4	102.4	102.1	103.0	104.2
5	98.6	100.1	100.5	94.9	90.8	92.0	101.1	101.3	101.2	102.6	103.7
6	97.9	99.2	99.3	93.2	89.7	91.6	100.9	101.2	101.0	102.9	103.8
7	96.8	98.0	97.7	90.4	88.7	91.4	100.8	102.0	102.5	103.8	104.6
8	96.2	97.2	97.0	89.3	88.1	91.2	101.0	103.2	103.4	105.2	107.1

RUN NUMBER 121

FLUID MASS FLOW RATE	=	293.04	LBM/HOUR
UNCORRECTED INLET BULK TEMPERATURE	=	83.00	DEGREES F
UNCORRECTED OUTLET BULK TEMPERATURE	=	88.90	DEGREES F
VOLTAGE DROP IN THE TEST SECTION	=	2.03	VOLTS
CURRENT TO THE TEST SECTION	=	162.50	AMPS
ROOM TEMPERATURE	=	85.10	DEGREES F
BULK BATH TEMPERATURE	=	87.00	DEGREES F

OUTSIDE SURFACE TEMPERATURES - DEGREES F

	1	2	3	4	5	6	7	8	9	10	11
1	94.2	94.8	95.0	86.5	85.2	86.6	97.4	100.9	102.0	102.9	103.9
2	94.7	95.1	95.5	87.0	85.2	86.7	97.4	100.7	101.5	102.0	103.4
3	95.5	95.9	96.6	87.8	85.7	87.2	97.2	100.1	100.6	100.5	101.5
4	96.6	97.3	98.0	92.4	87.3	87.9	96.6	99.3	99.9	99.3	100.1
5	96.3	97.8	98.2	92.8	88.5	88.3	96.3	98.7	98.7	98.7	99.7
6	95.7	97.0	97.0	90.8	87.2	87.7	96.4	98.4	98.2	99.2	99.8
7	94.9	95.9	95.7	87.8	85.9	86.9	96.6	98.9	99.4	100.0	100.7
8	94.4	95.1	95.0	86.8	85.2	86.5	96.9	99.9	100.2	101.4	103.0

RUN NUMBER 131

FLUID MASS FLOW RATE	=	366.18	LBM/HOUR
UNCORRECTED INLET BULK TEMPERATURE	=	88.10	DEGREES F
UNCORRECTED OUTLET BULK TEMPERATURE	=	93.00	DEGREES F
VOLTAGE DROP IN THE TEST SECTION	=	2.01	VOLTS
CURRENT TO THE TEST SECTION	=	162.50	AMPS
ROOM TEMPERATURE	=	89.80	DEGREES F
BULK BATH TEMPERATURE	=	94.00	DEGREES F

OUTSIDE SURFACE TEMPERATURES - DEGREES F

	1	2	3	4	5	6	7	8	9	10	11
1	98.5	99.2	99.1	90.9	89.9	90.6	99.9	104.6	106.1	107.0	107.8
2	98.9	99.5	99.5	91.3	90.0	90.7	99.9	104.4	105.7	106.1	107.2
3	99.6	100.2	100.5	92.0	90.5	91.2	99.8	103.7	104.7	104.7	105.3
4	100.4	101.5	101.8	96.6	92.0	92.2	99.3	102.9	104.0	103.4	103.9
5	100.2	101.9	102.0	97.1	93.3	92.7	99.0	102.4	103.0	102.7	103.4
6	99.7	101.2	100.8	95.0	91.9	92.0	99.0	102.3	102.7	103.1	103.5
7	99.0	100.3	99.7	91.8	90.7	91.0	99.2	102.8	103.4	103.9	104.7
8	98.6	99.6	99.1	91.0	90.1	90.6	99.4	103.8	104.1	105.2	106.7

RUN NUMBER 141

FLUID MASS FLOW RATE	=	414.26	LBM/HOUR
UNCORRECTED INLET BULK TEMPERATURE	=	84.60	DEGREES F
UNCORRECTED OUTLET BULK TEMPERATURE	=	88.60	DEGREES F
VOLTAGE DROP IN THE TEST SECTION	=	2.00	VOLTS
CURRENT TO THE TEST SECTION	=	162.50	AMPS
ROOM TEMPERATURE	=	91.30	DEGREES F
BULK BATH TEMPERATURE	=	90.00	DEGREES F

OUTSIDE SURFACE TEMPERATURES - DEGREES F

	1	2	3	4	5	6	7	8	9	10	11
1	94.6	95.2	95.4	87.1	86.2	86.4	94.9	100.0	101.6	103.1	103.7
2	95.1	95.5	95.7	87.5	86.2	86.5	94.9	99.9	101.4	102.5	103.2
3	95.6	96.1	96.6	88.1	86.8	87.3	94.9	99.2	100.5	101.2	101.4
4	96.3	97.3	97.7	92.9	88.4	88.3	94.5	98.5	99.8	100.0	100.0
5	96.2	97.7	98.0	93.4	89.7	88.8	94.4	98.0	99.1	99.1	99.4
6	95.8	97.1	96.9	91.2	88.3	88.1	94.2	97.9	98.8	99.3	99.5
7	95.1	96.2	95.9	88.1	87.0	86.8	94.3	98.4	99.4	100.2	100.6
8	94.7	95.5	95.4	87.3	86.4	86.3	94.5	99.2	100.1	101.5	102.7

RUN NUMBER 151

FLUID MASS FLOW RATE	=	489.42	LBM/HOUR
UNCORRECTED INLET BULK TEMPERATURE	=	74.40	DEGREES F
UNCORRECTED OUTLET BULK TEMPERATURE	=	78.40	DEGREES F
VOLTAGE DROP IN THE TEST SECTION	=	2.00	VOLTS
CURRENT TO THE TEST SECTION	=	162.50	AMPS
ROOM TEMPERATURE	=	85.30	DEGREES F
BULK BATH TEMPERATURE	=	90.00	DEGREES F

OUTSIDE SURFACE TEMPERATURES - DEGREES F

	1	2	3	4	5	6	7	8	9	10	11
1	84.8	86.0	86.0	77.6	76.4	76.3	83.7	89.3	91.3	93.2	94.1
2	85.1	86.2	86.4	78.1	76.5	76.5	83.7	89.1	90.6	92.5	93.8
3	85.5	86.7	87.1	78.9	77.1	77.4	83.7	88.6	89.8	91.4	92.2
4	85.9	87.6	88.1	83.7	78.7	78.5	83.5	87.9	89.6	90.5	91.1
5	85.9	87.9	88.1	84.2	80.1	79.1	83.4	87.5	89.0	89.9	90.4
6	85.7	87.4	87.3	81.9	78.5	78.4	83.2	87.4	88.6	90.0	90.4
7	85.2	86.7	86.4	78.8	77.1	77.0	83.3	87.9	89.5	90.6	90.9
8	84.9	86.2	86.0	77.8	76.4	76.5	83.4	88.7	89.9	91.7	93.2

RUN NUMBER 172

FLUID MASS FLOW RATE	=	646.22	LBM/HOUR
UNCORRECTED INLET BULK TEMPERATURE	=	78.00	DEGREES F
UNCORRECTED OUTLET BULK TEMPERATURE	=	81.10	DEGREES F
VOLTAGE DROP IN THE TEST SECTION	=	2.06	VOLTS
CURRENT TO THE TEST SECTION	=	162.50	AMPS
ROOM TEMPERATURE	=	86.30	DEGREES F
BULK BATH TEMPERATURE	=	82.00	DEGREES F

OUTSIDE SURFACE TEMPERATURES - DEGREES F

	1	2	3	4	5	6	7	8	9	10	11
1	87.8	89.0	89.1	80.5	79.6	79.5	84.0	89.0	91.8	94.4	95.8
2	87.9	89.2	89.5	80.8	79.8	79.8	84.1	89.1	91.5	94.0	95.6
3	88.3	89.6	90.1	81.3	80.2	80.5	84.1	88.9	91.0	93.1	94.2
4	88.7	90.3	90.6	86.0	81.8	81.5	84.6	88.6	90.8	92.4	93.2
5	88.8	90.5	91.0	86.5	83.2	82.0	84.9	88.3	90.4	92.0	92.7
6	88.6	90.1	90.3	84.3	81.6	81.3	84.2	88.2	90.1	92.1	92.7
7	88.2	89.5	89.5	81.0	80.4	80.1	83.9	88.4	90.7	92.7	93.4
8	88.0	89.1	89.2	80.4	79.8	79.6	83.8	88.7	90.9	93.5	95.1

RUN NUMBER 182

FLUID MASS FLOW RATE	=	725.43	LBM/HOUR
UNCORRECTED INLET BULK TEMPERATURE	=	78.90	DEGREES F
UNCORRECTED OUTLET BULK TEMPERATURE	=	81.70	DEGREES F
VOLTAGE DROP IN THE TEST SECTION	=	2.03	VOLTS
CURRENT TO THE TEST SECTION	=	160.00	AMPS
ROOM TEMPERATURE	=	88.50	DEGREES F
BULK BATH TEMPERATURE	=	84.00	DEGREES F

OUTSIDE SURFACE TEMPERATURES - DEGREES F

	1	2	3	4	5	6	7	8	9	10	11
1	88.3	89.5	89.8	81.5	80.8	80.6	83.7	88.2	91.1	94.1	95.3
2	88.4	89.6	90.1	81.9	81.0	80.8	83.8	88.3	90.8	93.8	95.1
3	88.7	90.0	90.6	82.5	81.5	81.6	83.9	88.4	90.5	93.1	93.9
4	89.0	90.6	91.4	86.9	83.2	82.7	84.5	88.3	90.4	92.6	93.1
5	89.0	90.8	91.4	87.5	84.8	83.3	84.9	88.2	90.2	92.2	92.6
6	89.0	90.5	90.8	85.1	82.9	82.6	84.1	88.0	89.9	92.3	92.6
7	88.7	90.0	90.1	82.4	81.5	81.2	83.8	88.1	90.4	92.8	93.5
8	88.5	89.6	89.6	81.6	80.9	80.7	83.6	88.2	90.5	93.4	94.8

APPENDIX B

CALIBRATION DATA

TABLE VII

CALIBRATION DATA FOR CALIBRATION OF OUTSIDE SURFACE THERMOCOUPLES

Station Number	Δ = (Saturated Steam Temperature) - (Thermocouple Reading), °F Peripheral Position							
	1	2	3	4	5	6	7	8
1	1.1	1.1	1.4	1.0	1.4	0.9	1.3	1.2
2	1.2	0.9	0.7	1.0	0.6	1.0	1.1	1.0
3	1.2	1.4	1.2	1.1	1.0	0.7	1.2	1.3
4	1.8	1.8	1.5	1.0	1.1	1.4	0.9	1.3
5	1.7	2.3	1.9	1.5	0.9	0.9	1.3	1.5
6	1.5	2.2	1.1	1.1	1.1	0.9	1.0	1.0
7	0.7	0.5	0.5	1.4	1.4	1.2	0.9	0.4
8	0.5	0.9	1.0	0.8	0.8	0.9	1.1	0.9
9	1.0	0.7	0.7	0.4	0.3	0.6	0.3	0.6
10	0.5	0.4	0.8	0.8	0.8	0.3	0.8	0.8
11	0.9	0.8	0.6	1.0	0.5	0.8	0.3	0.6

Note: In addition to this, water at room temperature was passed through the test section. The temperature difference between the water at room temperature and surface thermocouple was negligible. No correction was applied to surface thermocouples.

TABLE VIII

CALIBRATION DATA FOR INLET AND OUTLET BULK TEMPERATURES DURING IN-SITU CALIBRATION OF SURFACE THERMOCOUPLES

Saturated Steam Temperature, °F	Thermocouple Correction, °F Inlet	Thermocouple Correction, °F Outlet	Average Room Temperature, °F
210.23	-0.77	1.13	76.7

The corrected inlet and outlet bulk temperatures are obtained as follows:

$$(T_{in})_{corrected} = T_{in} - 0.77 \frac{(T_{in} - T_{room})}{(210.23 - 76.7)}$$

All temperatures are in degrees Fahrenheit. Inlet and outlet electrodes were located about 3.60 ft (1100 mm) from electrodes located at the far end of the U-bend. The saturated temperature of steam at atmospheric pressure was determined from steam tables. The above correction factors were found from data obtained after 10 hours of operation.

TABLE IX

CALIBRATION DATA FOR HEAT LOSS FROM THE TEST SECTION

Average temperature of saturated steam in test section	210.2 °F
Average room temperature during calibration	76.7 °F
Amount of condensate collected	0.6615 lbm/hr
Amount of condensate collected just before inlet to the test section	0.1190 lbm/hr
Heat of vaporization of water at 210.2 °F	971.74 Btu/lbm

The heat loss from the test section was correlated in the following manner.

1. Amount of condensate condensed in pipeline and test section was determined. Thus heat loss from the pipeline and test section was determined.

2. Amount of condensate condensed in the pipeline alone was determined and thus the heat loss from the pipeline.

3. The heat loss from the test section was determined by subtracting (2) from (1). Therefore heat loss in the test section was

   $$= (970.74)\ (0.6615 - 0.1190)\ \text{Btu/hr}$$

   $$= 527.2\ \text{Btu/hr}$$

4. The heat loss from the test section was determined by following the correlation

   $$Q_{loss} = \frac{572.2\ (T_{avg} - T_{room})}{(210.2 - 76.7)}\ ;\ \text{Btu/hr}$$

   where

   $$T_{avg} = (T_{in_{corrected}} + T_{out_{corrected}})/2.0,\ °\text{F}.$$

APPENDIX C

PHYSICAL PROPERTIES

A. Ethylene Glycol

The following correlations were used to compute the physical properties of ethylene glycol (11).

1. Density in kg/m^3

$$\rho = 1000.0/[0.924848 + 6.2796 \times 10^{-4} (T - 65) + 9.2444 \times 10^{-7} (T - 65)^2 + 3.0570 \times 10^{-9} (T - 65)^3]$$

where

T = temperature in °C

Range: 4.5°C to 100°C;

$$1 \text{ kg/m}^3 = 0.62428 \times 10^{-1} \frac{\text{lbm}}{\text{ft}^3}$$

2. Viscosity in NS/m^2

$$\mu = 0.16746 - 5.4455 \times 10^{-3} (T) + 8.3752 \times 10^{-5} (T)^2 - 7.3076 \times 10^{-7} (T)^3 + 3.7748 \times 10^{-9} (T)^4 - 1.1386 \times 10^{-11} (T)^5 + 1.8487 \times 10^{-14} (T)^6 - 1.2463 \times 10^{-17} (T)^7$$

where

T = temperature in °F

Range: 20°F to 350°F;

$1 NS/m^2 = 2.42 \times 10^3$ lbm/hr-ft

3. Specific heat in Btu/lbm-°F

$$C_p = 5.18956 \times 10^{-1} + 6.2290 \times 10^{-4} (T)$$

where

T = temperature in °F

Range: 6°F to 350°F;

1J/Kg-K = 6.238846 Btu/lbm-°F

4. Thermal conductivity in Btu/hr-ft-°F

$$k = 0.18329 - 0.24191 \times 10^{-3} (T)$$

where

T = temperature in °F

Range: 50°F to 350°F;

1W/m-K = 0.57779 Btu/hr-ft-°F

5. Coefficient of thermal expansion in 1/°C

$$\rho = -\frac{1}{\rho}\frac{d\rho}{dT}$$

$$\beta = \rho[6.2796 \times 10^{-4} + 1.84888 \times 10^{-6} (T - 65) + 9.171 \times 10^{-9} [T - 65]^2$$

where

ρ = density in gm/cm^3, and T = temperature in °C

Range: 4.5°C to 171°C

B. Stainless Steel

The following correlations developed by Singh (6) were used to compute the physical properties of stainless steel.

1. Electrical resistivity in ohms-in.^{2}/in.

$$= 2.601 \times 10^{-5} + 1.37904 \times 10^{-8} (T) + 8.5158 \times 10^{-12} (T^2) - 10.11924 \times 10^{-17} (T^3)$$

where

T = temperature in °F

2. Thermal conductivity in Btu/hr-ft-°F

$$k = 7.8034 + 0.51691 \times 10^{-2} (T) - 0.88501 \times 10^{-6} (T^2)$$

where

T = temperature in °F;

1W/m-k = 0.57779 Btu/hr-ft°F

APPENDIX D

SHELL BALANCE TO DETERMINE INSIDE WALL TEMPERATURE AND INTERNAL RADIAL FLUX

To determine inside wall temperature and radial heat flux, a shell balance around the tube wall was made. The following end conditions were assumed:

1. Radial heat flux is significant. Axial and angular heat fluxes are negligible.

2. Electrical resistivity and thermal conductivity could be evaluated at outside wall temperature (6).

3. Heat losses to surrounding are present but small.

4. Steady state condition exists.

Boundary conditions:

1. $\partial T/\partial r = 0$ at $r = r_2$ (see Figure 21).

2. $T = T_s = T_{\text{outside surface temperature}}$ at $r = r_2$.

Rate of thermal energy input at r

$$= (2\pi rL)q_r \tag{D.1}$$

Rate of thermal energy output at $r + \Delta r$

$$= [2\pi(r + \Delta r)L]q_{r+\Delta r} \tag{D.2}$$

Rate of generation of thermal energy due to electrical dissipation

$$= (j^2\rho)\ 2\pi r\Delta rL \tag{D.3}$$

where

$$j = \frac{I}{\text{cross sectional area}} = \text{current density, A/m}^2$$

and ρ is the resistivity, ohm-m^2/m. Now making energy balance we get,

Input - Output + Generation = Accumulation.

where accumulation is zero since the steady state assumption has been

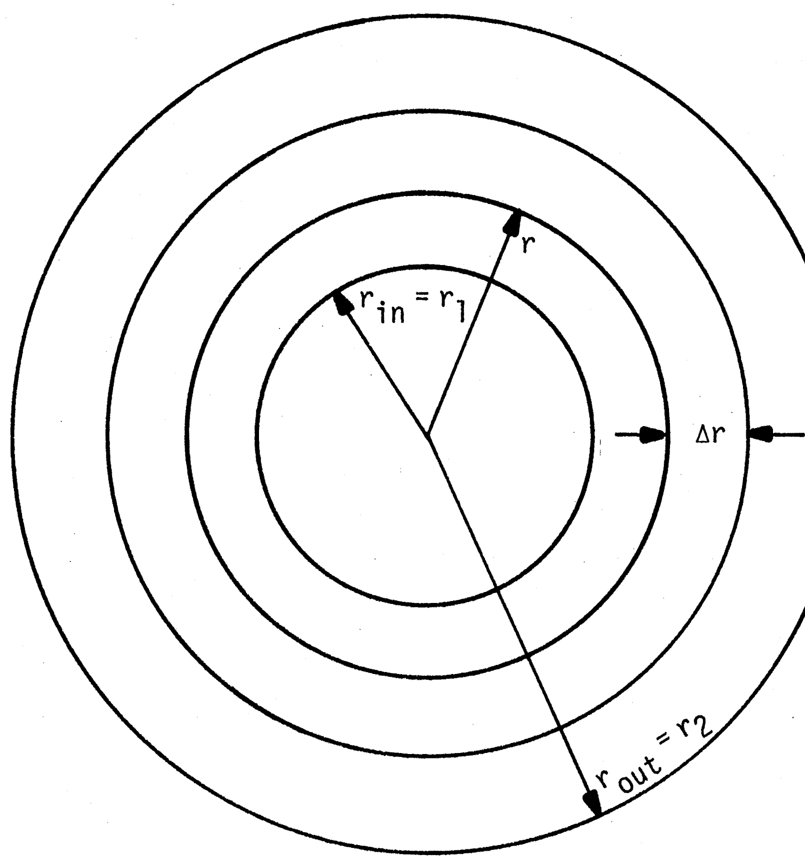

Figure 21. Shell Balance Around the Tube Wall

made. Substituting various terms, the following equation is obtained.

$$(2\rho rL)q_r - [2\pi(r + \Delta r)L]q_{r+\Delta r} + j^2\rho 2\pi r\Delta rL = 0 \tag{D.4}$$

Dividing by $2\pi\Delta rL$, rearranging terms, and taking the limit as $\Delta r \to 0$, the following equation was obtained.

$$\lim_{\Delta r \to 0} \frac{rq_{r+\Delta r} - rq_r}{\Delta r} = j^2\rho r$$

$$\therefore \quad \frac{\partial(rq_r)}{\partial r} = j^2\rho r \tag{D.5}$$

Integrating Equation (D.5) with respect to r, the following expres- was obtained:

$$rq_r = \frac{j^2\rho r^2}{2} + C_1 \tag{D.6}$$

$$q_r = \frac{j^2\rho r}{2} + \frac{C_1}{r}$$

where C_1 is the constant of integration. C_1 is evaluated later by applying the boundary conditions. q_r is the radial heat flux. This is given by

$$q_r = -k' \frac{\partial T}{\partial r} \tag{D.7}$$

where k' is the thermal conductivity of the tube material. Thermal conductivity k' was evaluated at the outside wall surface temperature. The terms for q_r were substituted in Equation (D.6) to obtain the equation (D.8). Equation (D.8) was then integrated with respect to r.

$$-k \frac{\partial T}{\partial r} = \frac{j^2\rho r}{2} + \frac{C_1}{r} \tag{D.8}$$

$$\therefore -kT = \frac{j^2\rho r^2}{4} + C_1 \ln r + C_2 \tag{D.9}$$

C_2 is the constant of integration. Applying boundary condition 1, $\partial T/\partial r = 0$ at $r = r_2$, $C_1 = j^2\rho r_2^2/2$ was obtained. Applying boundary condition 2, $T = T_s$ at $r = r_2$,

$$C_2 = -k'T_s - \frac{j^2\rho r_2^2}{4} + \frac{j^2\rho r_2^2}{2} \ \ln r_2$$

was obtained. Substituting for C_1 and C_2 in Equation (D.9) and rearranging terms, the following equation was obtained.

$$(T_s - T) = \frac{j^2\rho}{k'}\left[\left(\frac{r^2 - r_2^2}{4}\right) + \frac{r_2^2}{2} \ \ln \left(\frac{r_2}{r}\right)\right] \tag{D.10}$$

At $T = T_{\text{inside surface temperature}}$, $r = r_1$. Equation (D.11) was obtained by substituting the above condition. This, on rearrangement of the terms, gave Equation (D.12).

$$T_s - T_{\substack{\text{inside}\\\text{surface}\\\text{temperature}}} = \frac{j^2\rho}{k'}\left[\left(\frac{r_1^2 - r_2^2}{4}\right) + \frac{r_2^2}{2} \ \ln \left(\frac{r_2}{r_1}\right)\right] \tag{D.11}$$

$$\therefore T_{\substack{\text{inside}\\\text{surface}\\\text{temperature}}} = T_s - \frac{j\rho^2}{k'}\left[\left(\frac{r_1^2 - r_2^2}{4}\right) + \frac{r_2^2}{2} \ \ln \left(\frac{r_2}{r_1}\right)\right. \tag{D.12}$$

The local radial heat flux was obtained by substituting for constant C_1 in Equation (D.6).

$$q_r = \frac{j^2\rho}{2r_1}\left(r_1^2 - r_2^2\right) \tag{D.13}$$

Thus, in this fashion radial heat flux and local inside wall temperatures were determined.

APPENDIX E

SAMPLE CALCULATION

Calculations for data run 151 are presented here. The physical quantities measured for data run 151 are presented in Appendix A.

Calculation of the Heat Balance

Power input rate, Btu/hr

Power input = (2) (current to each straight section)

x (voltage drop across the test section)

x (3.41213)

= (2) (81.25) (2.0) (3.41213)

= 1108.9 Btu/hr

Heat loss = Q_{loss}, Btu/hr

$$Q_{loss} = 527.2\ (76.4 - 85.3)/(210.2 - 76.7)$$

$$= -35.1 \text{ Btu/hr}$$

Heat input rate = Q_{input}, Btu/hr

$$Q_{input} = [\text{power input} - Q_{loss}]$$

$$= [1108.9 - (-35.1)]$$

$$= 1144.0 \text{ Btu/hr}$$

Heat output rate = Q_{output}, Btu/hr

$$Q_{output} = (W)\ (C_p)\ [T_{bout} - T_{bin}]$$

The inlet and outlet bulk fluid temperatures measured by thermocouples were corrected, based on their calibration correction factor. Calibration data for these thermocouples are given in Table VIII (Appendix B).

Corrected inlet fluid temperature

$$= T_{bin} - (.77)\ [\frac{(T_{bin} - T_{room})}{(210.2 - 76.7)}$$

$$= 74.4 - (0.77)\ [\frac{(74.4 - 85.3)}{(210.2 - 76.7)}]$$

$$= 74.46\ °F^{*}$$

$$= 74.50\ °F$$

Corrected outlet fluid temperature

$$= T_{bout} + 1.13\ [\frac{(T_{bout} - T_{room})}{(210.2 - 76.7)}]$$

$$= 78.4 + 1.13\ [\frac{(78.4 - 85.3)}{(210.2 - 76.7)}]$$

$$= 78.34\ °F$$

$$= 78.30\ °F$$

Average bulk fluid temperature

$$= \frac{1}{2}\ (T_{bin} + T_{bout}),\ °F$$

$$= \frac{1}{2}\ (74.45 + 78.34),\ °F$$

$$= 76.4\ °F$$

Specific heat for ethylene glycol from Appendix C,

$$C_p = 5.18956 \times 10^{-1} + 6.229 \times 10^{-4}\ (T) \quad \text{at} \quad T = 76.4°F$$

$$C_p = 0.5665\ \text{Btu/lbm°F}$$

$$Q_{output} = (489.42)\ (0.5665)\ (78.34 - 74.46),\ \text{Btu/hr}$$

$$= 1075.7\ \text{Btu/hr}$$

Percent error in heat balance

$$= \frac{(Q_{input} - Q_{output})}{Q_{input}} \times 100$$

$$= [\frac{(1144.0 - 1075.7)}{1144.0}] \times 100$$

$$= 5.97\%$$

---

*Kept to two digits in order to compare with computer output.

Calculation of Local Inside Wall Temperature and the Inside Wall Radial Heat Flux

As indicated in Chapter V, a shell balance was made around the tube wall to calculate inside wall temperatures and radial heat fluxes. The equations are derived in Appendix D. Using Equations (D.12) and (D.13), the inside wall temperature and radial flux are calculated for station 8 and peripheral position 1 as shown below:

$T_{\text{inside wall temperature}}$

$$= T_s - \frac{j^2\rho}{k'} \left[\left(\frac{r_1^2 - r_2^2}{4}\right) + \frac{r_2^2}{2} \; n \left(\frac{r_2}{r_1}\right)\right], \ ^\circ F$$

Electrical resistivity ρ and thermal conductivity K are evaluated using correlations developed by Singh (6).

Electrical resistivity in ohms-in.^{2}/in.

$$\rho = 2.601 \times 10^{-5} + 1.37904 \times 10^{-8} (T) + 8.5158 \times 10^{-12} (T^2)$$
$$- 10.11924 \times 10^{-17} (T^3)$$

At T = 89.3 °F,

$$\rho = 2.7309 \times 10^{-5} \text{ ohm-in.}^2\text{/in.}$$
$$\rho = 6.9360 \times 10^{-7} \text{ ohm-m}^2\text{/m}$$

Thermal conductivity K in Btu/hr-ft-°F

$$k' = 7.8034 + 0.51691 \times 10^{-2} (T) - 0.88501 \times 10^{-6} (T^2)$$

At T = 89.3 °F,

$$k' = 8.2579 \text{ Btu/(hr-ft-°F)}$$
$$k' = 7.9401 \text{ W/m-°F}$$

Current density j^2 in A^2/m^4

$$j^2 = \left(\frac{81.25}{9.01951 \times 10^{-5}}\right)^2, \quad A^2/m^4$$

$$j^2 = 8.114856615 \times 10^{11}, \quad A^2/m^4$$

$T_{\text{inside wall temperature}}$

$$= 89.3 - \frac{8.114856615 \times 10^{11} \times 6.936 \times 10^{-7}}{7.9401}$$

$$\left[\frac{(-2.871 \times 10^{-5})}{4} + 4.5362 \times 10^{-5}\ (0.1902)\right],\ °F$$

$T_{\text{inside wall temperature}} = 89.2\ °F$

Inside radial heat flux, Btu/(hr-ft^2)

$$q_r = -k'\frac{\partial T}{\partial r} = \frac{j^2\rho}{2(r_1)}\,(r_1^2 - r_2^2)$$

$$= \frac{8.114856615 \times 10^{11} \times 6.936 \times 10^{-7}}{2 \times 7.875 \times 10^{-3}}\left[\left(\frac{0.01575}{2}\right)^2\right.$$

$$\left. - \left(\frac{0.01905}{2}\right)^2\right]$$

$$= -1025.9\ W/m^2$$

$$q_r = +k'\frac{\partial T}{\partial r} = +325.3\ \text{Btu/(hr-ft}^2)$$

The local heat transfer for station 8 and peripheral position 1 was calculated as follows:

Local heat transfer coefficient

$$= \frac{q_r}{(T_{w_{8-1}} - T_{b_8})}$$

The bulk temperature T_{b_8} was calculated using

$$T_{b_8} = T_{b_{in}} + (T_{b_{out}} - T_{b_{in}})(\frac{AL_8}{AL_{total}})$$

AL_{total} = Total heating length

$$T_{b_8} = 74.46 + (78.34 - 74.46)(\frac{10.2503}{18})$$

$$= 76.66 \text{ °F}$$

$$= 76.70 \text{ °F}$$

Local heat transfer coefficients

$$= \frac{325.3}{(89.20 - 76.66)}, \text{ Btu/(hr-ft}^2\text{-°F)}$$

$$= 25.96 \text{ Btu/(hr-ft}^2\text{-°F)}$$

$$= 26.00 \text{ Btu/(hr-ft}^2\text{-°F)}$$

The peripheral average local heat transfer coefficient at station 8 was obtained as follows:

$$\bar{h} = (\frac{1}{8}) \sum_{j=1}^{8} h_{ij}$$

$$= (\frac{1}{8})\ (26.0 + 26.4 + 27.5 + 29.2 + 30.3 + 30.6 + 29.2 + 27.3)$$

$$= 28.30 \text{ Btu/(hr-ft}^2\text{-°F)}$$

Tables X to XIV give the values of outside surface temperatures, the computed inside wall temperatures, the inside radial heat fluxes, the local heat transfer coefficients, and the average local heat transfer coefficients for relevant stations.

Physical Properties

Using the correlations given in Appendix C, calculate viscosity, specific heat, thermal conductivity, density, and thermal expansion coefficient of ethylene glycol.

TABLE X

RUN 151--OUTSIDE SURFACE TEMPERATURES, °F

Thermocouple* Peripheral Location	Thermocouple Station Number										
	1	2	3	4	5	6	7	8	9	10	11
1	84.8	86.0	86.0	77.6	76.4	76.3	83.7	89.3	91.3	93.2	94.1
2	85.1	86.2	86.4	78.1	76.5	76.5	83.7	89.1	90.6	92.5	93.8
3	85.5	86.7	87.1	78.9	77.1	77.4	83.7	88.6	89.8	91.4	92.2
4	85.9	87.6	88.1	83.7	78.7	78.5	83.5	87.9	89.6	90.5	91.1
5	85.9	87.9	88.1	84.2	80.1	79.1	83.4	87.5	89.0	89.9	90.4
6	85.7	87.4	87.3	81.9	78.5	78.4	83.2	87.4	89.6	90.0	90.4
7	85.2	86.7	86.4	78.8	77.1	77.0	83.3	87.9	89.5	90.6	90.9
8	84.9	86.2	86.0	77.8	76.4	76.5	83.4	88.7	89.9	91.7	93.2

*Peripheral position of each thermocouple as in Figure 3.

TABLE XI

RUN 151--INSIDE WALL TEMPERATURES, °F

Thermocouple Peripheral Location	Thermocouple Station Number 1	2	3	7	8	9	10	11
1	84.7	85.9	85.9	83.6	89.2	91.2	93.1	94.0
2	85.0	86.1	86.3	83.6	89.0	90.5	92.4	93.7
3	85.4	86.6	87.0	83.6	88.5	89.7	91.3	92.1
4	85.8	87.5	88.0	83.4	87.8	89.5	90.4	91.0
5	85.8	87.8	88.0	83.3	87.4	88.9	89.8	90.3
6	85.6	87.3	87.2	83.1	87.3	88.5	89.9	90.3
7	85.1	86.6	86.3	83.2	87.8	89.4	90.5	90.8
8	84.8	86.1	85.9	83.3	88.6	89.8	91.6	93.1

TABLE XII

RUN 151--INSIDE RADIAL HEAT FLUXES, BTU/(HR-FT^2)

Thermocouple Peripheral Location	Thermocouple Station Number							
	1	2	3	7	8	9	10	11
1	324.4	324.7	324.7	324.2	325.3	325.6	326.0	326.1
2	324.5	324.7	324.7	324.2	325.2	325.5	325.9	326.1
3	324.6	324.8	324.9	324.2	325.1	325.4	325.6	325.8
4	324.6	325.0	325.0	324.2	325.0	325.3	325.5	325.6
5	324.6	325.0	325.0	324.2	324.9	325.2	325.4	325.5
6	324.6	324.9	324.9	324.2	324.9	325.1	325.5	325.5
7	324.5	324.8	324.7	324.2	325.0	325.3	325.5	325.6
8	324.5	324.7	324.7	324.2	325.2	325.4	325.7	326.0

TABLE XIII

RUN 151--LOCAL HEAT TRANSFER COEFFICIENT, BTU/(HR-FT^2-°F)

Thermocouple Peripheral Location	Thermocouple Station Number 1	2	3	7	8	9	10	11
1	34.6	33.3	34.1	45.3	26.0	22.8	20.9	20.4
2	33.6	32.6	32.7	45.3	26.4	24.0	21.8	20.8
3	32.2	31.0	30.5	45.3	27.5	25.5	23.6	23.1
4	31.0	28.6	27.9	46.6	29.2	25.9	25.2	25.1
5	31.0	27.9	27.9	47.2	30.3	27.2	26.4	26.5
6	31.6	29.1	30.0	48.7	30.6	28.1	26.2	26.5
7	33.2	31.0	32.7	47.9	29.2	26.1	25.0	25.5
8	34.3	32.6	34.1	47.2	27.3	25.3	23.1	21.6

TABLE XIV

RUN 151--AVERAGE LOCAL HEAT TRANSFER COEFFICIENT, BTU/(HR-FT^2-°F)

Thermocouple Station Number 1	2	3	7	8	9	10	11
32.7	30.8	31.2	46.7	28.3	25.6	24.0	23.7

1. Viscosity

$$\mu = 0.16746 - 5.4455 \times 10^{-3} (T) + 8.3752 \times 10^{-5} (T)^2$$
$$- 7.3076 \times 10^{-7} (T)^3 + 3.7748 \times 10^{-9} (T)^4$$
$$- 1.1386 \times 10^{-11} (T)^5 + 1.8487 \times 10^{-14} (T)^6$$
$$- 1.2463 \times 10^{-17} (T)^7$$

where T is measured in degrees F.

At T_{bath} = 90.00 °F

$$\mu = 0.16746 - 5.4455 \times 10^{-3} (90) + 8.3752 (90)^2$$
$$- 7.3076 \times 10^{-7} (90)^3 + 3.7748 \times 10^{-9} (90)^4$$
$$- 1.1386 \times 10^{-11} (90)^5 + 1.8487 \times 10^{-14} (90)^6$$
$$- 1.2463 \times 10^{-17} (90)^7$$

$$\mu = 1.2684 \times 10^{-2} \text{ NS/m}^2$$

$$\mu = 30.69 \text{ lbm/hr-ft}$$

Viscosity at the film temperature is calculated as follows:

$$T_{film} = [(\frac{1}{8} \sum_{j=1}^{8} T_{\text{inside wall temperature}} + T_{bulk_i}]/2.0$$

For station 8,

$$T_{film} = [\frac{1}{8} (89.2 + 89.0 + 88.5 + 87.8 + 87.4 + 87.3 + 87.8$$
$$+ 88.6) + 76.7]/2.0$$
$$= 82.4 \text{ °F}$$

Viscosity at film temperature = 82.4 °F

$$\mu = 1.4798 \times 10^{-2} \text{ Ns/m}^2$$

μ = 35.81 lbm/hr-ft

2. Specific heat

$$C_p = 5.18956 \times 10^{-1} + 6.2290 \times 10^{-4}\ (T)$$

where T is °F. At film temperature, T_{film} = 82.4.

$$C_p = 5.18956 \times 10^{-1} + 6.2290 \times 10^{-4}\ (82.4)$$

$$C_p = 0.5702 \text{ Btu/(lbm-°F)}$$

3. Thermal conductivity

$$k = 0.18329 - 0.24191 \times 10^{-3}\ (T)$$

At T_{film} = 82.4

$$k = 1.6335 \times 10^{-1} \text{ Btu/(hr-ft-°F)}$$

4. Density

$$\rho = 1000.0/[0.924848 + 6.2796 \times 10^{-4}\ (T - 65) + 9.2444 \times 10^{-7}\ (T - 65)^2 + 3.057 \times 10^{-9}\ (T - 65)^3]$$

where T is in °C.

At T_{film} = 82.4 °F = 28.0 °C

$$\rho = 1000.0/[0.924848 + 6.2796 \times 10^{-4}\ (28 - 65) + 9.2444 \times 10^{-7}\ (28 - 65)^2 + 3.057 \times 10^{-9}\ (28 - 65)^3]$$

$$\rho = 1.1077 \times 10^3 \text{ kg/m}^3$$

$$= 69.2 \text{ lbm/ft}^3$$

5. Coefficient of thermal expansion

$$\beta = -\frac{1}{\rho}\frac{d\rho}{dT}$$

$$= \rho[6.2796 \times 10^{-4} + 1.84888 \times 10^{-6} (T - 65)$$

$$+ 9.171 \times 10^{-9} (T - 65)^2], \quad \rho \text{ in gm/cm}^3$$

At T_{film} = 28.0 °C

$$\beta = 1.1077 [6.2796 \times 10^{-4} + 1.84888 \times 10^{6} (28 - 65)$$

$$+ 9.171 \times 10^{-9} (28 - 65)^2]$$

$$\beta = 6.3372 \times 10^{-4}/°C$$

$$= 3.5206 \times 10^{-4}/°F$$

Dimensionless Numbers

1. Reynolds number: Re

$$Re = \frac{4W}{d_i \pi \mu}$$

where d_i is in ft.

At T_{bath} = 82.4 °F

$$Re = \frac{(4)(489.42 \text{ lbm/hr})}{(5.1666 \times 10^{-2} \text{ ft})(3.14159)(30.69 \text{ lbm/hr-ft})}$$

$$Re = 392.9$$

Reynolds number at film temperature, T_{film} = 82.4 °F

$$Re = \frac{4W}{d_i \pi \mu}$$

$$= \frac{(4)(489.92 \text{ lbm/hr})}{(5.1666 \times 10^{-2} \text{ ft})(3.14159)(35.81)}$$

$= 337.1$

2. Prandtl number: Pr

$$Pr = (C_p)(\mu)/k$$

$$= (0.5702)(35.81)/(1.6335 \times 10^{-1})$$

$$= 125.0$$

3. Peripheral average Nusselt number: Nu

$$Nu = (\bar{h})(d_i)/k$$

$$Nu = (28.3)\ (5.1666 \times 10^{-2})/1.6335 \times 10^{-1})$$

$$Nu = 9.0$$

4. Graetz number: Gz

$$Gz = WC_p/kL$$

$$= (489.42)(0.5702)/(1.6335 \times 10^{-1})\ (1.25)$$

$$= 1366.7$$

5. Grashof number: Gr

$$Gr = (d_i)^3\ (\rho)^2\ (g)\ (\beta)\ (\overline{T}_{wi} - T_{bulki})/\mu^2$$

$$Gr = \frac{(1.3792 \times 10^{-4})(69.2)^2(4.17 \times 10^8)(3.5206 \times 10^{-4})(88.2-76.7)}{(35.81)^2}$$

$$Gr = 871.0$$

6. Rayleigh number: Ra

$$Ra = (Gr)\ (Pr)$$

$$= (871)\ (125.0)$$

$$= 108{,}875.$$

APPENDIX F

CALCULATED RESULTS

RUN NUMBER 103

```
REYNOLDS NUMBER              =   64.269
PRANDTL NUMBER               =   93.460
HEAT INPUT=AMP*VOLT*C-JL=  1081.618   BTU/HR
HEAT OUTPUT=M*CP*(T2-T1)=  1021.259   BTU/HR
HEAT LOSS                    =   66.136   BTU/HR
AVERAGE REYNOLDS NUMBER =   85.076
% ERROR IN HEAT BALANCE =    5.580
```

LOCAL HEAT TRANSFER COEFFICIENT - BTU/(HR-SQ.FT-DEG.F)

	1	2	3	7	8	9	10	11
1	45.7	63.1	67.3	23.8	23.9	23.9	24.1	24.3
2	39.7	57.5	58.9	23.6	25.2	24.8	26.4	25.4
3	33.9	47.6	47.1	24.3	29.2	29.1	31.7	30.9
4	29.4	37.8	37.9	25.7	34.7	34.2	39.1	38.3
5	30.5	35.3	37.1	27.8	37.0	38.6	43.2	41.2
6	33.3	39.6	42.8	26.7	36.6	38.1	39.6	40.2
7	39.7	46.9	54.9	25.8	32.3	32.8	34.6	33.0
8	44.5	56.6	66.0	24.5	27.0	29.1	28.9	26.2

AVERAGE LOCAL HEAT TRANSFER COEFFICIENT - BTU/(HR-SQ.FT-DEG.)

1	2	3	7	8	9	10	11
37.1	48.0	51.5	25.4	30.7	31.3	33.4	32.4

AVERAGE LOCAL HEAT TRANSFER COEFFICIENT - BTU/(HR-SQ.FT-DEG.F) BY SECOND DEF.

1	2	3	7	8	9	10	11
36.2	46.2	49.0	25.3	30.0	30.4	32.2	31.2

RUN NUMBER 103

INSIDE SURFACE TEMPERATURES - DEGREES F

	1	2	3	7	8	9	10	11
1	100.7	103.4	104.4	113.8	115.1	116.7	119.7	122.7
2	101.8	103.9	105.1	113.9	114.4	116.2	118.5	122.1
3	103.2	105.1	106.5	113.5	112.6	114.2	116.4	119.8
4	104.7	106.9	108.2	112.3	110.8	112.5	114.4	117.7
5	104.3	107.5	108.4	111.8	110.2	111.4	113.6	117.1
6	103.4	106.5	107.2	112.3	110.3	111.5	114.3	117.3
7	101.8	105.2	105.5	112.7	111.5	112.9	115.5	119.1
8	100.9	104.0	104.5	113.4	113.5	114.2	117.4	121.7

INSIDE RADIAL HEAT FLUXES - BTU/(SQ.FT.-HR)

	1	2	3	7	8	9	10	11
1	327.4	327.9	328.1	329.8	330.1	330.4	330.9	331.5
2	327.6	328.0	328.2	329.8	329.9	330.3	330.7	331.4
3	327.8	328.2	328.5	329.8	329.6	329.9	330.3	330.9
4	328.1	328.5	328.6	329.5	329.3	329.6	329.9	330.5
5	328.0	328.6	328.6	329.4	329.1	329.4	329.8	330.4
6	327.9	328.5	328.6	329.5	329.2	329.4	329.9	330.5
7	327.6	328.2	328.3	329.6	329.4	329.6	330.1	330.8
8	327.4	328.0	328.1	329.7	329.8	329.9	330.5	331.3

BULK FLUID TEMPERATURES - DEGREES F

1	2	3	7	8	9	10	11
93.5	98.2	99.5	99.9	101.3	102.9	106.0	109.1

CORRECTED INLET BULK TEMPERATURE= 88.6 DEG. F

CORRECTED OUTLET BULK TEMPERATURE= 110.9 DEG. F

RUN NUMBER 114

REYNOLDS NUMBER = 164.460
PRANDTL NUMBER = 110.692
HEAT INPUT=AMP*VOLT*C-QL= 1088.474 BTU/HR
HEAT OUTPUT=M*CP*(T2-T1)= 1025.205 BTU/HR
HEAT LOSS = -2.052 BTU/HR
AVERAGE REYNOLDS NUMBER = 182.886
% ERROR IN HEAT BALANCE = 5.813

LOCAL HEAT TRANSFER COEFFICIENT - BTU/(HR-SQ.FT-DEG.F)

	1	2	3	7	8	9	10	11
1	34.6	40.5	41.1	26.4	22.4	21.8	21.2	21.3
2	32.2	38.5	38.6	26.1	22.4	23.0	22.7	22.0
3	29.2	34.7	33.7	26.1	23.5	25.2	25.4	25.5
4	26.6	29.6	28.6	26.6	25.6	27.6	28.4	28.4
5	27.2	28.0	28.3	27.3	28.1	29.9	29.4	29.7
6	29.0	30.4	31.7	27.7	28.3	30.5	28.6	29.5
7	32.2	34.4	37.7	28.0	26.4	26.7	26.5	27.4
8	34.3	37.6	41.1	27.5	24.0	24.8	23.7	22.6

AVERAGE LOCAL HEAT TRANSFER COEFFICIENT - BTU/(HR-SQ.FT-DEG.)

1	2	3	7	8	9	10	11
30.7	34.2	35.1	27.0	25.1	26.2	25.8	25.8

AVERAGE LOCAL HEAT TRANSFER COEFFICIENT - BTU/(HR-SQ.FT-DEG.F) BY SECOND DEF.

1	2	3	7	8	9	10	11
30.4	33.7	34.4	26.9	24.9	25.9	25.4	25.4

RUN NUMBER 114

INSIDE SURFACE TEMPERATURES - DEGREES F

	1	2	3	7	8	9	10	11
1	96.0	96.5	96.9	101.4	104.1	105.1	106.7	107.9
2	96.7	96.9	97.4	101.5	104.1	104.3	105.7	107.4
3	97.7	97.8	98.6	101.5	103.4	103.1	104.2	105.4
4	98.8	99.4	100.3	101.3	102.3	102.0	102.9	104.1
5	98.5	100.0	100.4	101.0	101.2	101.1	102.5	103.6
6	97.8	99.1	99.2	100.8	101.1	100.9	102.8	103.7
7	96.7	97.9	97.6	100.7	101.9	102.4	103.7	104.5
8	96.1	97.1	96.9	100.9	103.1	103.3	105.1	107.0

INSIDE RADIAL HEAT FLUXES - BTU/(SQ.FT.-HR)

	1	2	3	7	8	9	10	11
1	316.5	316.6	316.7	317.5	318.0	318.2	318.5	318.7
2	316.7	316.7	316.8	317.5	318.0	318.0	318.3	318.6
3	316.8	316.9	317.0	317.5	317.9	317.8	318.0	318.2
4	317.0	317.1	317.3	317.5	317.7	317.6	317.8	318.0
5	317.0	317.3	317.3	317.4	317.5	317.5	317.7	317.9
6	316.9	317.1	317.1	317.4	317.5	317.4	317.8	317.9
7	316.7	316.9	316.8	317.4	317.6	317.7	317.9	318.1
8	316.6	316.7	316.7	317.4	317.8	317.8	318.2	318.5

BULK FLUID TEMPERATURES - DEGREES F

1	2	3	7	8	9	10	11
86.9	88.7	89.2	89.4	89.9	90.5	91.7	92.9

CORRECTED INLET BULK TEMPERATURE= 84.9 DEG. F

CORRECTED OUTLET BULK TEMPERATURE= 93.6 DEG. F

RUN NUMBER 121

REYNOLDS NUMBER = 221.581
PRANDTL NUMBER = 117.217
HEAT INPUT=AMP*VOLT*C-QL= 1122.132 BTU/HR
HEAT OUTPUT=M*CP*(T2-T1)= 993.206 BTU/HR
HEAT LOSS = 3.443 BTU/HR
AVERAGE REYNOLDS NUMBER = 245.729
% ERROR IN HEAT BALANCE = 11.489

LOCAL HEAT TRANSFER COEFFICIENT - BTU/(HR-SQ.FT-DEG.F)

	1	2	3	7	8	9	10	11
1	33.4	35.7	36.3	29.0	22.7	21.7	21.6	21.4
2	31.8	34.6	34.4	29.0	23.0	22.4	22.9	22.1
3	29.5	31.9	30.9	29.5	24.0	23.9	25.6	25.3
4	26.8	28.1	27.3	31.2	25.5	25.2	28.2	28.3
5	27.5	26.9	26.8	32.1	26.8	27.7	29.8	29.3
6	29.0	28.8	29.7	31.8	27.4	28.9	28.5	29.1
7	31.2	31.9	33.7	31.2	26.3	26.2	26.6	26.9
8	32.7	34.6	36.3	30.3	24.4	24.6	23.9	22.7

AVERAGE LOCAL HEAT TRANSFER COEFFICIENT - BTU/(HR-SQ.FT-DEG.)

1	2	3	7	8	9	10	11
30.2	31.6	31.9	30.5	25.0	25.1	25.9	25.6

AVERAGE LOCAL HEAT TRANSFER COEFFICIENT - BTU/(HR-SQ.FT-DEG.F) BY SECOND DEF.

1	2	3	7	8	9	10	11
30.1	31.3	31.5	30.5	24.9	24.9	25.6	25.3

RUN NUMBER 121

INSIDE SURFACE TEMPERATURES - DEGREES F

	1	2	3	7	8	9	10	11
1	94.1	94.7	94.9	97.3	100.8	101.9	102.8	103.8
2	94.6	95.0	95.4	97.3	100.6	101.4	101.9	103.3
3	95.4	95.8	96.5	97.1	100.0	100.5	100.4	101.4
4	96.5	97.2	97.9	96.5	99.2	99.8	99.2	100.0
5	96.2	97.7	98.1	96.2	98.6	98.6	98.6	99.6
6	95.6	96.9	96.9	96.3	98.3	98.1	99.1	99.7
7	94.8	95.8	95.6	96.5	98.8	99.3	99.9	100.6
8	94.3	95.0	94.9	96.8	99.8	100.1	101.3	102.9

INSIDE RADIAL HEAT FLUXES - BTU/(SQ.FT.-HR)

	1	2	3	7	8	9	10	11
1	326.2	326.3	326.3	326.7	327.4	327.6	327.8	327.9
2	326.3	326.3	326.4	326.7	327.4	327.5	327.6	327.9
3	326.4	326.5	326.6	326.7	327.2	327.3	327.3	327.5
4	326.6	326.7	326.9	326.6	327.1	327.2	327.1	327.2
5	326.5	326.8	326.9	326.5	327.0	327.0	327.0	327.2
6	326.4	326.7	326.7	326.6	326.9	326.9	327.1	327.2
7	326.3	326.5	326.4	326.6	327.0	327.1	327.2	327.4
8	326.2	326.3	326.3	326.7	327.2	327.3	327.5	327.8

BULK FLUID TEMPERATURES - DEGREES F

1	2	3	7	8	9	10	11
84.3	85.6	85.9	86.0	86.4	86.8	87.6	88.4

CORRECTED INLET BULK TEMPERATURE= 83.0 DEG. F

CORRECTED OUTLET BULK TEMPERATURE= 88.9 DEG. F

RUN NUMBER 131

REYNOLDS NUMBER =	317.105	
PRANDTL NUMBER =	108.310	
HEAT INPUT=AMP*VOLT*C-OL=	1111.453	BTU/HR
HEAT OUTPUT=M*CP*(T2-T1)=	1036.015	BTU/HR
HEAT LOSS =	3.034	BTU/HR
AVERAGE REYNOLDS NUMBER =	332.051	
% ERROR IN HEAT BALANCE =	6.787	

LOCAL HEAT TRANSFER COEFFICIENT - BTU/(HR-SQ.FT-DEG.F)

	1	2	3	7	8	9	10	11
1	35.6	36.9	38.6	35.6	24.1	22.3	22.0	21.8
2	34.1	35.7	36.8	35.6	24.5	22.9	23.3	22.7
3	31.8	33.2	33.1	36.0	25.8	24.6	25.9	26.1
4	29.5	29.3	29.3	38.1	27.6	25.9	28.9	29.3
5	30.0	28.3	28.8	39.5	28.8	28.1	30.7	30.7
6	31.5	30.1	32.2	39.5	29.0	28.9	29.6	30.4
7	33.7	32.8	36.0	38.5	27.8	27.2	27.6	27.4
8	35.2	35.3	38.6	37.7	25.6	25.7	24.9	23.5

AVERAGE LOCAL HEAT TRANSFER COEFFICIENT - BTU/(HR-SQ.FT-DEG.)

1	2	3	7	8	9	10	11
32.7	32.7	34.2	37.6	26.7	25.7	26.6	26.5

AVERAGE LOCAL HEAT TRANSFER COEFFICIENT - BTU/(HR-SQ.FT-DEG.F) BY SECOND DEF.

1	2	3	7	8	9	10	11
32.5	32.4	33.8	37.5	26.5	25.5	26.3	26.1

RUN NUMBER 131

INSIDE SURFACE TEMPERATURES - DEGREES F

	1	2	3	7	8	9	10	11
1	98.4	99.1	99.0	99.8	104.5	106.0	106.9	107.7
2	98.8	99.4	99.4	99.8	104.3	105.6	106.0	107.1
3	99.5	100.1	100.4	99.7	103.6	104.6	104.6	105.2
4	100.3	101.4	101.7	99.2	102.8	103.9	103.3	103.8
5	100.1	101.8	101.9	98.9	102.3	102.9	102.6	103.3
6	99.6	101.1	100.7	98.9	102.2	102.6	103.0	103.4
7	98.9	100.2	99.6	99.1	102.7	103.3	103.8	104.6
8	98.5	99.5	99.0	99.3	103.7	104.0	105.1	106.6

INSIDE RADIAL HEAT FLUXES - BTU/(SQ.FT.-HR)

	1	2	3	7	8	9	10	11
1	327.0	327.1	327.1	327.2	328.1	328.4	328.5	328.7
2	327.0	327.1	327.1	327.2	328.0	328.3	328.4	328.6
3	327.2	327.3	327.3	327.2	327.9	328.1	328.1	328.2
4	327.3	327.5	327.6	327.1	327.8	328.0	327.9	327.9
5	327.3	327.6	327.6	327.0	327.7	327.8	327.7	327.9
6	327.2	327.4	327.4	327.0	327.7	327.7	327.8	327.9
7	327.0	327.3	327.2	327.1	327.7	327.9	327.9	328.1
8	327.0	327.2	327.1	327.1	327.9	328.0	328.2	328.5

BULK FLUID TEMPERATURES - DEGREES F

1	2	3	7	8	9	10	11
89.2	90.2	90.5	90.6	90.9	91.3	91.9	92.6

CORRECTED INLET BULK TEMPERATURE= 88.1 DEG. F

CORRECTED OUTLET BULK TEMPERATURE= 93.0 DEG. F

RUN NUMBER 141

REYNOLDS NUMBER = 332.338
PRANDTL NUMBER = 115.915
HEAT INPUT=AMP*VOLT*C-QL= 1127.467 BTU/HR
HEAT OUTPUT=M*CP*(T2-T1)= 934.730 BTU/HR
HEAT LOSS = -18.525 BTU/HR
AVERAGE REYNOLDS NUMBER = 348.024
% ERROR IN HEAT BALANCE = 17.095

LOCAL HEAT TRANSFER COEFFICIENT - BTU/(HR-SQ.FT-DEG.F)

	1	2	3	7	8	9	10	11
1	36.3	37.2	37.4	40.0	25.1	22.8	21.4	21.4
2	34.4	36.0	36.2	40.0	25.3	23.2	22.3	22.1
3	32.7	33.8	32.9	40.0	26.8	24.7	24.4	25.1
4	30.6	30.1	29.6	42.1	28.4	26.1	26.8	28.1
5	30.9	29.0	28.9	42.6	29.7	27.6	29.0	29.6
6	22.1	30.6	31.9	43.7	29.9	28.3	28.5	29.3
7	34.4	33.4	35.4	43.2	28.6	26.9	26.4	26.7
8	35.9	36.0	37.4	42.1	26.8	25.5	23.9	22.8

AVERAGE LOCAL HEAT TRANSFER COEFFICIENT - BTU/(HR-SQ.FT-DEG.)

1	2	3	7	8	9	10	11
33.4	33.3	33.7	41.7	27.6	25.6	25.3	25.6

AVERAGE LOCAL HEAT TRANSFER COEFFICIENT - BTU/(HR-SQ.FT-DEG.F) BY SECOND DEF.

1	2	3	7	8	9	10	11
33.3	33.0	33.4	41.7	27.5	25.5	25.1	25.3

RUN NUMBER 141

INSIDE SURFACE TEMPERATURES - DEGREES F

	1	2	3	7	8	9	10	11
1	94.5	95.1	95.3	94.8	99.9	101.5	103.0	103.6
2	95.0	95.4	95.6	94.8	99.8	101.3	102.4	103.1
3	95.5	96.0	96.5	94.8	99.1	100.4	101.1	101.3
4	96.2	97.2	97.6	94.4	98.4	99.7	99.9	99.9
5	96.1	97.6	97.9	94.3	97.9	99.0	99.0	99.3
6	95.7	97.0	96.8	94.1	97.8	98.7	99.2	99.4
7	95.0	96.1	95.6	94.2	98.3	99.3	100.1	100.5
8	94.6	95.4	95.3	94.4	99.1	100.0	101.4	102.6

INSIDE RADIAL HEAT FLUXES - BTU/(SQ.FT.-HR)

	1	2	3	7	8	9	10	11
1	326.2	326.3	326.4	326.3	327.2	327.5	327.8	327.9
2	326.3	326.4	326.4	326.3	327.2	327.5	327.7	327.8
3	326.4	326.5	326.6	326.3	327.1	327.3	327.4	327.5
4	326.5	326.7	326.8	326.2	327.0	327.2	327.2	327.2
5	326.5	326.8	326.9	326.2	326.9	327.1	327.1	327.1
6	326.5	326.7	326.7	326.2	326.8	327.0	327.1	327.1
7	326.3	326.5	326.5	326.2	326.9	327.1	327.3	327.3
8	326.3	326.4	326.4	326.2	327.1	327.2	327.5	327.7

BULK FLUID TEMPERATURES - DEGREES F

1	2	3	7	8	9	10	11
85.5	86.3	86.6	86.6	86.9	87.2	87.7	88.2

CORRECTED INLET BULK TEMPERATURE= 84.6 DEG. F

CORRECTED OUTLET BULK TEMPERATURE= 88.6 DEG. F

RUN NUMBER 151

```
REYNOLDS NUMBER           =  392.631
PRANDTL NUMBER            =  140.257
HEAT INPUT=AMP*VOLT*C-UL= 1144.072  BTU/HR
HEAT OUTPUT=M*CP*(T2-T1)= 1075.487  BTU/HR
HEAT LOSS                 =  -35.130  BTU/HR
AVERAGE REYNOLDS NUMBER =  336.011
% ERROR IN HEAT BALANCE =    5.995
```

LOCAL HEAT TRANSFER COEFFICIENT - BTU/(HR-SQ.FT-DEG.F)

	1	2	3	7	8	9	10	11
1	34.6	33.3	34.1	45.3	26.0	22.8	20.9	20.4
2	33.6	32.6	32.7	45.3	26.4	24.0	21.8	20.8
3	32.2	31.0	30.5	45.3	27.5	25.5	23.6	23.1
4	31.0	28.6	27.9	46.6	29.2	25.9	25.2	25.1
5	31.0	27.9	27.9	47.2	30.3	27.2	26.4	26.5
6	31.6	29.1	30.0	48.7	30.6	28.1	26.2	26.5
7	33.2	31.0	32.7	47.9	29.2	26.1	25.0	25.5
8	34.3	32.6	34.1	47.2	27.3	25.3	23.1	21.6

AVERAGE LOCAL HEAT TRANSFER COEFFICIENT - BTU/(HR-SQ.FT-DEG.)

1	2	3	7	8	9	10	11
32.7	30.8	31.2	46.7	28.3	25.6	24.0	23.7

AVERAGE LOCAL HEAT TRANSFER COEFFICIENT - BTU/(HR-SQ.FT-DEG.F) BY SECOND DEF.

1	2	3	7	8	9	10	11
32.6	30.6	31.1	46.7	28.2	25.5	23.9	23.5

RUN NUMBER 151

INSIDE SURFACE TEMPERATURES - DEGREES F

	1	2	3	7	8	9	10	11
1	84.7	85.9	85.9	83.6	89.2	91.2	93.1	94.0
2	85.0	86.1	86.3	83.6	89.0	90.5	92.4	93.7
3	85.4	86.6	87.0	83.6	88.5	89.7	91.3	92.1
4	85.8	87.5	88.0	83.4	87.8	89.5	90.4	91.0
5	85.8	87.8	88.0	83.3	87.4	88.9	89.8	90.3
6	85.6	87.3	87.2	83.1	87.3	88.5	89.9	90.3
7	85.1	86.6	86.3	83.2	87.8	89.4	90.5	90.8
8	84.8	86.1	85.9	83.3	88.6	89.8	91.6	93.1

INSIDE RADIAL HEAT FLUXES - BTU/(SQ.FT.-HR)

	1	2	3	7	8	9	10	11
1	324.4	324.7	324.7	324.2	325.3	325.6	326.0	326.1
2	324.5	324.7	324.7	324.2	325.2	325.5	325.9	326.1
3	324.6	324.8	324.9	324.2	325.1	325.4	325.6	325.8
4	324.6	325.0	325.0	324.2	325.0	325.3	325.5	325.6
5	324.6	325.0	325.0	324.2	324.9	325.2	325.4	325.5
6	324.6	324.9	324.9	324.2	324.9	325.1	325.4	325.5
7	324.5	324.8	324.7	324.2	325.0	325.3	325.5	325.6
8	324.5	324.7	324.7	324.2	325.2	325.4	325.7	326.0

BULK FLUID TEMPERATURES - DEGREES F

1	2	3	7	8	9	10	11
75.3	76.1	76.4	76.4	76.7	76.9	77.5	78.0

CORRECTED INLET BULK TEMPERATURE= 74.5 DEG. F

CORRECTED OUTLET BULK TEMPERATURE= 78.3 DEG. F

RUN NUMBER 172

REYNOLDS NUMBER = 440.916
PRANDTL NUMBER = 131.891
HEAT INPUT=AMP*VOLT*C-QL= 1168.853 BTU/HR
HEAT OUTPUT=M*CP*(T2-T1)= 1105.138 BTU/HR
HEAT LOSS = -26.643 BTU/HR
AVERAGE REYNOLDS NUMBER = 467.000
% ERROR IN HEAT BALANCE = 5.451

LOCAL HEAT TRANSFER COEFFICIENT - BTU/(HR-SQ.FT-DEG.F)

	1	2	3	7	8	9	10	11
1	36.2	34.0	34.3	75.1	35.6	27.8	23.5	21.9
2	35.8	33.3	32.9	73.4	35.2	28.5	24.1	22.2
3	34.3	32.0	31.1	73.4	36.0	29.8	25.9	24.5
4	32.9	30.0	29.1	65.9	37.2	30.3	27.4	26.5
5	32.6	29.4	28.6	62.2	38.5	31.5	28.3	27.6
6	33.2	30.5	30.5	71.8	39.0	32.5	28.1	27.6
7	34.7	32.4	32.9	76.3	38.1	30.6	26.7	26.1
8	35.4	33.7	34.0	78.7	36.8	30.1	25.1	23.0

AVERAGE LOCAL HEAT TRANSFER COEFFICIENT - BTU/(HR-SQ.FT-DEG.)

1	2	3	7	8	9	10	11
34.4	31.9	31.7	72.2	37.1	30.1	26.1	24.9

AVERAGE LOCAL HEAT TRANSFER COEFFICIENT - BTU/(HR-SQ.FT-DEG.F) BY SECOND DEF.

1	2	3	7	8	9	10	11
34.3	31.8	31.6	71.8	37.0	30.1	26.0	24.7

RUN NUMBER 172

INSIDE SURFACE TEMPERATURES - DEGREES F

	1	2	3	7	8	9	10	11
1	87.7	88.9	89.0	83.9	88.9	91.7	94.3	95.7
2	87.8	89.1	89.4	84.0	89.0	91.4	93.9	95.5
3	88.2	89.5	90.0	84.0	88.8	90.9	93.0	94.1
4	88.6	90.2	90.7	84.5	88.5	90.7	92.3	93.1
5	88.7	90.4	90.9	84.8	88.2	90.3	91.9	92.6
6	88.5	90.0	90.2	84.1	88.1	90.0	92.0	92.6
7	88.1	89.4	89.4	83.8	88.3	90.6	92.6	93.3
8	87.9	89.0	89.1	83.7	88.6	90.8	93.4	95.0

INSIDE RADIAL HEAT FLUXES - BTU/(SQ.FT.-HR)

	1	2	3	7	8	9	10	11
1	325.0	325.2	325.2	324.3	325.2	325.7	326.2	326.5
2	325.0	325.2	325.3	324.3	325.2	325.7	326.1	326.4
3	325.1	325.3	325.4	324.3	325.2	325.6	326.0	326.2
4	325.2	325.4	325.5	324.4	325.1	325.5	325.8	326.0
5	325.2	325.5	325.6	324.5	325.1	325.5	325.8	325.9
6	325.1	325.4	325.4	324.3	325.1	325.4	325.8	325.9
7	325.1	325.3	325.3	324.3	325.1	325.5	325.9	326.0
8	325.0	325.2	325.2	324.3	325.2	325.6	326.0	326.3

BULK FLUID TEMPERATURES - DEGREES F

1	2	3	7	8	9	10	11
78.7	79.3	79.5	79.6	79.8	80.0	80.4	80.8

CORRECTED INLET BULK TEMPERATURE= 78.0 DEG. F

CORRECTED OUTLET BULK TEMPERATURE= 81.1 DEG. F

RUN NUMBER 182

REYNOLDS NUMBER	=	516.070	
PRANDTL NUMBER	=	130.028	
HEAT INPUT=AMP*VOLT*C-OL	=	1140.638	BTU/HR
HEAT OUTPUT=M*CP*(T2-T1)	=	1109.104	BTU/HR
HEAT LOSS	=	-32.379	BTU/HR
AVERAGE REYNOLDS NUMBER	=	528.251	
% ERROR IN HEAT BALANCE	=	2.765	

LOCAL HEAT TRANSFER COEFFICIENT - BTU/(HR-SQ.FT-DEG.F)

	1	2	3	7	8	9	10	11
1	36.4	34.0	33.5	95.9	41.4	30.6	24.4	23.0
2	36.0	33.6	32.4	93.0	40.9	31.5	25.0	23.3
3	34.8	32.2	30.9	90.4	40.3	32.4	26.4	25.5
4	33.7	30.4	28.6	77.1	40.9	32.8	27.6	27.3
5	33.7	29.8	28.6	70.2	41.4	33.5	28.6	28.5
6	33.7	30.7	30.3	65.5	42.5	34.6	28.3	28.5
7	34.8	32.2	32.4	93.0	41.9	32.8	27.1	26.4
8	35.6	33.6	33.5	98.9	41.4	32.4	25.8	23.8

AVERAGE LOCAL HEAT TRANSFER COEFFICIENT - BTU/(HR-SQ.FT-DEG.)

1	2	3	7	8	9	10	11
34.9	32.1	31.3	88.0	41.3	32.6	26.6	25.8

AVERAGE LOCAL HEAT TRANSFER COEFFICIENT - BTU/(HR-SQ.FT-DEG.F) BY SECOND DEF.

1	2	3	7	8	9	10	11
34.8	32.0	31.2	86.9	41.3	32.5	26.6	25.6

RUN NUMBER 182

INSIDE SURFACE TEMPERATURES - DEGREES F

	1	2	3	7	8	9	10	11
1	88.2	89.4	89.7	83.6	88.1	91.0	94.0	95.2
2	88.3	89.5	90.0	83.7	88.2	90.7	93.7	95.0
3	88.6	89.9	90.5	83.8	88.3	90.4	93.0	93.8
4	88.9	90.5	91.3	84.4	88.2	90.3	92.5	93.0
5	88.9	90.7	91.3	84.8	88.1	90.1	92.1	92.5
6	88.9	90.4	90.7	84.0	87.9	89.8	92.2	92.5
7	88.6	89.9	90.0	83.7	88.0	90.3	92.7	93.4
8	88.4	89.5	89.7	83.5	88.1	90.4	93.3	94.7

INSIDE RADIAL HEAT FLUXES - BTU/(SQ.FT.-HR)

	1	2	3	7	8	9	10	11
1	315.2	315.4	315.4	314.3	315.1	315.7	316.2	316.4
2	315.2	315.4	315.5	314.4	315.2	315.6	316.1	316.4
3	315.2	315.5	315.6	314.4	315.2	315.5	316.0	316.1
4	315.3	315.6	315.7	314.5	315.2	315.5	315.9	316.0
5	315.3	315.6	315.7	314.6	315.1	315.5	315.8	315.9
6	315.3	315.5	315.6	314.4	315.1	315.4	315.9	315.9
7	315.2	315.5	315.5	314.4	315.1	315.5	316.0	316.1
8	315.2	315.4	315.4	314.3	315.1	315.5	316.1	316.3

BULK FLUID TEMPERATURES - DEGREES F

1	2	3	7	8	9	10	11
79.6	80.1	80.3	80.3	80.5	80.7	81.0	81.4

CORRECTED INLET BULK TEMPERATURE= 79.0 DEG. F

CORRECTED OUTLET BULK TEMPERATURE= 81.6 DEG. F

APPENDIX G

COMPUTER PROGRAM LISTING

```
$JOB TIME=10, NOSUBCHK
      DIMENSION COEFF(11,8),ACOEFF(11),BLNUSS(11,8),ANUSSL(11)
      DIMENSION AL(11),QFL(11),BCOEF(11)
      DIMENSION OUT(8)
      REAL MW,L,LTOTAL,IRENO,IQFLUX
      DIMENSION GRS(11),IRENO(11),PRD(11),PAL(11),GRAEZ(11)
      COMMON TOSURF(11,8),TISURF(11,8),TCONDK(11,8)
      COMMON TBULK(11),FILMTM(11),TIMSUF(11),T(11)
      COMMON COND(11),SPHT(11),ROU(11),VISC(11),BETA(11)
      COMMON TIN,TOUT,QLOSST
      COMMON TROOM,VOLTS,TAMPS,MW,NRON,TBATH
      COMMON L(11),LTOTAL,DIN,DOUT
      COMMON CDEN,CDENSQ,RESIST(11,8)
      COMMON ICFLUX(11,8)
      L(1)=4.00
      L(2)=7.7499
       L(3)=8.8161
      L(4)=0.0
      L(5)=0.0
      L(6)=0.0
      L(7)=0.1509
      L(8)=1.25
      L(9)=2.5
      L(10)=5.0
      L(11)=7.5
       LTOTAL=23.00
      AL(1)=4.0
      AL(2)=7.7499
      AL(3)=8.8161
      AL(4)=0.0
      AL(5)=0.0
      AL(6)=0.0
      AL(7)=9.1501
      AL(8)=10.2503
      AL(9)=11.5
      AL(10)=14.0
      AL(11)=16.5
      ALTCT=18.0
      READ(5,10)NRUN
   10 FORMAT(I3)
      CALL READS
      CALL CORECT
C     CALCULATION OF CURRENT DENSITY J. THIS IS USED TO CALCULATE INSIDE
C     SURFACE TEMPERATURE AND RADIAL HEAT FLUX.
C
      XAREA=0.0000901951
      CDEN=(0.5*TAMPS)/XAREA
       CDENSC=CDEN*CDEN
      G=4.17EC8
      DIN=0.05167
      DOUT=0.C6250
      CALL ERSTVT
      CALL THCOND
      CALL ISURFT
      CALL IFLUX
C     CALCULATION OF BULK TEMPERATURE FOR STATION 1 - 11
C
      DO 325 IST=1,11
      TBULK(IST)=TIN+((TOUT-TIN)*AL(IST)/ALTCT)
  325 CONTINUE
```

```
C     CALCULATION OF LOCAL HEAT TRANSFER COEFFICIENT -  STATION 1 - 3
C
      DO 350 IST=1,3
       DO 350 IPR=1,8
      COEFF(IST,IPR)=IQFLUX(IST,IPR)/(TISURF(IST,IPR)-TBULK(IST))
  350 CONTINUE
C     CALCULATION OF LOCAL HEAT TRANSFER COEFFICIENT -  STATION 7 - 11
      DO 375 IST=7,11
      DO 375 IPR=1,8
      COEFF(IST,IPR)=IQFLUX(IST,IPR)/(TISURF(IST,IPR)-TBULK(IST))
  375 CONTINUE
C     CALCULATION OF AVERAGE LOCAL HEAT TRANSFER COEFFICIENT -  STATION
C     1 - 3
      DO 2 IST=1,3
      ACOF=0.0
      DO 3 IPR=1,8
      ACOF=ACOF+COEFF(IST,IPR)
    3 CONTINUE
      ACOEFF(IST)=ACOF/8.0
    2 CONTINUE
C     CALCULATION OF AVERAGE LOCAL HEAT TRANSFER COEFFICIENT -  STATION
C     7 - 11
      DO 4 IST=7,11
       BCOF=0.0
      DO 6 IPR=1,8
      BCOF=BCOF+COEFF(IST,IPR)
    6 CONTINUE
      ACOEFF(IST)=BCOF/8.0
    4 CONTINUE
C     CALCULATES MEAN INSIDE SURFACE TEMPERATURES -  STATION - 1 - 3
      DO 650 IST=1,3
      TI=0.0
      DO 660 IPR=1,8
      TI=TI+TISURF(IST,IPR)
  660 CONTINUE
      TIMSUF(IST)=TI/8.0
  650 CONTINUE
C     CALCULATES MEAN INSIDE SURFACE TEMPERATURES -  STATION  7 - 11
C
      DO 675 IST=7,11
      S=0.0
      DO 680 IPR=1,8
      S=S+TISURF(IST,IPR)
  680 CONTINUE
      TIMSUF(IST)=S/8.0
  675 CONTINUE
C     CALCULATES AVERAGE HEAT FLUX AT EACH STATION TO CALCULATE AVERAGE
C     HEAT TRANSFER COEFFICIENT BY SECOND METHOD
      DO 651 IST=1,3
      FL=0.0
      DO 652 IPR=1,8
      FL=FL+IQFLUX(IST,IPR)
  652 CONTINUE
      QFL(IST)=FL/8.0
  651 CONTINUE
      DO 653 IST=7,11
      SFL=0.0
      DO 654 IPR=1,8
      SFL=SFL+IQFLUX(IST,IPR)
  654 CONTINUE
```

```
      QFL(IST)=SFL/8.0
  653 CONTINUE
C***************************************                *************************
C     CALCULATES AVERAGE HEAT FLUX AT EACH STATION TO CALCULATE AVERAGE
C     HEAT TRANSFER COEFFICIENT BY SECOND METHOD
C
      DO 656 IST=1,3
      BCOEFF(IST)=QFL(IST)/(TIMSUF(IST)-TBULK(IST))
  656 CONTINUE
      DO 657 IST=7,11
      BCOEFF(IST)=QFL(IST)/(TIMSUF(IST)-TBULK(IST))
  657 CONTINUE
C     CALCULATES FILM TEMPERATURE BY ARITHMETIC AVERAGE OF BULK AND
C     MEAN INSIDE SURFACE TEMPERATURES   STATION  1 - 3
      DO 700 IST=1,3
      FILMTM(IST)=(TIMSUF(IST)+TBULK(IST))/2.0
  700 CONTINUE
C     CALCULATES FILM TEMPERATURE BY ARITHMETIC AVERAGE OF BULK AND
C     MEAN INSIDE SURFACE TEMPERATURES   STATION  7 - 11
      DO 725 IST=7,11
      FILMTM(IST)=(TIMSUF(IST)+TBULK(IST))/2.0
  725 CONTINUE
      CALL PHROP
C     CALCULATES LOCAL NUSSELT NUMBER  STATION  1 - 3
C
      DO 450 IST=1,3
      DO 450 IPR=1,8
      BLNUSS(IST,IPR)=COEFF(IST,IPR)*DIN/COND(IST)
  450 CONTINUE
C     CALCULATES LOCAL NUSSELT NUMBER STATION 7 - 11
C
      DO 475 IST=7,11
      DO 475 IPR=1,8
      BLNUSS(IST,IPR)=COEFF(IST,IPR)*DIN/COND(IST)
  475 CONTINUE
C     CALCULATES AVERAGE LOCAL NUSSELT NUMBER  STATION 1 - 3
      DO 510 IST=1,3
      SUM=0.0
      DO 500 IPR=1,8
      SUM=SUM+BLNUSS(IST,IPR)
  500 CONTINUE
      ANUSSL(IST)=SUM/8.0
  510 CONTINUE
C     CALCULATES AVERAGE LOCAL NUSSELT NUMBER  STATION 7 - 11
      DO 520 IST=7,11
      BSUM=0.0
      DO 525 IPR=1,8
      BSUM=BSUM+BLNUSS(IST,IPR)
  525 CONTINUE
      ANUSSL(IST)=BSUM/8.0
  520 CONTINUE
C     CALCULATES LOCAL GRAETZ NUMBER  STATION 1 - 3
C
      DO 550 IST=1,3
      GRAEZ(IST)=MW*SPHT(IST)/(COND(IST)*L(IST))
  550 CONTINUE
C     CALCULATES LOCAL GRAETZ NUMBER  STATION 7 - 11
C
      DO 575 IST=7,11
      GRAEZ(IST)=MW*SPHT(IST)/(COND(IST)*L(IST))
```

```
  575 CONTINUE
C     ****************************************************************
C
C     CALCULATION OF HEAT INPUT
       QI=(TAMPS*VOLTS*3.41213)-QLOSST
       TCBA=(TIN+TOUT)/2.0
       SHEAT=5.18956E-1 +6.2290E-4*TCBA
       QOUT=MW*SHEAT*(TOUT-TIN)
       BISC=2.42*(1.6746E2 -5.4455*TBATH +8.3752E-2*TBATH*TBATH
      $-7.3076E-4*TBATH*TBATH*TBATH +3.7748E-6*TBATH**4 -1.1386E-8*
      $TBATH**5 +1.8487E-11*TBATH**6 -1.2463E-14*TBATH**7)
       RENO=4*MW/(DIN*BISC*3.14159)
       QPER=100.0*(QI-QOUT)/QI
C
       ACOND=241.91*(7.576925-4 -1.0E-6*TCBA)
       CISC=2.42*(1.6746E2 -5.4455*TCBA +8.3752E-2*TCBA*TCBA -7.3076E-4
      $*TCBA*TCBA*TCBA +3.7748E-6*TCBA**4 -1.1386E-8*TCBA**5 +1.8487E-11
      $*TCBA**6 -1.2463E-14*TCBA**7)
C
       PRNO=(SHEAT*CISC)/ACOND
C     CALCULATES GRASHOF NUMBER AT EACH STATION
       DCUBE=DIN*DIN*DIN
       DO 730 IST=1,3
       GRS(IST)=DCUBE*G*BETA(IST)*ROU(IST)**2*(TIMSUF(IST)-TBULK(IST))/(V
      $ISC(IST)*VISC(IST))
  730 CONTINUE
C     CALCULATES GRASHOF NUMBER AT EACH STATION
       DO 740 IST =7,11
       GRS(IST)=DCUBE*G*BETA(IST)*ROU(IST)**2*(TIMSUF(IST)-TBULK(IST))/(V
      $ISC(IST)*VISC(IST))
  740 CONTINUE
C     CALCULATES LOCAL REYNOLDS NUMBER  STATION  1 - 3
       DO 750 IST=1,3
       IRENO(IST)=4*(MW/(VISC(IST)*DIN*3.14159))
  750 CONTINUE
C     CALCULATES LOCAL REYNOLDS NUMBER  STATION  7 - 11
       DO 760 IST=7,11
       IRENO(IST)=4*(MW/(VISC(IST)*DIN*3.14159))
  760 CONTINUE
       IRENO(4)=0.0
       IRENO(5)=0.0
       IRENO(6)=0.0
C     CALCULATES AVERAGE REYNOLDS NUMBER
       BRENO=0.0
       DO 751 IST=1,11
       BRENO=BRENO+IRENO(IST)
  751 CONTINUE
       ARENO=BRENO/8.0
       DO 770 IST=1,3
       PRD(IST)=(SPHT(IST)*VISC(IST))/COND(IST)
  770 CONTINUE
       DO 780 IST=7,11
       PRD(IST)=(SPHT(IST)*VISC(IST))/COND(IST)
  780 CONTINUE
       DO 790 IST=1,3
       RAL(IST)=GRS(IST)*PRD(IST)
  790 CONTINUE
       DO 800 IST=7,11
       RAL(IST)=GRS(IST)*PRD(IST)
  800 CONTINUE
```

```
      WRITE(6,111)
  111 FORMAT(1H1)
      WRITE(6,112)NRUN
  112 FORMAT(23X,15('-')/23X,'RUN NUMBER   ',I3/23X,15('-')//)
      WRITE(6,113)
  113 FORMAT(8X,'  INSIDE SURFACE TEMPERATURES - DEGREES F'//
     $9X,'1',6X,'2',7X,'3',7X,'7',7X,'8',7X,'9',7X,'10',6X,'11',//)
      DO 114 IPR=1,8
      J=1
      DO 116 IST=1,11
      IF(IST.GE.4.AND.IST.LE.6) GO TO 116
      OUT(J)=TISURF(IST,IPR)
      J=J+1
  116 CONTINUE
  114 WRITE(6,117)IPR,(OUT(K),K=1,8)
  117 FORMAT(3X,I1,2X,F6.1,1X,F6.1,6(2X,F6.1))
      WRITE(6,211)
  211 FORMAT(//)
      WRITE(6,118)
  118 FORMAT(8X,'  INSIDE RADIAL HEAT FLUXES - BTU/(SQ.FT.-HR)'//
     $9X,'1',6X,'2',7X,'3',7X,'7',7X,'8',7X,'9',7X,'10',6X,'11',//)
      DO 119 IPR=1,8
      J=1
      DO 121 IST=1,11
      IF(IST.GE.4.AND.IST.LE.6) GO TO 121
      OUT(J)=IQFLUX(IST,IPR)
      J=J+1
  121 CONTINUE
  119 WRITE(6,122)IPR,(OUT(K),K=1,8)
  122 FORMAT(3X,I1,2X,F6.1,1X,F6.1,6(2X,F6.1))
      WRITE(6,123) .
  123 FORMAT(//,8X,'  BULK FLUID TEMPERATURES - DEGREES F'//,
     $10X,'1',6X,'2',7X,'3',7X,'7',7X,'8',7X,'9',7X,'10',6X,'11',//)
      J=1
      DO 124 IST=1,11
      IF(IST.GE.4.AND.IST.LE.6) GO TO 126
      OUT(J)=TBULK(IST)
      J=J+1
  126 CONTINUE
  124 CONTINUE
      WRITE(6,127)(OUT(K),K=1,8)
  127 FORMAT(6X,3(1X,F6.1),5(2X,F6.1))
      WRITE(6,128)TIN,TOUT
  128 FORMAT(//8X,'  CORRECTED INLET BULK TEMPERATURE= ',F6.1,' DEG. F '
     $,//8X,'  CORRECTED OUTLET BULK TEMPERATURE=',F6.1,' DEG. F ')
      WRITE(6,11)
   11 FORMAT(1H1)
      WRITE(6,312)NRUN,RENO,PRNO,QI,QOUT,QLOSST,ARENO,QPER
  312 FORMAT(23X,15('-')/23X,'RUN NUMBER   ',I3/23X,15('-')//
     $        10X,'REYNOLDS NUMBER            =',F9.3/
     $        10X,'PRANDTL NUMBER             =',F9.3/
     $        10X,'HEAT INPUT=AMP*VOLT*C-QL=',F9.3,2X,'BTU/HR'/
     $        10X,'HEAT OUTPUT=M*CP*(T2-T1)=',F9.3,2X,'BTU/HR'/
     $        10X,'HEAT LOSS                  =',F9.3,2X,'BTU/HR'/
     $        10X,'AVERAGE REYNOLDS NUMBER =',F9.3/
     $        10X,'% ERROR IN HEAT BALANCE =',F9.3)
      WRITE(6,129)
  129 FORMAT(//,8X,'  LOCAL HEAT TRANSFER COEFFICIENT - BTU/(HR-SQ.FT-DE
     $G.F)'//,9X,'1',6X,'2',7X,'3',7X,'7',7X,'8',7X,'9',7X,'10',6X,'11',
     $//)
```

```
      DO 131 IPR=1,8
      J=1
      DO 132 IST=1,11
      IF(IST.GE.4.AND.IST.LE.6) GO TO 132
      OUT(J)=COEFF(IST,IPR)
      J=J+1
  132 CONTINUE
  131 WRITE(6,133)IPR,(OUT(K),K=1,8)
  133 FORMAT(3X,I1,2X,F6.1,1X,F6.1,6(2X,F6.1))
      WRITE(6,134)
  134 FORMAT(//,8X,'  AVERAGE LOCAL HEAT TRANSFER COEFFICIENT - BTU/(HR-
     $SQ.FT-DEG.F)'//10X,'1',6X,'2',6X,'3',7X,'7',7X,'8',7X,'9',7X,'10',6
     $X,'11',//)
      J=1
      DO 136 IST=1,11
      IF(IST.GE.4.AND.IST.LE.6) GO TO 137
      OUT(J)=ACOEFF(IST)
      J=J+1
  137 CONTINUE
  136 CONTINUE
      WRITE(6,138)(OUT(K),K=1,8)
  138 FORMAT(6X,3(1X,F6.1),5(2X,F6.1))
      WRITE(6,139)
  139 FORMAT(//8X,'  AVERAGE LOCAL HEAT TRANSFER COEFFICIENT - BTU/(HR-S
     $Q.FT-DEG.F) BY SECOND DEF.'//10X,'1',6X,'2',6X,'3',7X,'7',7X,'8',7
     $X,'9',7X,'10',6X,'11',//)
      J=1
      DO 141 IST=1,11
      IF(IST.GE.4.AND.IST.LE.6) GO TO 142
      OUT(J)=BCOEF(IST)
      J=J+1
  142 CONTINUE
  141 CONTINUE
      WRITE(6,143)(OUT(K),K=1,8)
  143 FORMAT(6X,3(1X,F6.1),5(2X,F6.1))
      WRITE(6,24)
   24 FORMAT(1H1)
      WRITE(6,72)
   72 FORMAT(//1X,'AVERAGE LOCAL NUSSELT NUMBER')
   63 FORMAT(/10X,'1',7X,'2',7X,'3')
   66 FORMAT(/10X,'7',6X,'8',5X,'9',5X,'10',7X,'11')
   69 FORMAT(5X,F8.1,2F7.1)
   71 FORMAT(5X,F8.1,4F7.1)
      WRITE(6,63)
      WRITE(6,69)(ANUSSL(IST),IST=1,3)
      WRITE(6,66)
      WRITE(6,71)(ANUSSL(IST),IST=7,11)
      WRITE(6,76)
   76 FORMAT(//1X,'AVERAGE LOCAL GRAETZ NUMBER')
      WRITE(6,63)
      WRITE(6,69)(GRAEZ(IST),IST=1,3)
      WRITE(6,66)
      WRITE(6,71)(GRAEZ(IST),IST=7,11)
      WRITE(6,79)
   79 FORMAT(//1X,'LOCAL AVERAGE GRASHOF NUMBER')
      WRITE(6,63)
      WRITE(6,99)(GRS(IST),IST=1,3)
   99 FORMAT(1X,3F9.2)
      WRITE(6,66)
      WRITE(6,101)(GRS(IST),IST=7,11)
```

```
  101 FORMAT(1X,5F9.2)
      WRITE(6,83)
   83 FORMAT(1H1)
      WRITE(6,84)
   84 FORMAT(//1X,'LOCAL AVERAGE REYNOLDS NUMBER')
      WRITE(6,63)
      WRITE(6,69)(IRENO(IST),IST=1,3)
      WRITE(6,66)
      WRITE(6,71)(IRENO(IST),IST=7,11)
      WRITE(6,88)
   88 FORMAT(//1X,'LOCAL AVERAGE PRANDTL NUMBER')
      WRITE(6,63)
      WRITE(6,69)(PRD(IST),IST=1,3)
      WRITE(6,66)
      WRITE(6,71)(PRD(IST),IST=7,11)
C
      WRITE(6,92)
   92 FORMAT(//1X,'LOCAL RAYLEIGH NUMBER')
      WRITE(6,91)
   91 FORMAT(7X,'1',8X,'2',9X,'3')
      WRITE(6,93)(RAL(IST),IST=1,3)
   93 FORMAT(5X,3F9.1)
      WRITE(6,96)
   96 FORMAT(//9X,'7',8X,'8',8X,'9',8X,'10',8X,'11')
      WRITE(6,94)(RAL(IST),IST=7,11)
   94 FORMAT(5X,5F9.1)
      WRITE(6,98)
   98 FORMAT(1H1)
      STOP
      END
C     ****************************************************************
C     ****************************************************************

      SUBROUTINE READS
      REAL MW,L,LTOTAL,IRENO,IQFLUX
      COMMON TOSURF(11,8),TISURF(11,8),TCONDK(11,8)
      COMMON TBULK(11),FIL4TM(11),TIMSUF(11),T(11)
      COMMON COND(11),SPHT(11),ROU(11),VISC(11),BETA(11)
      COMMON TIN,TOUT,QLOSST
      COMMON TROOM,VOLTS,TAMPS,MW,NRUN,TBATH
      COMMON L(11),LTOTAL,DIN,DOUT
      COMMON CDEN,CDENSQ,RESIST(11,8)
      COMMON IQFLUX(11,8)
      WRITE(6,104)
  104 FORMAT(1H1)
C    READS PHYSICAL QUANTITIES MEASURED
      READ(5,1)NRUN,MW,TIN,TOUT,VOLTS,TAMPS,TROOM,TBATH
    1 FORMAT(I10,7F10.0)
      READ(5,2)((TOSURF(IST,IPR),IPR=1,8),IST=1,11)
    2 FORMAT(8F10.0)
C    WRITES PHYSICAL QUANTITIES MEASURED IN TABLE FORMAT
      WRITE(6,101)NRUN,MW,TIN,TOUT,VOLTS,TAMPS,TROOM,TBATH
  101 FORMAT(33X,15('-')/33X,'RUN NUMBER  ',I3/33X,15('-')//
     115X,'FLUID MASS FLOW RATE                    =',F8.2,2X,'LBM/HOUR'/
     $15X,'UNCORRECTED INLET BULK TEMPERATURE      =',F8.2,2X,'DEGREES F'/
     $15X,'UNCORRECTED OUTLET BULK TEMPERATURE     =',F8.2,2X,'DEGREES F'/
     415X,'VOLTAGE DROP IN THE TEST SECTION        =',F8.2,2X,'VOLTS'/
     515X,'CURRENT TO THE TEST SECTION             =',F8.2,2X,'AMPS'/
     $15X,'ROOM TEMPERATURE                        =',F8.2,2X,'DEGREES F'/
     715X,'BULK BATH TEMPERATURE                   =',F8.2,2X,'DEGREES F'/
```

```
      8)
C     WRITES TITLE FOR OUTSIDE SURFACE TEMPERATURE
      WRITE(6,102)
  102 FORMAT(//20X,'  OUTSIDE SURFACE TEMPERATURES - DEGREES F'//
     $9X,'1',6X,'2',6X,'3',6X,'4',6X,'5',6X,'6',6X,'7',6X,'8',6X,'9',6X
     $'10',5X,'11'//)
      WRITE(6,103)(IPR,(TOSURF(IST,IPR),IST=1,11),IPR=1,8)
  103 FORMAT(3X,I1,F8.1,10F7.1)
      RETURN
      END
C     SUBROUTINE CORECT CORRECTS BULK TEMPERATURES AND CALCULATES HEAT
C     LOSS FROM THE TEST SECTION

      SUBROUTINE CORECT
      REAL MW,L,LTOTAL,IRENO,IQFLUX
      COMMON TOSURF(11,8),TISURF(11,8),TCONDK(11,8)
      COMMON TBULK(11),FILMTM(11),TIMSUF(11),T(11)
      COMMON COND(11),SPHT(11),ROU(11),VISC(11),BETA(11)
      COMMON TIN,TOUT,QLOSST
      COMMON TROOM,VOLTS,TAMPS,MW,NRUN,TBATH
      COMMON L(11),LTOTAL,DIN,DOUT
      COMMON CDEN,CDENSQ,RESIST(11,8)
      COMMON IQFLUX(11,8)
      TIN=TIN-0.77/(210.23-76.7)*(TIN-TROOM)
      TOUT=TOUT+1.13/(210.23-76.7)*(TOUT-TROOM)
C     CALCULATES HEAT LOSS FROM THE TEST SECTION
C       CONSTANTS 527.2,210.23, AND 76.7 ARE OBTAINED FROM CALIBRATION
C       DATA
      QLOSST=527.2/(210.23-76.7)*((TIN+TOUT)/2.0-TROOM)
      RETURN
      END
C
C
C

      SUBROUTINE THCOND
      REAL MW,L,LTOTAL,IRENO,IQFLUX
      COMMON TOSURF(11,8),TISURF(11,8),TCONDK(11,8)
      COMMON TBULK(11),FILMTM(11),TIMSUF(11),T(11)
      COMMON COND(11),SPHT(11),ROU(11),VISC(11),BETA(11)
      COMMON TIN,TOUT,QLOSST
      COMMON TROOM,VOLTS,TAMPS,MW,NRUN,TBATH
      COMMON L(11),LTOTAL,DIN,DOUT
      COMMON CDEN,CDENSQ,RESIST(11,8)
      COMMON IQFLUX(11,8)
C     TCONDK IN WATT/METER-DEGREES F
      DO 12 IST=1,11
      DO 12 IPR=1,8
      TCONDK(IST,IPR)=0.961516*(7.8034 +0.51691E-2*TOSURF(IST,IPR)
     $ -0.88501E-6*TOSURF(IST,IPR)*TOSURF(IST,IPR))
   12 CONTINUE
      RETURN
      END
C

      SUBROUTINE ERSTVT
      REAL MW,L,LTOTAL,IRENO,IQFLUX
      COMMON TOSURF(11,8),TISURF(11,8),TCONDK(11,8)
      COMMON TBULK(11),FILMTM(11),TIMSUF(11),T(11)
      COMMON COND(11),SPHT(11),ROU(11),VISC(11),BETA(11)
      COMMON TIN,TOUT,QLOSST
```

```
      COMMON TROOM,VOLTS,TAMPS,MW,NRUN,TBATH
      COMMON L(11),LTOTAL,DIN,DOUT
      COMMON CDEN,CDENSQ,RESIST(11,8)
      COMMON IOFLUX(11,8)
C     RESIST(IST,IPR)  IN OHMS METER IN THIS EQUATION
      DO 12 IST=1,11
      DO 12 IPR=1,8
      RESIST(IST,IPR)=0.0254*(0.2601E-4 + 0.137904E-7*TOSURF(IST,IPR) +
     $0.951585E-11*TOSURF(IST,IPR)*TOSURF(IST,IPR) -0.10119E-15*TOSURF
     $(IST,IPR)**3)
   12 CONTINUE
      RETURN
      END
C     SUBROUTINE IFLUX CALCULATES RADIAL HEAT FLUXES

      SUBROUTINE IFLUX
      REAL MW,L,LTOTAL,IRENO,IOFLUX
      COMMON TOSURF(11,8),TISURF(11,8),TCONDK(11,8)
      COMMON TBULK(11),FILMTM(11),TIMSUF(11),T(11)
      COMMON COND(11),SPHT(11),ROU(11),VISC(11),BETA(11)
      COMMON TIN,TOUT,OLOSST
      COMMON TROOM,VOLTS,TAMPS,MW,NRUN,TBATH
      COMMON L(11),LTOTAL,DIN,DOUT
      COMMON CDEN,CDENSQ,RESIST(11,8)
      COMMON IOFLUX(11,8)
C      IN THE CALCULATION OF IOFLUX 5.778477E-4 IS CONSTANAT.
       THIS CONSTANT COMES FROM THE TERM : 0.5*(R1**2-R2**2)/R1
       AND CONVERSION FACTOR FROM
C     WATT/(SQ.METER) TO BTU/(HR-SQ. FEET).
      DO 75 IST=1,3
      DO 75 IPR=1,8
      IOFLUX(IST,IPR)=(CDENSQ*RESIST(IST,IPR))*5.778477E-4
   75 CONTINUE
      DO 125 IST=7,11
      DO 125 IPR=1,8
      IOFLUX(IST,IPR)=(CDENSQ*RESIST(IST,IPR))*5.778477E-4
  125 CONTINUE
      RETURN
      END
C     SUBROUTINE ISURFT CALCULATES INSIDE SURFACE TEMPERATURES

      SUBROUTINE ISURFT
      REAL MW,L,LTOTAL,IRENO,IOFLUX
      COMMON TOSURF(11,8),TISURF(11,8),TCONDK(11,8)
      COMMON TBULK(11),FILMTM(11),TIMSUF(11),T(11)
      COMMON COND(11),SPHT(11),ROU(11),VISC(11),BETA(11)
      COMMON TIN,TOUT,OLOSST
      COMMON TROOM,VOLTS,TAMPS,MW,NRUN,TBATH
      COMMON L(11),LTOTAL,DIN,DOUT
      COMMON CDEN,CDENSQ,RESIST(11,8)
      COMMON IOFLUX(11,8)
C     IN THE EQUATION FOR THE CALCULATION OF THE INSIDE WALL TEMPRATURE
C      1.454146E-6 IS OBTAINED FROM THE EXPRESSION:  ((R1**2)-(R2**2))/4.
      + 0.5
C      *(R2**2)*LN(R2/R1). R1 AND R2 ARE RADIAL FROM SHELL BALANCE.
C      LN DENOTES NATURAL LOGARITHM IN THE ABOVE EXPRESSION
      DO 15 IST=1,3
      DO 15 IPR=1,8
      TISURF(IST,IPR)=TOSURF(IST,IPR)-((CDENSQ*RESIST(IST,IPR))/TCONDK(I
     $ST,IPR))*1.454146E-6
   15 CONTINUE
      DO 25 IST=7,11
```

```
      DO 25 IPR=1,8
      TISURF(IST,IPR)=TOSURF(IST,IPR)-((CDENSQ*RESIST(IST,IPR))/TCONDK(I
     $ST,IPR))*1.4541E-6
   25 CONTINUE
      RETURN
      END
C     SUBROUTINE PHROP EVALUATES PROPERTIES OF ETHYLENE GLYCOL AT FILM
C     TEMPERATURE
C
      SUBROUTINE PHROP
      REAL MW,L,LTOTAL,IRENO,IQFLUX
      COMMON TOSURF(11,8),TISURF(11,8),TCONDK(11,8)
      COMMON TBULK(11),FILMTM(11),TIMSUF(11),T(11)
      COMMON COND(11),SPHT(11),ROU(11),VISC(11),BETA(11)
      COMMON TIN,TOUT,QLOSST
      COMMON TROOM,VOLTS,TAMPS,MW,NRUN,TBATH
      COMMON L(11),LTOTAL,DIN,DOUT
      COMMON CDEN,CDENSQ,RESIST(11,8)
      COMMON IQFLUX(11,8)
C     *****    SPHT IN BTU/(LBM-DEG F)
C     *****    COND IN BTU/(HR-FT-DEG F)
C     *****    ROU IN LBM/CUBIC FEET
C     *****    1.8 IS A CONVERSION FACTOR. IT CONVERTS DEG. C TO DEF. F
C     THIS IS IN BETA EXPRESSION.
      DO 10 IST=1,3
      SPHT(IST)=5.18956E-1 +6.2290E-4*FILMTM(IST)
   10 CONTINUE
      DO 20 IST=7,11
      SPHT(IST)=5.18956E-1 +6.2290E-4*FILMTM(IST)
   20 CONTINUE
C
      DO 30 IST=1,3
      COND(IST)=241.91*(7.57692E-4 -1.0E-6*FILMTM(IST))
   30 CONTINUE
      DO 40 IST=7,11
      COND(IST)=241.91*(7.57692E-4 -1.0E-6*FILMTM(IST))
   40 CONTINUE
C
      DO 50 IST=1,3
      VISC(IST)=2.42*(1.6746E2 -5.4455*FILMTM(IST) +8.3752E-2*FILMTM(IST
     $)*FILMTM(IST) -7.30765E-4*FILMTM(IST)*FILMTM(IST)*FILMTM(IST) +3.77
     $485E-6*FILMTM(IST)**4 -1.1386E-8*FILMTM(IST)**5 +1.8487E-11*FILMTM(
     $IST)**6 -1.2463E-14*FILMTM(IST)**7)
   50 CONTINUE
      DO 60 IST=7,11
      VISC(IST)=2.42*(1.6746E2 -5.4455*FILMTM(IST) +8.3752E-2*FILMTM(IST
     $)*FILMTM(IST) -7.30765E-4*FILMTM(IST)*FILMTM(IST)*FILMTM(IST) +3.77
     $485E-6*FILMTM(IST)**4 -1.1386E-8*FILMTM(IST)**5 +1.8487E-11*FILMTM(
     $IST)**6 -1.2463E-14*FILMTM(IST)**7)
   60 CONTINUE
C
      DO 70 IST=1,3
      T(IST)=10.0*(FILMTM(IST)-32.0)/18.0
   70 CONTINUE
      DO 80 IST=7,11
      T(IST)=10.0*(FILMTM(IST)-32.0)/18.0
   80 CONTINUE
C
      DO 90 IST=1,3
```

```
      ROU(IST)=62.428/(0.924848 +6.2796E-4*(T(IST)-65) +9.2444E-7*(T(IST
     $)-65)**2 +3.057E-9*(T(IST)-65)**3)
   90 CONTINUE
      DO 100 IST=7,11
      ROU(IST)=62.428/(0.924848 +6.2796E-4*(T(IST)-65) +9.2444E-7*(T(IST
     $)-65)**2 +3.057E-9*(T(IST)-65)**3)
  100 CONTINUE
C
      DO 110 IST=1,3
      BETA(IST)=ROU(IST)*(6.2796E-4 +9.2444E-7*(T(IST)-65.)*2 +3.057E-9*
     $(T(IST)-65.)**2*3.)/62.428/1.8
  110 CONTINUE
      DO 120 IST=7,11
      BETA(IST)=ROU(IST)*(6.2796E-4 +9.2444E-7*(T(IST)-65.)*2 +3.057E-9*
     $(T(IST)-65.)**2*3.)/62.428/1.8
  120 CONTINUE
      RETURN
      END

$ENTRY
```

Nomenclature for Computer Program

ACOEFF	average local heat transfer coefficient calculated by Equation (6.2), Btu/(hr-ft^2-°F)
ACOND	thermal conductivity of the ethylene glycol evaluated at average of inlet and outlet bulk temperature, Btu/(hr-ft-°F)
AL	location of the station number on the test section to evaluate bulk temperature, ft
ANUSSL	average local Nusselt number
ARENO	average Reynolds number
BCOEF	average local heat transfer coefficient calculated by Equation (6.3), Btu/(hr-ft^2-°F)
BETA	coefficient of volume expansion of ethylene glycol, 1/°C
BISC	viscosity of the ethylene glycol evaluated at bulk bath temperature, lbm/(ft-hr)
BLNUSS	local Nusselt number
CDEN	current density, A/m^2
CDENSQ	current density square, A^2/M^4
CISC	viscosity of ethylene glycol evaluated at average of inlet and outlet bulk temperature
COEFF	local heat transfer coefficient, Btu/(hr-ft^2-°F)
COND	conductivity of ethylene glycol evaluated at film temperature, Btu/(hr-ft-°F)
CORECT	subroutine CORECT
DIN	inside diameter, ft
DOUT	outside diameter, ft
ERSTVT	subroutine to evaluate electrical resistivity of stainless steel 304
FILMTM	film temperature, °F
G	gravitational constant, ft/hr^2
GRAEZ	local Graetz number

GRS	local Grashof number
IFLUX	subroutine to evaluate radial heat fluxes
IPR	peripheral index
IQFLUX	local radial heat flux, Btu/(hr-ft^2)
IREND	local Reynolds number
IST	station number index
L	location of the station number on the test section, ft
LTOTAL	total length of the test section
MW	mass flow rate, lbm/hr
NRUN	run number
OUT	dummy variable to transfer values
PHROP	subroutine to evaluate physical properties of ethylene glycol
PRD	local Prandtl number evaluated at film temperature
PRNO	Prandtl number evaluated at the average of inlet and outlet bulk temperature
QFL	average radial heat flux, Btu/(hr-ft^2)
QI	heat input, Btu/hr
QLOSST	heat loss from the test section, Btu/hr
QOUT	heat output, Btu/hr
QPER	percent error in heat balance
RAL	Rayleigh number
READS	subroutine reads data and writes them in table format
RENO	Reynolds number evaluated at bath temperature
RESIST	resistivity of stainless steel 304, (ohm-m^2)/m
ROU	density of ethylene glycol, lbm/ft^3
SHEAT	specific heat of ethylene glycol evaluated at average of inlet and outlet bulk temperature
T	temperature variable to convert from °F to °C

TAMPS	current to the test section, ampere
TBATH	bulk bath temperature, °F
TBULK	bulk temperature at a station, °F
TCBA	average of inlet and outlet bulk temperature, °F
TCONDK	conductivity of stainless steel, watt/meter-°F
THCOND	subroutine to evaluate conductivity of the stainless steel 304
TIMSUF	mean inside surface temperature, °F
TIN	inlet bulk temperature, °F
TISURF	local inside surface temperature, °F
TOSURF	local outside surface temperature, °F
TOUT	outlet bulk temperature, °F
TROOM	room temperature, °F
VISC	viscosity of ethylene glycol evaluated at film temperature, lbm/(ft-hr)
VOLTS	voltage drop across the test section, volts
XAREA	cross sectional area, ft^2 or m^2

VITA

Nitin D. Mehta

Candidate for the Degree of

Master of Science

Thesis: LAMINAR FLOW HEAT TRANSFER IN A PIPE PRECEDED BY A 180° BEND

Major Field: Chemical Engineering

Biographical:

Personal Data: Born in Bombay, India, July 13, 1954, the son of Mr. and Mrs. D. V. Mehta.

Education: Graduated from The New Era School, Bombay, India, in June, 1971; received the Bachelor of Science in Chemical Engineering degree from Oklahoma State University in May, 1978; completed requirements for the Master of Science degree in Chemical Engineering at Oklahoma State University in December, 1979.

Professional Experience: Graduate teaching assistant, School of Chemical Engineering, Oklahoma State University, from January, 1978, to May, 1979.